Schweizerische Eidgenossenschaft
Confédération suisse
Confederazione Svizzera
Confederaziun svizra

Federal Department of the Environment, Transport, Energy and Communications DETEC

Swiss Federal Office of Energy SFOE
Energy Research and Cleantech Division

Final report dated 30th of June 2024 / revised 20th of December 2024

Optimized adsorption heat pump for increased efficiency in district heating networks

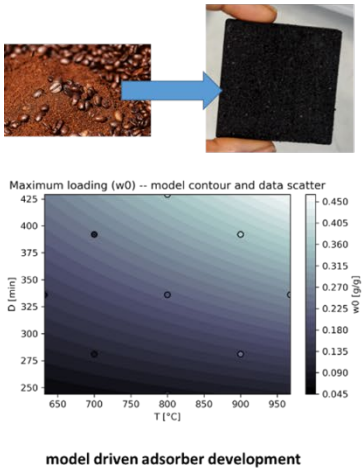

model driven adsorber development

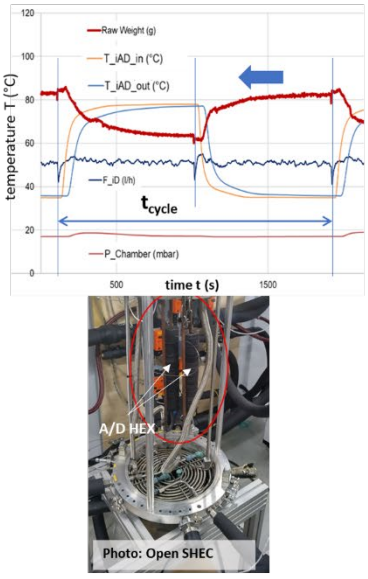

adsorption/desorption HEX characterisation

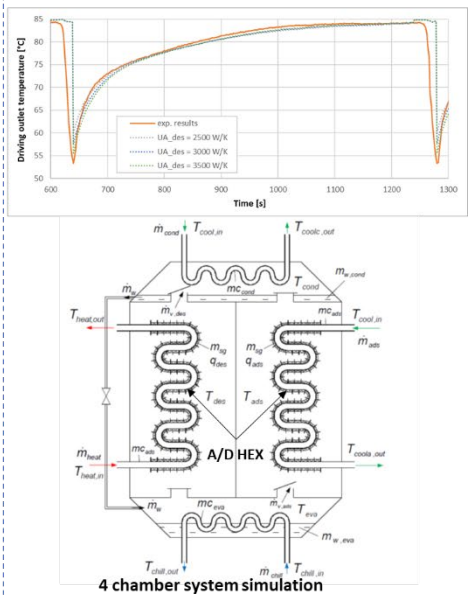

4 chamber system simulation

Source: © CharacSorb 2022

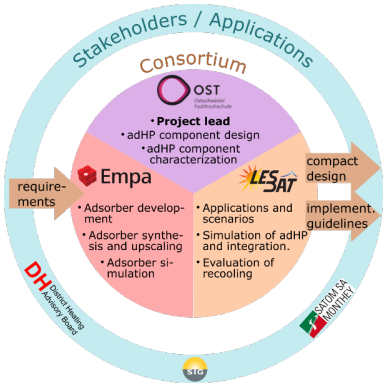

Date: 30th June 2024

Location: Yverdon-Les-Bain, Dübendorf, Rapperswil

Publisher:
Swiss Federal Office of Energy SFOE
Energy Research and Cleantech
CH-3003 Bern
www.bfe.admin.ch

Subsidy recipients:
OST Ostschweizer Fachhochschule, SPF Institut für Solartechnik
Oberssestrasse 10, CH-8640 Rapperswil
www.spf.ch

Empa, Building Energy Materials and Components Group
Überlandstrasse 129, CH-8600 Dübendorf
www.empa.ch

HEIG-VD LESBAT
Avenue des Sport 20, CH-1401 Yverdon-les-Bain
https://heig-vd.ch

Authors:
Alexis Duret, Xavier Jobard; HEIG-VD LESBAT, alexis.duret@heig-vd.ch, xavier.jobard@heig-vd.ch;
Sandra Galmarini, Empa Building Energy Materials and Components Group, sandra.galmarini@empa.ch;
Kevin Meili, Paul Gantenbein, Xavier Daguenet, SPF Institut für Solartechnik, kevin.meili@ost.ch, paul.gantenbein@ost.ch, xavier.daguenet@ost.ch.

SFOE project coordinators:
Stephan Renz, info@renzconsulting.ch

SFOE contract number: SI/502258-01

Zusammenfassung

Sorptionswärmepumpen können auf der Basis von erneuerbarer Fernwärme oder Abwärme Kälte bereitstellen und somit den Anwendungsbereich der Fernwärmenetze (FWN) erweitern sowie bestehende erneuerbare Wärmequellen besser nutzen. Andererseits können Sorptionswärmepumpen in Fernwärme-Übergabestationen auch Wärme bereitstellen bei gleichzeitiger Reduktion der Temperatur des Rücklaufs im Fernwärmenetz, dies im Vergleich zu einer Übergabestation mit Standard-Wärmetauscher. Damit wird die Effizienz des Fernwärmenetzes erhöhen. Kommerziell verfügbare Sorptionsmaschinen sind jedoch nicht auf FWN ausgelegt. Deshalb werden neue, ideal auf die Temperauren und Anwendungen in Fernwärmenetzen abgestimmt Sorptionsmaterialien entwickelt und in einen für Sorptionsmaschinen bestimmte Wärme- & Stoffübertrager eingebaut.

Die Betriebsbedingungen einer Adsorptionswärmepumpe (adHP) wurden in einem Fernwärmenetz für zwei verschiedene Betriebsmodi definiert: (1) Kühlbetrieb zur Bereitstellung von Kälte für Gebäude, welche an das Fernwärmenetz angeschlossen sind, unter Verwendung von Wärme aus dem FNW und (2) FNW-Rücklauftemperaturreduktion zur Verbesserung der Effizienz des Netzes. Die ermittelten technischen und wirtschaftlichen Anforderungen bzw. Randbedingungen stellen keine grösseren Hindernisse für die Entwicklung und Anwendung der Technologie dar. Die derzeitigen Netztemperaturen sind anwendbar und die Kosten für Maschinen mit hoher Leistung (> 100 kW) sind bereits wettbewerbsfähig. Ein Workshop mit Betreibern von Fernwärmenetzen wurde im Rahmen eines 5-7-Treffens zur Absenkung der Netztemperaturen durchgeführt.

Im Projekt wurde zudem ein numerisches Modell der adHP modifiziert. Das aktualisierte Modell wurde dann kalibriert und anhand experimenteller Messungen, durchgeführt im SPF-Prüfstand, validiert. Dieses validierte Modell wurde schliesslich verwendet, um die Leistung der adHP-Technologien im Rücklauftemperaturreduktionsmodus zu bestimmen. Diese ermittelte Leistung wurde wiederum mit jener von kommerziell verfügbaren adHP verglichen. Da mit der neuen Entwicklung keine Leistungsverbesserung erkennbar war, wurden die Fallstudien mit den verfügbaren Modellen durchgeführt. In einer Fallstudie zum Temperaturreduktionsmodus wurde eine aktive Unterstation zwischen einem Niedertemperatur-Unternetz und einem 90 °C-Hauptnetz eingebunden. Dabei hat das Unternetz einen Vorlauf mit 50 °C/65 °C, sowie einen Rücklauf mit 40 °C/50 °C und versorgt ein Viertel bestehend aus 33 Gebäuden (5 MW Leistung, 9 GWh*Jahr^{-1} Bedarf). Die Ergebnisse zeigen, dass der Einbau der Unterstation eine Reduzierung der Rücklauftemperaturen um 10 K und eine Investitionsrückzahlung von weniger als 5 und 7 Jahren ermöglicht, wobei Kostenreduktionsgradienten von 0.67 bzw. 0.51 CHF*MWh^{-1}*K^{-1} berücksichtigt werden. Eine Fallstudie zur Kühlanwendung in einer Gewerbezone wurde durchgeführt, in welcher zwei Szenarien verglichen wurden: 1) Business as Usual (BAU) mit dezentralen Kompressionskältemaschinen und 2) Fernkühlung (District Cooling) unter Einbindung einer Sorptionskältemaschine, die vom Fernwärmenetz (DHN) betrieben wird. Das DC-Szenario (89.6 CHF*MWh^{-1}) ist teurer als das BAU-Szenario (72.5 CHF*MWh^{-1}). Dies mit höheren Investitionskosten (~21 % vs. 7.2 %) und zusätzlichen Kosten für das Kaltwassernetz. Die Kosten im BAU-Szenario werden hauptsächlich durch den Bedarf an elektrischer Energie (92.8 %) bestimmt, während das DC-Szenario eine ausgewogenere Kostenverteilung zwischen Wärme (32.8 %) und Elektrizität (42.9 %) aufweist. Dies kann die Volatilität der Energiepreise abschwächen.

Die Modellierung unterstützte zudem die Sorbent-Optimierung und führte zu vielversprechenden Sorptionsmaterialien. Die Herstellung des Sorbent-Materials wurde erfolgreich hochskaliert. Für den geplanten Wärme- und Stoffaustascher (A/D HEX 2) wurden Aktivkohle-Monolithe hergestellt.

Weiter wurde der im früheren SNF THRIVE Projekt entwickelte und mit Aktivkohle bestückte A/D Wärme- und Stoffaustauscher (A/D HEX 1) im erweiterten Prüfstand charakterisiert. Das Design eines Wärme- und Massentauschers der zweiten Generation (A/D HEX 2) wurde fertiggestellt (hydraulische Verteilung, Lamellen und Sorptionsmonolith-Layout) sowie mit selbst entwickelten Verfahren und Werkzeugen hergestellt. Nun zeigen jedoch die Ergebnisse der Messkampagne von A/D HEX 2 keine signifikant anderen Ergebnisse als jene zur ersten Version: um etwa 30 % geringere Leistungen im Kühlmodus und etwas bessere (+5 %) im Wärmenetzmodus. Angesichts der hohen (Sorbat)

Dampfmengen, die zu Beginn eines Zyklus adsorbiert und desorbiert werden (hohe Kinetik), scheint das Sorbent-Material selbst nicht (Leistungs-) limitierend zu sein, sondern eher die Umsetzung bzw. Implementierung in die Wärme transportierenden Elemente (Limitierung durch den Wärmeübergang). Weitere Untersuchungen, wie z.B. 3D-Modellierung, um die Zahl der Versuche zu reduzieren, wären notwendig, um diese Hypothese zu bestätigen.

Résumé

Les pompes à chaleur à sorption peuvent fournir du froid à partir de sources de chaleur renouvelable ou de chaleur résiduelle, ce qui élargit le champ d'application des réseaux de chaleur et permet de mieux utiliser les sources de chaleur renouvelables existantes. D'autre part, les pompes à chaleur à sorption dans les stations de transfert de chaleur peuvent également fournir de la chaleur tout en réduisant de manière significative la température de retour du réseau de chaleur par rapport à une station avec un échangeur de chaleur ordinaire, augmentant ainsi l'efficacité de l'approvisionnement en chauffage urbain. Cependant, les machines à sorption disponibles dans le commerce ne sont pas conçues pour les réseaux de chaleur. C'est pourquoi de nouveaux matériaux de sorption idéalement adaptés aux températures et aux applications des réseaux de chauffage urbain sont en cours de développement et incorporés dans un échangeur de chaleur et de masse conçu pour les pompes à chaleur à adsorption réversible.

Les conditions de fonctionnement de la pompe à chaleur par adsorption (adHP) intégrée dans un réseau de chauffage urbain ont été définies pour deux modes différents : (1) mode de refroidissement pour fournir du froid aux bâtiments connectés au réseau de chauffage urbain en utilisant la chaleur du réseau et (2) mode de réduction de la température de retour pour améliorer l'efficacité du réseau de chaleur. Les contraintes techniques et économiques identifiées ne présentent de frein majeur au développement de la technologie. Les niveaux de température des réseaux actuelles sont adaptés et les coûts sont déjà compétitifs pour les machines de forte puissances (> 100 kW). Un atelier a été effectué avec les opérateurs de réseaux de chauffage à distance lors d'un 5 à 7 sur l'abaissement de la température des réseaux.

En outre, le modèle numérique de l'adHP a été modifié. Le modèle mis à jour a ensuite été calibré et validé par rapport aux mesures expérimentales réalisées sur le banc d'essai du SPF. Le modèle validé a finalement été utilisé pour cartographier les performances des technologies adHP en mode de réduction de la température de retour et pour le mode rafraichissement. Les performances ont été comparées à celles d'une adHP disponible commercialement et des données issues de la litérature. Comme les performances des nouveaux développements ne présentaient pas d'amélioration au niveau des performances, les études de cas ont été effectuée avec les modèles disponibles. Un cas d'étude en mode réduction des températures a été effectués en intégrant une sous-station active entre un sous-réseaux basse température (aller : 50 °C/65 °C, retour : 40 °C/50 °C) alimentant un quartier de 33 bâtiments (5 MW de puissance et 9 $GWh*an^{-1}$ de consommation) et un réseau structurant à 90 °C. Les résultats montrent que la sous-station active permet de réduire les températures de retour de 10 K et des retours sur investissement inférieurs à 5 et 7 ans en considérant respectivement des gradients de réduction des coûts de 0.67 et 0.51 $CHF*MWh^{-1}*K^{-1}$. Une étude de cas pour l'application de refroidissement d'une zone commerciale a été menée, comparant deux scénarios : 1) Business as Usual (BAU) avec des machines frigorifiques à compression décentralisés, et 2) Froid a distance (FaD) intégrant un machine à sorption alimentée par le chauffage à distance(CaD) Le scénario FaD (89.6 $CHF*MWh^{-1}$) est plus coûteux que le scénario BAU (72.5 $CHF*MWh^{-1}$), avec un amortissement des investissements plus élevé (~21 % contre 7.2 %) et des coûts supplémentaires liés au réseau de FaD. Les coûts du scénario BAU sont principalement dus à l'électricité consommée (92.8 %), tandis que le scénario FaD présente une répartition des coûts plus équilibrée entre la chaleur (32.8 %) et l'électricité (42.9 %), atténuant ainsi la volatilité des tarifs énergétiques.

L'optimisation soutenue par la modélisation a conduit à des matériaux adsorbants très prometteurs, et la production de matériaux a pu être menée à bien à plus grande échelle. La production de sorbants pour le prototype final a été achevé.

Finalement, l'échangeur de chaleur et de masse A/D (A/D HEX 1) développé dans l'ancien projet SNF THRIVE transportant du carbone actif a été caractérisé sur le banc d'essai mis à jour. La conception d'un échangeur de chaleur et de masse de deuxième génération (A/D HEX 2) a été achevée (distribution hydraulique, ailettes et disposition du monolithe de sorption) et fabriquée à l'aide d'outils et de processus développés en interne. Malheureusement, les résultats de la campagne de caractérisation de l'A/D HEX 2 ne montrent pas de résultats significativement différents de la première version : performances inférieures de l'ordre de 30 % en mode rafraîchissement et légèrement meilleures (+5 %) en mode réseau de chaleur. Au vu des fortes quantités de vapeur adsorbées/désorbées en début de cycle, le matériau lui-même ne semble plas limitant mais plutôt sa mise en œuvre (limitation liée aux transferts thermique?). Des investigations supplémentaires (modellisation 3 D) seraient nécessaires afin de confirmer cette hypothèse.

Summary

Sorption heat pumps can provide cooling based on renewable district heat or waste heat, thus expanding the scope of district heating networks (DHN) and making better use of existing renewable heat sources. On the other hand, sorption heat pumps in district heat transfer stations can also provide heat while significantly reducing the return flow of the district heating network compared to a station with ordinary heat exchanger, thus increasing the efficiency of district heating supply. However, commercially available sorption machines are not designed for DHN. Therefore, new sorption materials ideally suited to the temperatures and applications in district heating networks are being developed and incorporated in a heat & mass exchanger designed for reversible adsorption heat pumps.

The Adsorption Heat Pump (adHP) operating conditions in a District Heating Network have been defined for two different modes: (1) cooling mode to supply cooling to building connected to the DHN using heat from the grid and (2) return temperature reduction mode to improve the efficiency of the grid. The technical and economic constraints identified do not present any major obstacles to the development of the technology. Current network temperature levels are suitable, and costs are already competitive for high-power machines (> 100 kW). A workshop was held with district heating network operators during a 5 à 7 on lowering network temperatures.

Furthermore, the adHP numerical model has been modified. The updated model has then been calibrated and validated against experimental measurements realized in the SPF test bench. The validated model has finally been used to map the performance of the adHP technologies in return temperature reduction mode. The performance has been compared to the performance of a commercially available adHP. As the new developments showed no improvement in performance, the case studies were carried out using available models. A case study in temperature reduction mode was carried out, integrating an active substation between a low-temperature subnetwork (outgoing: 50 °C/65 °C, return: 40 °C/50 °C) supplying a district of 33 buildings (5 MW of power and 9 $GWh*year^{-1}$ of consumption) and a 90°C structural network. The results show that the active substation enables return temperatures to be reduced by 10 K, with paybacks of less than 5 and 7 years respectively, considering cost reduction gradients of 0.67 and 0.51 $CHF*MWh^{-1}*K^{-1}$. A case study for a commercial zone's cooling application was conducted, comparing two scenarios: 1) Business as Usual (BAU) with decentralized compression chillers, and 2) District Cooling (DC) integrating a sorption chiller powered by the DHN. The DC scenario (89.6 $CHF*MWh^{-1}$) is more expensive than the BAU scenario (72.5 $CHF*MWh^{-1}$), with higher initial investment amortization (~21 % vs. 7.2 %) and additional costs from the chilled water network. The BAU scenario's costs are primarily driven by electricity (92.8 %), whereas the DC scenario has a more balanced cost distribution between heat (32.8%) and electricity (42.9 %), mitigating energy tariff volatility.

Modelling supported optimization led to highly promising sorbent materials and materials production has been successfully upscaled. The production of sorbents for the final prototype has been completed.

Finally, the A/D Heat and Mass Exchanger (A/D HEX 1) developed in the former SNF THRIVE project carrying active carbon sorbent was characterized on the updated test rig. The design of a second-generation Heat and Mass Exchanger (A/D HEX 2) has been completed (hydraulic distribution, fins and sorption monolith layout) and manufactured using in-house developed tools and processes. Unfortunately, the results of the A/D HEX 2 characterisation campaign do not show significantly different results from the first version: performance is around 30 % lower in the cooling mode and slightly better (+5 %) in the district heating mode. In view of the large quantities of vapour adsorbed and desorbed at the onset of the cycle, due to the high kinetic the material itself does not appear to be a limiting factor, but rather the way it is installed and laminated to the heat conducting elements i.e. heat transfer limited characteristic. Further investigations like 3D modelling and thus reduction of the experimental effort would be required to confirm this hypothesis.

Main findings

- The active substation integrating a sorption heat pump allows return temperatures to be reduced by 10 K and paybacks period shorter than 5 and 7 years, considering cost reduction gradients of 0.67 and 0.51 CHF/(MWh.C) respectively.
- Text BoxDistrict Cooling (DC) integrating a sorption chiller powered by the DHN shows cost slightly higher (about 21 %) than a decentralized chillers scenario (BAU) to cover the refrigeration and cooling demand of a commercial zone. However, the DC scenario has a more balanced cost distribution between heat (32.8%) and electricity (42.9%), mitigating future energy tariff volatility, whereas the BAU scenario's costs will be greatly influenced by the cost of electricity representing 92.8% of the total cost of the project.
- Techniques have been developed to manufacture a functional second-generation A/D heat and mass exchanger.
- Upscaling of both synthesis and pyrolysis protocol for monolithic carbon based on used coffee grounds with target properties and completion of production of ACs for the second prototype.

Abbreviations

List of Parameters & Abbreviations

AC	Activated Carbon
A/D HEX	Adsorption-Desorption heat exchanger (heat and mass exchanger)
AdHP	Adsorption Heat Pump
α	thermal diffusivity (m^2*s^{-1})
c	specific heat ($J*kg^{-1}*K^{-1}$)
C	Characteristic energy of adsorption ($J*g^{-1}$)
D	Diffusion coefficient (m^2*s^{-1})
DHN	District Heating Network
DHW	Domestic Hot Water
E	Heat (J)
ε	Porosity (-)
F	adsorption enthalpy ($J*g^{-1}$)
GUI	Graphical User Interface (NI LabVIEW) (-)
Δh_v	heat of evaporation of water ($J*kg^{-1}$)
γ	Gas concentration ($kg*m^{-3}$)
k_{50}	heat conductivity ($W*m^{-1}*K^{-1}$)
KPI	key performance indication (-)
m	mass (kg)
M	molecular mass ($g*mol^{-1}$)
N	Adsorption curve shape factor, exponente (-)
p	pressure (Pa)
R	gas constant ($J*K^{-1}*mol^{-1}$)
$R_{heat,\ mass}$	Heat transfer resistance ($K*W^{-1}$), mass transfer resistance
ρ	density ($kg*m^{-3}$)
s	thickness (m)
SCP	Specific Cooling Power ($W*kg_{Sorbent}^{-1}$)
SCG	Spent Cofee Grounds
SH	Space Heating
SHEC	Sorption Heat and mass Exchanger Characterization
T	Temperature (°C)
ΔT	Temperature difference (K), example: $\Delta T = T_{des} - T_{ads}$
t_{cycle}	Cycle time in the quasi-continuous adsorption & desorption process (s)
τ	adimensional time (-)
V	specific volume (cm^3*g^{-1})
UA	overall heat transfer coefficient ($W/(m^2K)$)
w	water adsorption characteristic w(p, T)
W	Water saturation capacity ($g*g^{-1}$)

List of Subscripts

a	adsorbate
ads	adsorption
c / cond	condensation

cooling	cooling mode
des	desorption
e / env	envelope
evap	evaporation
ext	external
f	fin / lamella
heat	subscript of heat transfer resistance R_{heat}
h / heating	heating mode
hot	hot temperature source used for desorption
m	mesoscopic
mass	subscript of mass transfer resistance R_{mass}
M	Macroscopic
μ	microscopic
i	initial
int	internal
s	adsorbent
sat	saturation
skel	skeletal
surf	surface
t	total
v, ν	vapor

1 Introduction

1.1 Background information and current situation

Due to climate change and the ensuing rise of the outdoor temperatures, the cooling demand in buildings will increase in the future (www.spf.ch/SolSimCC, 2022). Nevertheless, the heating demand in Switzerland [Gonseth et al., 2017] will remain high in wintertime. In order to achieve the energy turnaround for Switzerland and to reduce drastically greenhouse gas emissions (SWEET Call, 2020), innovative, integrated and eco-friendly heating and cooling solutions are required to supply the building stock as well as processes with heating and cooling. Today's decarbonisation strategy of the Swiss energy sector is based mainly on electrification with heat pumps and compression cooling machines. Indeed, compression heat pumps are the cheapest technical installations able to meet the MuKEn/MoPEc [EnDK, 2022] requirements. On the one hand, with Switzerland phasing out of nuclear power and increasing needs (energy demand), it is expected that more electricity will be imported from neighbouring countries like Germany, where the CO_2 footprint of the energy mix during peak load in winter is high [Padey et al., 2020]. On the other hand, during summer, large amounts of heat remain unused from waste incineration plants and other industrial processes because of the low heat demand during this season. This heat can be used in summer to power AdHP and supply eco-friendly and cost-effective cooling energy to various cooling consumers (buildings, retail salesrooms, industries…).
District heating networks (DHN) are a well-known solution for tackling two challenges:

a) lower the carbon footprint for heating in winter and

b) valorisation of otherwise unused "waste" heat.

However, DHN suffers from two important drawbacks, which limits their energy efficiency and operability:

- Low efficiency caused by high operating temperatures, especially high return temperatures (Rüetschi et al., 1997) that lead to extra cost (high thermal losses and high-volume flow rates to deliver one unit of useful heat).
- Low utilization of the DHN in summertime (only domestic hot water is used in the buildings) which leads to inefficient operation conditions.

The impacts of those two drawbacks are reduced heat distribution capacity for a given pipe diameter (due to limited temperature differences), high heat distribution costs (pumping energy and heat losses) and lower energy efficiency in the heating station (more energy to produce one unit of useful heat).

As shown during the SNF PNR70 THRIVE [Ruch et al., 2015] project and the Interreg PACs-CAD ["PACs-CAD – Interreg France-Suisse," 2024] project, the integration of reversible adsorption heat pumps into DHN allows for the use of untapped waste heat and increases energy efficiency of district heating networks.

1.2 Purpose of the project

Two particularly promising integrations of AdHP in DHN have been investigated in those two projects:

1. **Temperature reduction mode:** the use of high temperature from the DHN to satisfy relatively space heating at low temperature implies important exergy loses. In order to reduce those loses, an adHP could be integrated in a substation using the high temperature to drive the sorption cycle and the return flow as heat source to reduce the return temperature.
2. **Cooling mode:** in order to remain competitive compared to decentralized solution for space heating, DHW production and cooling, thermal grid should offer cooling service in summer time. By integrating an adHP in a substation, it is possible to use the high temperature of the DHN to provide cooling to the building.

Therefore, the knowledge and technologies developed in the SFOE CharacSorb project have two main purposes:

1. **DHN return temperature reduction** (figure 1 (a)): in this mode of operation[1], an AdHP is integrated in a substation at the building level (i.e., where the heat exchange between the thermal grid and the building takes place) and provides heat to the building. The AdHP uses the substation return flow as a heat source for the evaporator and thus reduces the temperature of the DHN return flow. With this mode of operation, it is possible to lower the return temperature of the district heating network to values below the return temperature of the building's space heat supply. This new active substation configuration offers DHN operators to better control the temperature difference in critical substations on their thermal grid. By increasing the temperature difference between the forward and return of the DHN, this new technology allows to save pumping energy or to increase the heat delivery capacity of a given thermal grid. Additionally, it also reduces heat losses since the return temperatures are lowered.
2. **Cooling production** (Figure 1 (b)): by integrating a reversible AdHP in a substation, it is possible to produce cooling for building application in summertime using heat from the DHN. This enables the DHN operators to offer a new energy service to their customers, while increasing the sale of heat in summertime and thus the profitability of the DHN. Since a major part of heat is either renewable or waste heat in Swiss DHN, this cold supply will also be renewable. The major challenge for this mode of operation is to dissipate and/or valorise condensation and adsorption heat at intermediate temperature (heat extracted from the adsorber and the condenser) without extra cost. Valorisation of this heat can be achieved by pre-heating domestic hot water.

[1] To operate an AdHP three temperature levels T_{des} (desorption), T_{ads} (adsorption), T_{low} (evaporation) are needed.

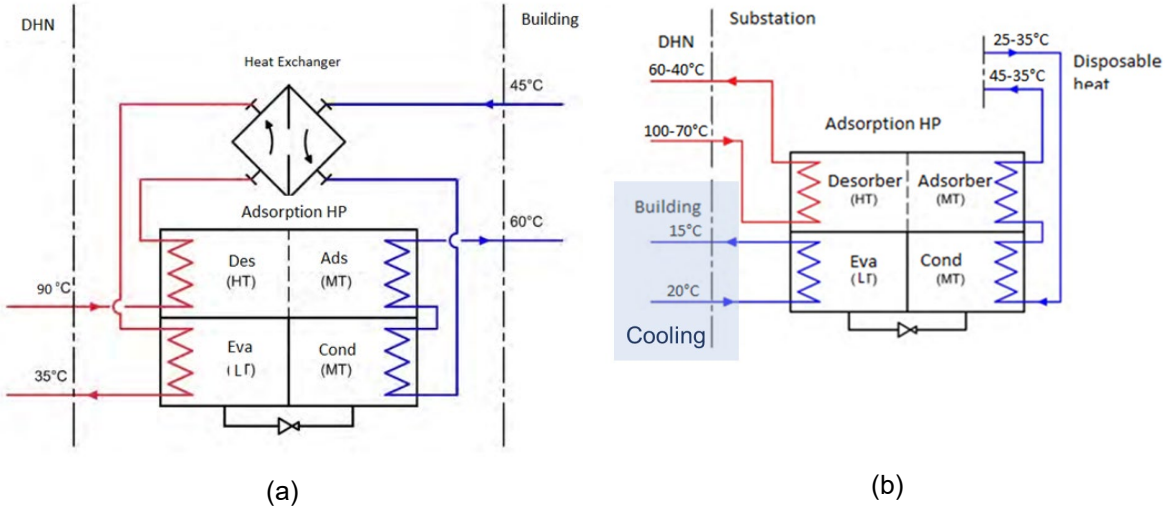

Figure 1: Hydraulic architecture of a Substation integrating an adsorption Heat Pump for (a) return temperature reduction and (b) cooling production.

1.3 Objectives

a) Definition of the **technical and operating constraints of a reversible AdHP integrated in a substation** in cooperation with the DHN advisory board.

b) **Extension of a physical reversible AdHP simulation model**, **including hydraulic implementation in DHN** for cooling application. The experimental measurements realized with the optimized HEX component with carbon sorbents will be used to calibrate/validate the numerical model.

c) Development of targeted **sorbent materials** – which allows a thermal **COP_{th} > 0.6 in the reversible heat pump** even in summer (cooling mode) and a high/optimal recooling temperature – to be able to valorise it for preheating of domestic hot water – as well as provides an adequate energy and power density.

d) Upscaling of the material synthesis to produce ~100 g sorbent and sorbent integration in **a custom designed adsorber-desorber HEX** with a cooling power of approx. **1 kW** with water sorbate**.** The **HEX will be characterised** for **DHN integration with a target thermal COP_{th} ~ 0.6 to 0.7 for cooling.** Scaling considerations to higher power will be performed.

e) **Technical and financial evaluation of the new sorption reversible substation** for the two targeted modes: a) return temperature reduction for heating and b) cooling, using validated simulation models.

f) Formulation of **practical implementation guidelines for reversible AdHPs in district heating networks** (**hydraulic implementation in DHN increasing the efficiency**) for **room air conditioning** application.

2 Procedures and methodology

2.1 Implementation constraints and cost guidelines for adHP application in DHN (WP1)

During the first step of the project, the **operational constraints** and **conditions of operation** of the Adsorption Heat Pump (AdHP) developed in the CharacSorb project were defined. Those inputs are crucial for the adsorbent and AdHP development. They have been used to simulate the performance of a substation including an AdHP. Two modes of operation were studied: (1) return temperature reduction mode and (2) cooling production mode with specific constraints for each mode. The operational constraints and conditions of operation were mainly defined by reviewing the **current conditions of operation of existing DHNs** in Switzerland and the **thermodynamic constraints** of AdHP cycle.

In a second stage, the **integration/cost guidelines and best practices** for the two modes of operation of a substation integrating a reversible adHP were compiled. Those guidelines are needed by DHN operators to evaluate the feasibility and attractiveness of adHP integration into their networks. It will promote the use of sorption technology coupled to DHN for increased efficiency and reliable renewable cooling production. Different hydraulic integration schemes between existing DHN and buildings have been developed. Those hydraulic scheme should allow maximizing the adHP performance while keeping investment and operational cost low.

The results obtained in WP1 are given in Section 3.1.

2.2 System performance simulation (WP2)

The performances of the new adsorption heat pump integrated in a substation have been evaluated by simulation in WP2 using inputs from WP1 (operating conditions), WP3 (properties of the heat and mass exchanger) and WP4 (new adsorbent materials properties). The numerical model has been developed recently during a phd thesis by A. Dalibard on Trnsys (Dalibard, 2017). This model has been modified and adapted to be integrated in a substation numerical model. Thanks to this model, the performance of the AdHP substation have been evaluated over a wide range of operating conditions in temperature reduction mode and for cooling applications.

2.3 Heat and mass exchanger characterization (WP3)

A/D HEX Characterization In the adsorber - desorber characterization the mass uptake w(t) in the adsorption and mass loss in the desorption cycling is measured. The amount of w(t) multiplied by the heat of evaporation (Δh_v) of the sorbate is used as a benchmark for the efficiency of the heat and mass exchanger. Therefore, the measurement setup of the SNF THRIVE project was modified. This comprised the modification of the external heat transfer fluid loops and additional sensors – like a new balance beam (HBK Plattformwägezelle 1-SP4MC6MR/7KG-1) of a higher (mass m +/- Δm of 0.5 g) resolution.

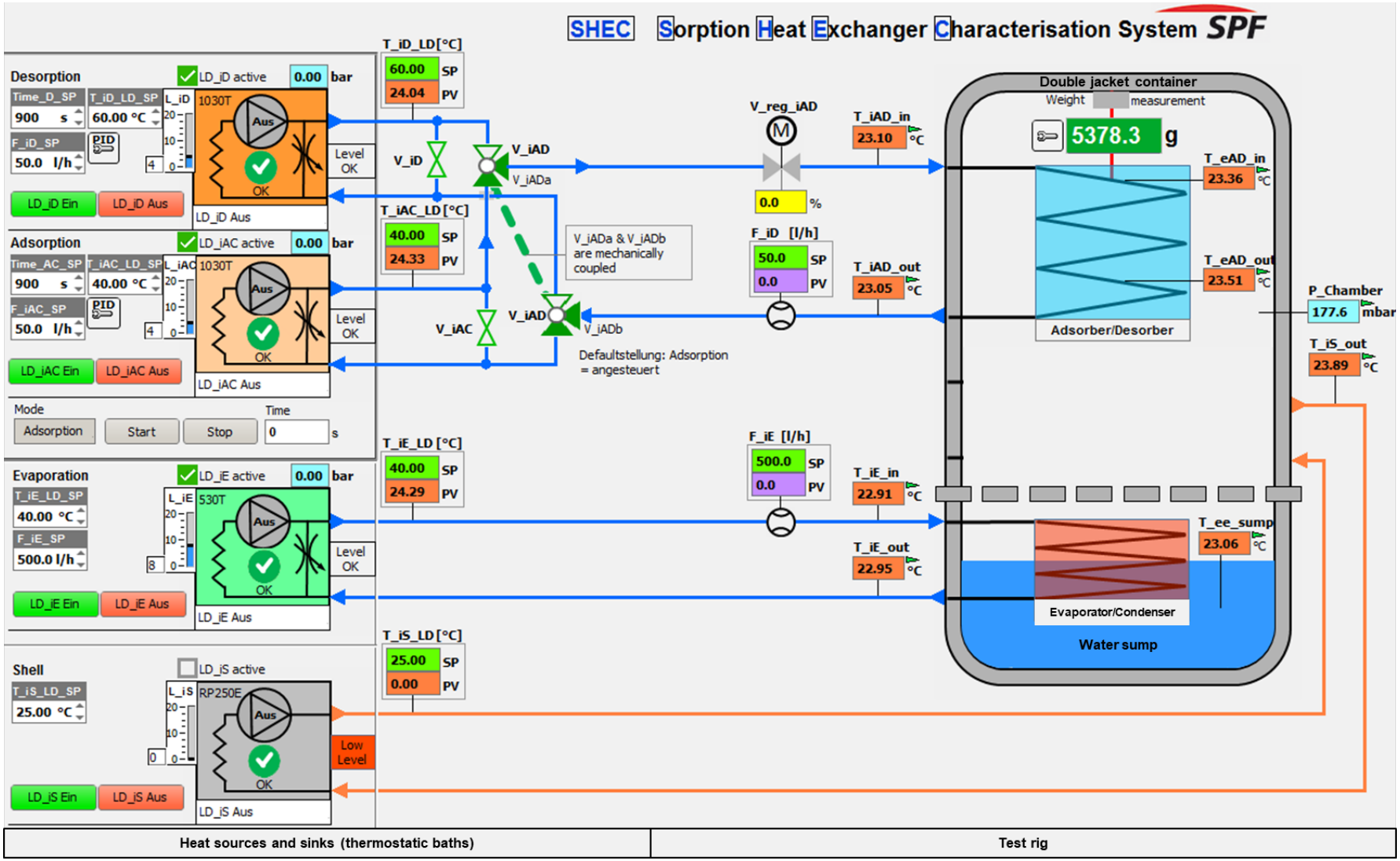

Figure 2: Graphical user interface (GUI) of the NI LabVIEW data acquisition system: 4 thermostatic baths as heat sources and heat sinks (left), single chamber setup with double jacket envelope, evaporator/condenser as well as adsorber/desorber (right), tubing and sensors.

Figure 2 shows the graphical user interface (GUI) of the NI LabVIEW data acquisition system. The principle of the setup with heat sources and heat sinks can be seen. Therefore, 3 thermostatic baths are used to perform adsorption and desorption (with the A/D HEX) as well as evaporation (evaporator) and condensation (condenser) of sorbate. With the 4th thermostat, the double jacked is tempered to avoid heat transfer from and to the environment (the inner vacuum envelope surface) from and to the A/D HEX. In Figure 3 part of the open single chamber with the installed A/D HEX I (suspended at the beam balance) is shown, and the right of this Figure shows a section of the activated carbon sorbent disks stack.

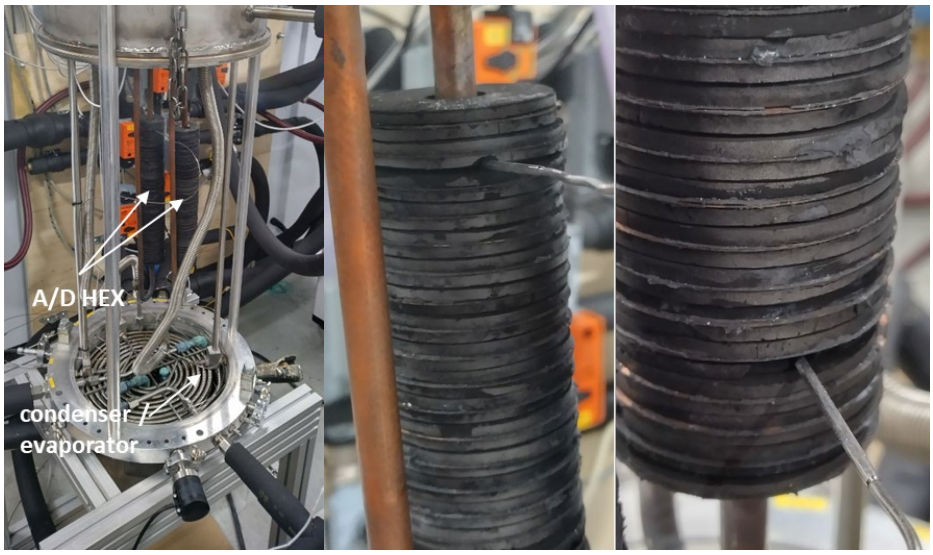

Figure 3: SHEC and installed activated carbon sorbent disks stack: photo of the open single chamber measurement setup (left) and a section of the A/D HEX I with clamped Pt 100 temperature sensors. The sorbent disks sandwich the heat conducting copper fins.

Prior to cyclic adsorption and desorption measurements with sorbate, a calibration procedure without sorbate has to be performed for each cycle time t_{cycle}. These calibrations account for all “virtual” mass changes induced by thermal expansion of the A/D HEX, pressure oscillations in the heat transfer fluid and any heat input from the surrounding. After the measurements with the sorbent-sorbate combination an appropriate data procedure follows to determine the efficiency parameters.

2.4 Sorbent development and characterization (WP4)

One of the key components in an AdHP are the A/D heat and mass transfer units carrying the sorbent material (A/D HEX). This is a research field where a high optimization potential remains (Aristov, 2013). However, in order to be able to optimize the sorption component, it is important to understand where the current main performance limitations come from (combined heat and mass diffusion, equilibrium sorption properties of sorbent). To be able to do so, the sorption model developed for HyCool was adapted to help determining the main performance limiting factors of the 1st A/D HEX (materials sorption capacity, heat and mass transfer – diffusion - within the material, material integration, HEX design) and guide the sorbent optimization for the 2nd A/D HEX.

The model was developed in OpenModelica, following the lumped-parameter approach described in (Piccoli et al., 2021). Using such an approach assumes that the global adsorption dynamic can be sufficiently well described as if happening at a single effective thermodynamic state (temperature, pressure, loading), instead of simulating the local variations of temperature, pressure and loading within

the adsorbent. Such a model includes only the heat and mass transfer within the material itself, therefore can be used as a term of comparison for different materials, boundary conditions and geometries, and not as a reference for whole AdHPs.

The model is composed of a temperature boundary condition (representing the HEX fin temperature), a heat transfer resistance (representing the conduction within the AC), a heat and mass balance (representing the adsorption reaction in the pores), a mass transfer resistance (representing the vapour diffusion in the pores), one pressure boundary conditions (representing the evaporator / condenser). All these elements are connected in this order, such that the adsorption dynamics calculated in the heat and mass balance depend on the materials properties and on the boundary conditions.

The temperature and pressure boundary conditions are modelled as square waves oscillating between the adsorption and desorption heat transfer fluid temperatures and evaporator and condenser pressure, respectively. Moreover, a control mechanism forbids flow reversal for the pressure boundary condition. More details can be found in (Piccoli et al., 2021). The mass transfer resistance within the monolith is modelled as microscopic surface diffusion and a transient 1-D macroscopic diffusion. For the macropore diffusion, the porosity is not limiting the mean free path of the gas and therefore only the total macroporosity is expected to influence macropore diffusion. Furthermore, given the characteristic lengths at play in the microscale and in the macroscale (r_μ~1 μm and s~1) the macroscopic diffusion is by far the limiting mechanism, especially at the beginning of the diffusive process. This is similar to the trends observed for coatings (Ammann et al., 2019). The state of the AC is determined by its properties, namely thermal diffusivity α, specific heat capacity c, envelope density ρ, thickness s and water adsorption characteristic w=$w(p, T)$.

In addition to originally planned activities, due to lower performance of the 1st gen prototype compared to predictions, the ageing of the THRIVE sorbent material and insufficient integration has been investigated and mitigation strategies developed.

3 Results and discussion

3.1 Implementation constraints and cost guidelines for adHP application in DHN (WP1)

3.1.1 Introduction

In the CharacSorb project, one of the initial tasks was to define the two operational modes of a substation integrating an adsorption heat pump (adHP). The first mode, termed "heating mode," involves using the adHP to reduce the return temperature of the district heating network (DHN) by utilizing the return flow as a low-temperature heat source, as detailed in section 3.1.2 of the report. The second mode, termed "cooling mode," involves using high-temperature heat from the DHN for cooling production, as described in section 3.1.3.

Following the definition of these operational modes, section 3.1.4 outlines the operational constraints and temperature requirements necessary for adHP integration into the DHN. These constraints and conditions guided the development of the adsorbent material and were essential for evaluating the performance of the CharacSorb heat and mass exchanger in both operational modes. Additionally, an assessment of the current costs of substations integrating commercially available adHPs was

conducted. Finally, a comprehensive guideline for the integration of adHPs in DHNs for both "heating" and "cooling" modes was proposed.

3.1.2 AdHP in DHN substation – Temperature reduction mode

The objective of this mode of operation is to use the temperature difference between the DHN forward flow and the secondary heating circuit return flow to drive the thermodynamic cycle and lower the DHN return flow temperature. This operating mode will thus be only feasible with an important temperature difference between the primary and secondary circuit. Thanks to this mode of operation the return temperature on the DHN could be lower than the return temperature on the secondary circuit.

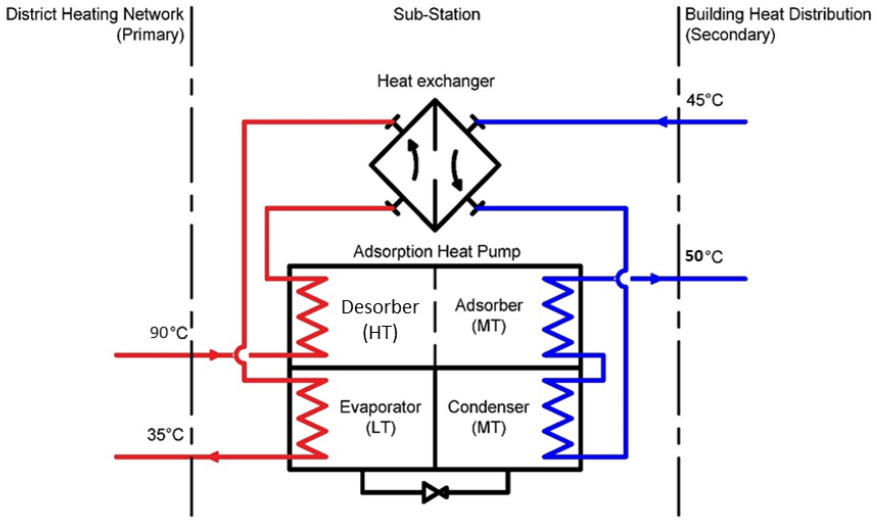

Figure 4: AdHP hydraulic integration in District Heating Network (DHN) substation in “heating” mode

The substation depicted in Figure 4 couples one regular plate heat exchanger (as found in classical substation) with an adsorption heat pump. The adHP operates according to a classical thermodynamic cycle:

1. **Heat Source (DHN):** Heat from the heat source (e.g., central boiler plant or renewable energy) supplies the desorber (HT).
2. **Desorption (HT):** In the desorber, heat induces the separation of the adsorbate (gas) from the adsorbent (solid). This endothermic reaction requires heat input.
3. **Condensation (MT):** The gaseous adsorbate then moves to the condenser (MT) or the secondary circuit (building). It releases its latent heat to the surroundings, enabling its condensation into liquid form.
4. **Expansion and Evaporation (LT):** The liquid adsorbate is expanded and sent to the evaporator (LT). The heat source, cooled a second time in a conventional exchanger, provides the energy required for the adsorbate's evaporation, preparing it for the next adsorption step.
5. **Adsorption (MT):** The gaseous adsorbate is brought into contact with the adsorbent in the adsorber (MT). This exothermic reaction releases heat, which is used for heating the secondary network.

The temperature evolution on each side of the substation incorporating an adHP is shown in Figure 5 below. On the DHN circuit, there are three successive temperature drops (red curve on Figure 5):

1. **Generator/desorber**: high temperature heat is used to desorb a refrigerant from an adsorbent.
2. **Conventional exchanger:** Cools the primary side with the heating circuit return flow below the condensation temperature of the refrigerant (necessary for proper thermodynamic operation of the adHP).
3. **Evaporator:** the refrigerant is evaporated with heat from the DHN return flow reducing the primary return temperature below the secondary return temperature.

On the other side, on the heating circuit, there are three temperature gains (blue curve on Figure 5):

1. **Conventional exchanger (HX):** the heat from the DHN is used to pre heat the heating circuit return flow (similarly to what happen in a standard substation)
2. **Condenser:** the refrigerant condensing heat is used to increase the Heat Transfer Fluid (HTF) temperature on the heating circuit side.
3. **Adsorber:** the heat of adsorption is here used to increase further the HTF temperature on the heating circuit to reach the final desired heating circuit forward temperature.

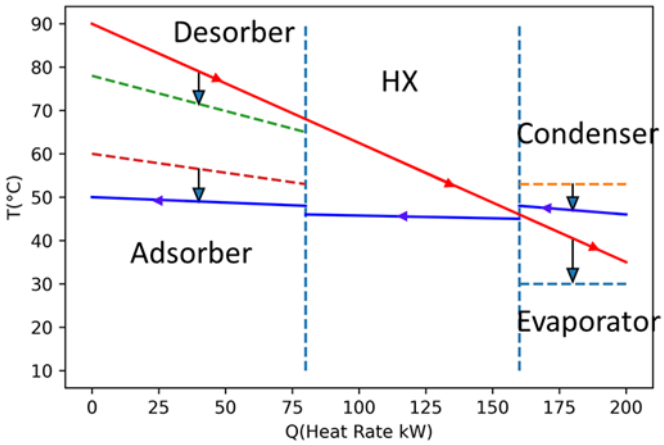

Figure 5: T-Q diagram of the substation shown in Figure 4 with a heating circuit operating with 45/50°C temperature regime and 90°C of forward temperature on the DHN

Performance

The coefficient of performance (COP) of the adHP in heating mode is around 1.5-1.8, indicating high energy efficiency. This means that the adHP can produce 1.5-1.8 units of heat for every unit of high temperature thermal energy consumed.

The new substation thermal performance can be evaluated using the concept of temperature efficiency, analogous to the analysis of classical heat exchangers. The efficiency (ε) is defined as the ratio of the potential heat gain ($T_{DHN,In}-T_{Heating,In}$) to the actual heat exchanged ($T_{DHN,In}-T_{DHN,Out}$):

$$\varepsilon = \frac{T_{DHN,In}-T_{DHN,Out}}{T_{DHN,In}-T_{Heating,In}} \qquad \text{Equation 1}$$

Figure 6 below compares the temperature profile of a standard substation with a simple heat exchanger with a substation incorporating an adHP. This figure illustrates the capacity of the adHP to cool down the DHN return flow at a temperature inferior to the secondary circuit return flow temperature.

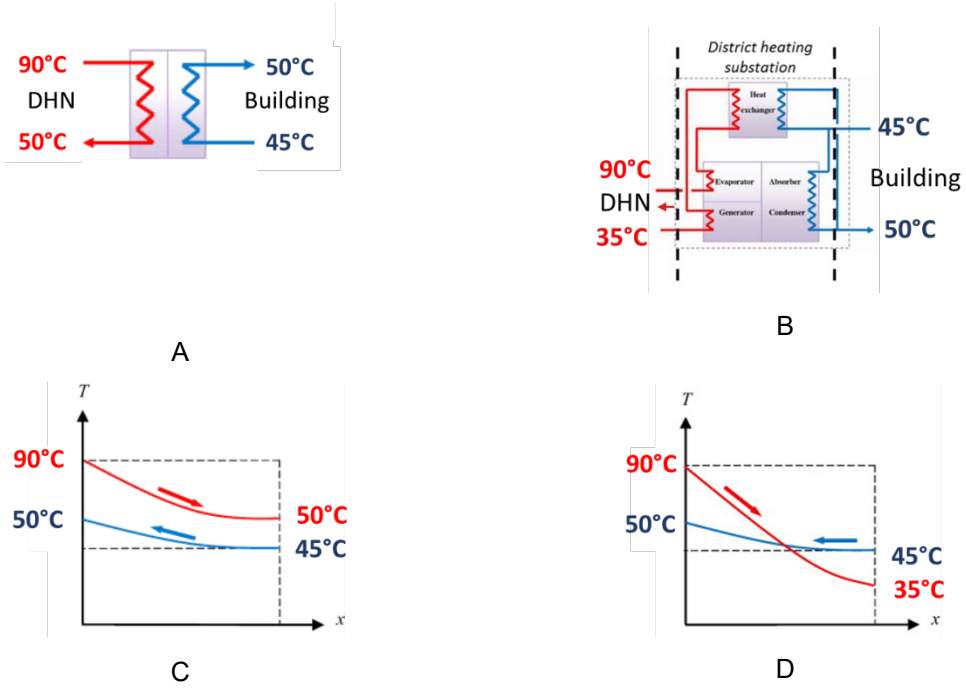

Figure 6: Hydraulic configuration and temperature profile for a standard substation substation with a plate heat exchanger (A and C) and a substation integrating an adHP (B and D)

In the example given above, the typical temperature efficiency of a standard substation is around 0.9 whereas for the substation with an adHP it is around 1.2.

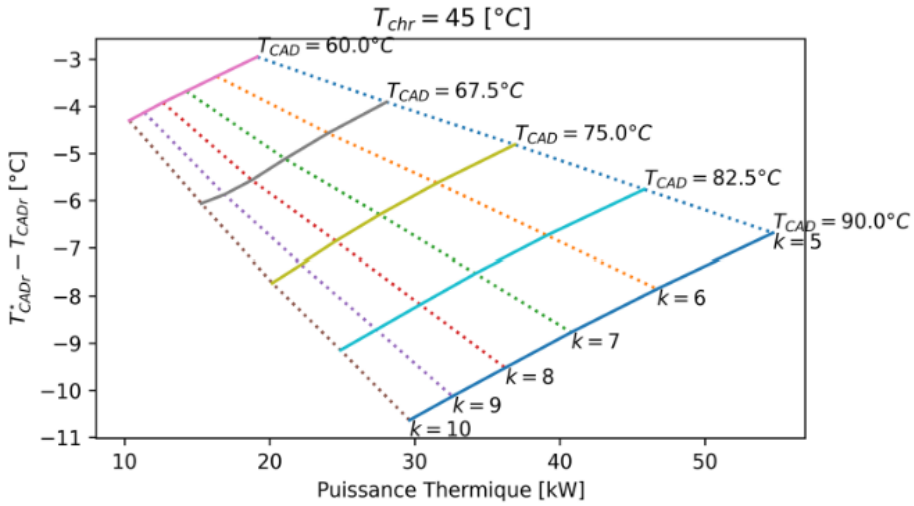

Figure 7: Temperature reduction potential ($T^*_{CADr} - T_{CADr}$) in heating mode for heating circuit return temperature of 45°C for different DHN forward temperature (T_{CAD}). k corresponds to the flowrate on the heating circuit over the flowrate on the DHN side

Figure 7 shows the potential temperature reduction on the DHN return flow for a heating circuit return temperature of 45°C, this temperature difference is calculated between the return temperature of the adHP substation and the return temperature of heat exchanger with an efficiency of 0.9 under the same

boundary conditions. This graph shows that to maximize the temperature reduction the forward DHN temperature should be as high as possible. For a typical DHN forward temperature of 90°C, the DHN temperature could be reduced up to 10°C compared to a standard substation with a plate heat exchanger.

This higher temperature efficiency of the substation incorporating adHP compared to a standard substation allows to satisfy the building heat demand with flow rate 30% lower on the DHN side. It illustrates well the advantage to use this technology for a DHN operator: with the same infrastructure, it is possible to distribute 30% more heat thanks to the adHP. This increase heat capacity distribution improves the DHN infrastructure amortization.

In addition, a temperature reduction of the return flow results often in a higher efficiency of heat production in the thermal power plant. For example, for a thermal grid using fresh wood chips boiler (moisture content up to 40%), the use of a condenser unit can increase the heat production by 20-25% for the same quantity of wood. A reduction in DHN return temperature can thus reduce significantly the wood consumption (up to 20 to 25%) and thus the heat production cost.

3.1.3 adHP in DHN substation – Cooling production mode

In the cooling mode, the adsorption heat pump integrated in the substation uses heat from the thermal grid to produce cooling (see Figure 8). The heat extracted from the building has then to be dissipated either in the environment using an aero cooler or valorized to satisfy a low temperature heat need. The heat rejection could for example be used for DHW production.

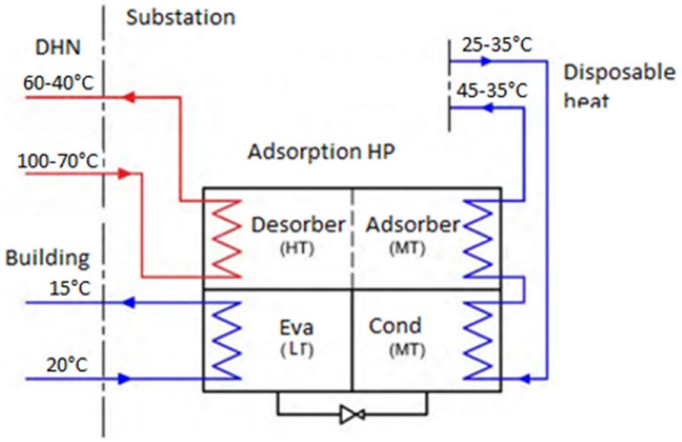

Figure 8: adHP integration in DHN substation in “cooling” mode

In cooling mode, adHP is operated as a chiller, utilizing the primary heat source (HT) from the district heating network to produce cooling energy (LT) for the building at the evaporator. The heat extracted from the building and residual heat from the work generation is dissipated to the environment through the absorber and condenser (MT).

The key components of the adHP in cooling mode are the following:

1. **Desorber (HT):** uses the heat from the DHN for the refrigerant desorption.
2. **Adsorber and Condenser (MT):** are used to evacuate heat to the environment. Alternatively, the rejected heat could be valorized locally to satisfy a medium to low temperature heat need (DHW production, …)
3. **Evaporator (LT):** absorbs heat from the building to evaporate the refrigerant at low pressure.

The cooling mode offers several important advantages:

1. **High-Temperature Heat Utilization:** Enables cooling production using high-temperature heat, which is abundant in summer and can be generated from sources like solar thermal panels or industrial waste heat.
2. **Efficient Utilization of District Heating Networks:** Consumes excess heat from DHN during summer for renewable cooling production, reducing environmental impact and improving energy efficiency.

The performance of adHP in the cooling mode is evaluated using the cooling COP (coefficient of performance) which is calculated as follow:

$$COP_{Cooling} = \frac{Q_{LT}}{Q_{HT}} \qquad Equation\ 2$$

where: Q_{LT} is the cooling energy supplied to the building and Q_{HT} the high temperature heat supplied by the DHN. In cooling mode, commercially available adHPs have COP of typically 0.6-08. The COP depends a lot on the operating temperature.

Operating an adHP in cooling mode using heat from a DHN offers several benefits:

1. **Sustainable Cooling Solution:** Provides an environmentally friendly cooling option by utilizing waste heat sources with a low electricity consumption.
2. **Enhances District Heating Network Efficiency:** Optimizes energy utilization within DHN by consuming excess heat during summer.
3. **Cost-Effective Cooling:** Offers a potentially cost-effective cooling solution compared to traditional chiller systems.

AdHPs in cooling mode present a promising technology for sustainable, efficient, and cost-effective cooling solutions, particularly in urban settings and applications involving DHN using industrial waste heat. As research and development progress, adHPs are expected to play an increasingly significant role in reducing energy consumption and environmental impact in the cooling sector.

3.1.4 Operational constraints and temperature level requirements for adHP integration in DHN

For the efficient integration of adHP in heating and cooling mode several technical and operating constraints have to be respected. In this section, those constraints are listed for the two modes of operation (cooling and heating).

Heating mode:

In heating mode, the DHN and building heating circuit temperature should respect the constraints described below. Those constraints guarantee good performances of the adHP and consequently an important reduction of the DHN return temperature compared to a standard substation with a plate heat exchanger.

The DHN forward temperature should be above the minimum desorption temperature. In case the temperature is too low, the amount of refrigerant which can be desorbed at a given pressure is too low. A typical minimum temperature is 60°C. In wintertime, most of the DHN operates at higher temperature (see Figure 9). This constraint should therefore be easily respected.

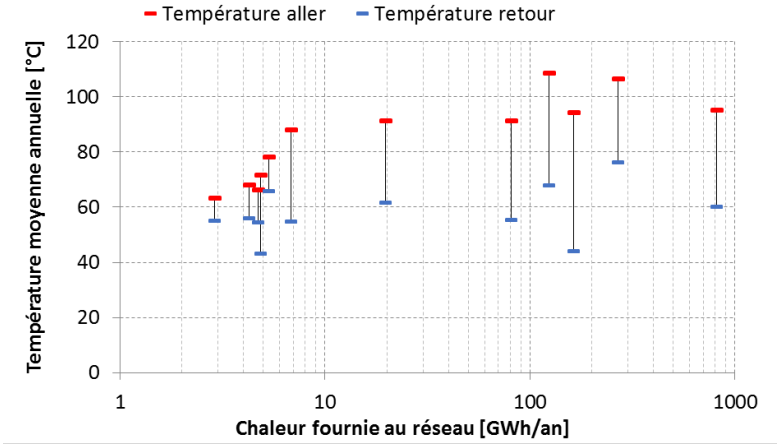

Figure 9: Forward and return temperature for different Swiss DHN as a function of the amount of heat delivered per year [Quiquerez, "Cycle de formation Energie-Environnement"]

The building heating circuit should be as low as possible in order to condense the refrigerant at low pressure. This low temperature condensation facilitates the refrigerant desorption. Too high condenser temperature limits the amount of refrigerant which is cycled between each cycle. In Geneva, one study [Quiquerez, "Températures de distribution de chauffage du parc immobilier genevois"] has shown that existing heating systems typically operate with a forward temperature ranging from 65°C at -10°C ambient temperature to 35°C at 15°C. The corresponding temperature difference varies between 10-15°C and falls below 5°C at milder ambient temperatures. (see Figure 10).

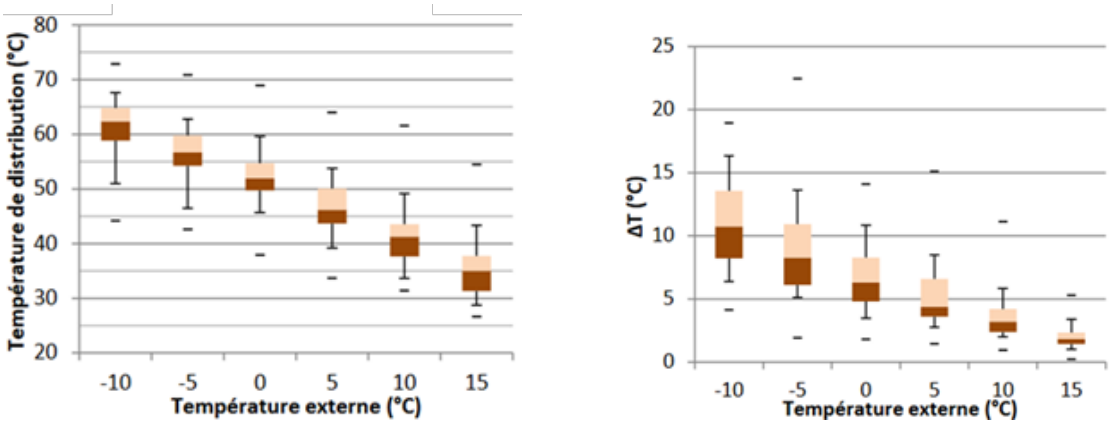

A. C.

Figure 10: Typical heating distribution system operating temperature measured over several buildings equipped with radiators in Geneva: A. heating system forward temperature as a function of ambient temperature, B. forward/return temperature difference as function of ambient temperature [Quiquerez, "Températures de distribution de chauffage du parc immobilier genevois"]

In addition, the difference between the heating system average temperature and the targeted DHN return temperature should be inferior to 20°C. And finally, the difference between the DHN forward and average heating temperature should be superior to 30°C in order to get a high COP.

The various constraints described above can be summarized with the following equations:

$$T_{DH,f} > 60°C \qquad \textit{Equation 3}$$

$$T_{SH,Avg} - T_{DH,r} < 20°C \qquad \textit{Equation 4}$$

$$T_{DH,f} - T_{SH,Avg} > 30°C \qquad \textit{Equation 5}$$

Where $T_{SH,Avg} = \frac{T_{SH,f}+T_{SH,r}}{2}$ is defined as the average temperature of the heating system, $T_{DH,f}$ and $T_{DH,r}$ are respectively the DHN forward and return temperature.

Using the equations given above, it is possible to estimate the heating system average temperature knowing the DHN forward temperature. For examples, for a DHN operating at 90°C in wintertime (typical value as shown in Figure 9), the heating system average temperature should be inferior to 60°C and the targeted DHN return temperature should be less than 40°C.

Cooling mode:

In cooling mode, the following three levels of temperature should be defined:

1. The desorber temperature: this temperature corresponds to the DHN forward temperature.
2. The adsorber and condenser temperature: this temperature corresponds to the temperature at which heat is evacuated from the building either in a cooling tower or for DHW pre heating.
3. The cooling temperature: the temperature used to cool down the building has an important impact on the COP of the adHP: the lower the temperature, the lower the COP.

In cooling mode, the temperature constraints are defined below. Those constraints guarantee good performances of the adHP and consequently an efficient conversion of DHN heat in cooling.

In order to have a sufficiently high cooling COP (>0.6), the DHN forward temperature should be above 60°C. A high COP is important because it limits the amount of DHN heat needed to produce cooling. It also limits the amount of heat to be rejected in the environment (or to be locally valorised). In addition, the DHN forward/return temperature difference at the desorber should be at least above 15°C in order to ensure that the cooling production will not reduce the DHN forward/return temperature difference. A small temperature difference results in higher cost for heat distribution (important pumping cost and higher heat losses) and limits the efficiency of heat production.

Concerning the temperature at which heat is evacuated from the building (adsorber and condenser), it has to be high enough in order to facilitate heat valorisation or dissipation. But on the other hand, it should be kept as low as possible in order to cycle enough refrigerant at each cycle: the lower the temperature, the higher the adHP cooling COP. A value below 40-45°C is typically given for commercially available adsorption chiller.

Finally, the cooling temperature should be low enough in order to efficiently extract heat from the building depending on the emission technology chosen (air handling unit, cold ceiling, …). On the other hand, it should not be too low to avoid water condensation and impeding the cooling COP. The forward cooling temperature should not be below 15°C and the return ideally around 20°C.

The temperature constraints for the cooling mode are summarized in the Figure 11 below.

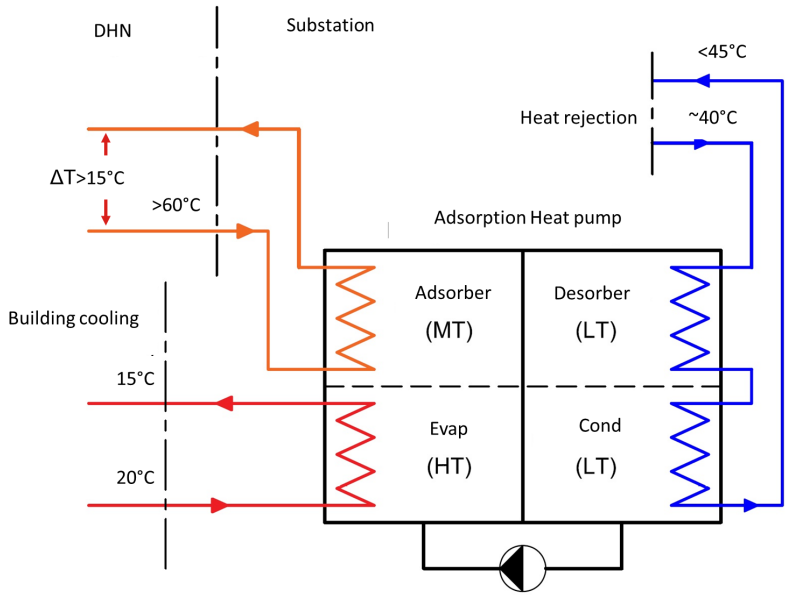

Figure 11: Summary of the temperature constraints for the cooling mode

3.1.5 AdHP integration guidelines and in DHN for the cooling and heating modes

The integration of an adsorption heat pump (adHP) into a district heating substation can significantly enhance the efficiency and sustainability of the network. In addition, it offers to the DHN operators the possibility to develop new energy services like cooling.

The most sensitive points to take into account for a successful integration in a substation are summarized below:

1. **Temperature levels:** first it is important to ensure that the temperature levels on the primary side and on the secondary side (building) respects the constraints described above. A respect of those constraints guarantees good performance of the adHP in both heating and cooling mode.
2. **Heating and cooling demand:** the adHP and the plate heat exchanger should be sized in order to satisfy the heating and cooling demand. It is therefore important to have a good estimation of the heating/cooling demand. The estimation should be based ideally on energy consumption measurements. If measurements or energy bills are not available, the estimation could also be done using SIA norms.
3. **Available volume:** adHP are relatively bulky compare to plate heat exchanger for identical thermal power. It is therefore important to make sure that the volume available in the boiler room is sufficient. For comparison, a 100kW adHP (in cooling mode) has a volume between 2 and 3m^3 [FAHRENHEIT, n.d.].
4. **Temperature difference on the primary side (DHN):** as mentioned above, for a successful integration in a DHN, it is important to ensure a forward/return temperature difference on the DHN of at least 15°C in cooling mode.
5. **DHW production:** the substation described above does not take into account DHW production. The DHW production could be realized using a dedicated heat exchanger inserted in parallel or in serial as depicted in Figure 12 below.

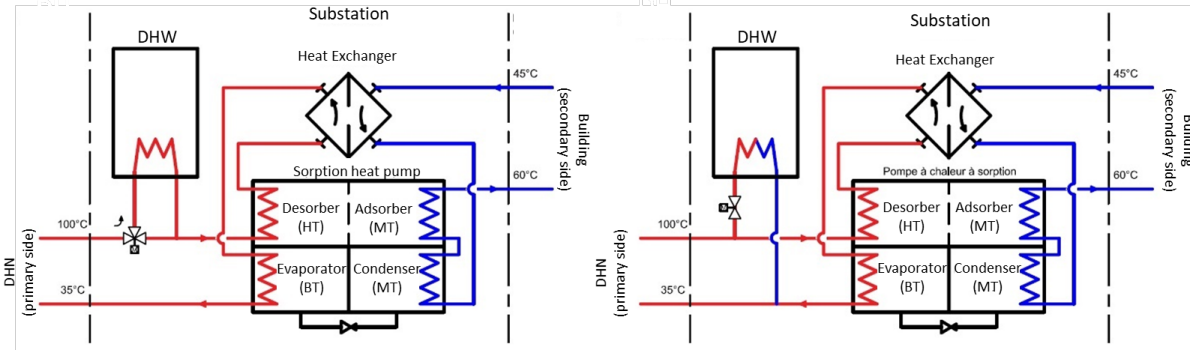

Figure 12: Two examples of possible hydraulic integration for DHW production: serial integration (left) and parallel integration (right)

Finally, in order to facilitate the amortization of the substation with an adHP, it is essential to maximize the number of hours where the adHP is operated. There are mainly two strategies to maximize the number of operating hours:

1. Reversible substation with adHP: a reversible substation can be used to reduce the DHN return temperature during the heating season and for cooling production in summer. This double functionality increases the adHP operating hours.
2. Integration of a substation with adHP between a high temperature DHN and a low temperature branch: it is more and more frequent that a low temperature DHN branch (new neighbourhood) are connected to high temperature existing DHN. Usually, the two thermal grids are hydraulically separated with a plate heat exchanger. This heat exchanger could be replaced by a substation with an adHP (sometimes called in the literature sorption Heat Exchanger). This application is very attractive for two reasons: (1) the large size of adHP needed bring important scale economy on the cost of the substation with adHP (see Figure 13 below) and (2) with this application, the adHP will be operated for longer period of time accelerating its amortization

3.1.6 AdHP cost – review of cost of commercially available adHP

It is essential to have an estimate of the cost of a substation including an adHP in order to assess and optimize the integration of this technology in an existing DHN. In particular, it is important to make sure that the financial benefits brought by this technology exceed the cost (including investment, maintenance and operating cost) of the substation. In this section, the cost of adHP as a function of its nominal power is estimated based on a literature review.

There is limited information available in the literature on the cost of commercially available adsorption heat pump. The main commercial application is cooling using either waste heat or solar heat. In order to estimate the cost of the substation including an adHP, two sources of data will be used:

1. For small adHP up to 50kW, the estimation will be based on a recent paper [AL-Hasni and Santori, „The Cost of Manufacturing Adsorption Chillers“] where a bottom-up estimation of the selling cost of a 10kW adHP have been done
2. For larger unit (above 50kW), the cost estimation will be based on a recent project [Schöpfer, „Absorption chillers”] where offers were asked to the major absorption chiller manufacturer. A cost-function has been derived from the data obtained.

In the first source of data for small adHP, the specific selling cost was evaluated to roughly 1’000€/kW or 1’000CHF/kW (with the current CHF/Euro exchange rate). This specific cost can be used to estimate the cost for adHP up to 50kW. Above, scale economy will certainly drive the specific cost down. As a comparison, a 10 kW adsorption chiller were bought in 2018 by HEIG-VD for a sum of ~17’000€ corresponding to a specific cost of 1’700€/kW.

For larger adHP, there is a lack of data. Indeed, the current market of adHP is focused on 10 kW unit and up to a maximum of 100kW. Moreover, the larger unit are often composed of smaller adHP operated in parallel. Consequently, to estimate the cost of adHP above 100kW, it has been chosen to used cost function derived for absorption chiller. In a 2015 report [Schöpfer, „Absorption chillers"], the cost function for absorption chiller from 100 to 1'000 kW were estimated based on offers obtained from 4 different manufacturers (see Figure 13).

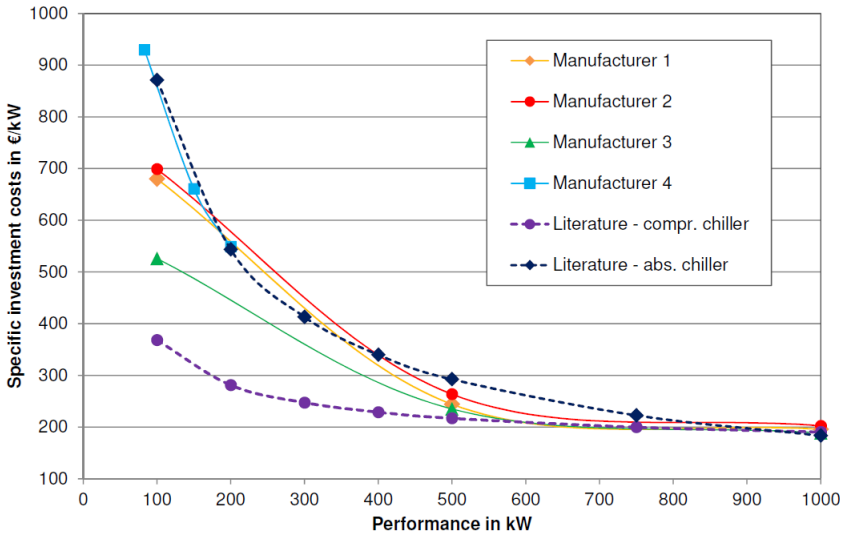

Figure 13: Specific cost of commercially available absorption chiller from 100 up to 1'000kW and comparison with cost function from the literature for absorption chiller and compression chiller [Schöpfer, „Absorption chillers"]

Figure 13 illustrates the important scale economy for sorption chiller with specific cost divided by a factor 3-4 between a 100 kW and a 1'000 kW depending on the manufacturer. A similar trend is also expected with adsorption chiller. This graph shows also that at 100kW, the specific cost varies from 500 up to almost 1'000 €/kW depending on the manufacturer. This specific cost is very close to the specific cost derived for a 10 kW adsorption chiller. Therefore, it seems reasonable to use data from absorption chiller to estimate the adHP chiller cost above 100kW. With those data, the cost a 100 kW adHP (cooling power) could be estimate between 50'000CHF up to 90'000CHF with a median value of 70'000CHF.

Using those cost function, it is possible to estimate the cost of 100kW substation including an adHP. The first step is to size the nominal thermal power of the adHP. Indeed, as depicted in Figure 4, the building heating needs are satisfied by combining heat transferred through the adHP with heat transfer through a regular heat exchanger. In a typical DHN (as shown in Figure 9), the forward/return temperature is in average 90/50°C. After the integration of an adHP, the return temperature could be reduced to 40°C (see Figure 7). So, one can estimate that roughly 20% percent of the heat is transferred to the building through the adHP corresponding to a 20kW nominal cooling power adHP. Using the recent adHP cost estimation, the cost of this 20kW adHP could be estimated to 20'360CHF. In addition, the cost of a regular substation has to be estimated. HSLU has developed an excel spreadsheet[2] to estimate the heating cost for various heat production technologies. Using this tool, the cost of 100kW has been estimated to ~15'800CHF. So in total, this substation with an adHP would cost 36'160CHF (only for the material). On top of that, the delivery and connection cost should be added. Those costs could also be estimated using the HSLU tool mentioned above to 4'300CHF and 102'000CHF. The total cost would therefore be 138'160CHF. The main cost driver is the connection cost to the DHN. Table 1 below gives a recapitulation of the cost's breakdown.

[2] Heizkostenvergleichsrechner 2.0 tools available on this website, last visit: 05.06.2024

Table 1: Cost breakdown of a 100kW substation integrating an adHP

Items	Cost [CHF]
Standard substation	15 800
adHP (20kW cooling power)	20 360
Connection fees (100kW nominal power)	102 000
TOTAl Cost	**138 160**

This substation could also be operated in cooling mode to cool the building during summertime. It is important to note that the peak cooling power, especially for older buildings with limited thermal insulation and small window surfaces, is always lower than the peak heating power, even when accounting for the effects of global warming [Silva u. a., „Opportunities for Passive Cooling to Mitigate the Impact of Climate Change in Switzerland“].

For a typical existing multi-family building, the annual heating needs are in the range of 100-200 kWh/m² (including domestic hot water) [Streicher u. a., „Analysis of Space Heating Demand in the Swiss Residential Building Stock“.], corresponding to a peak thermal demand of 40-70 W/m² (estimated with 2,700 equivalent full load hours). In contrast, for the same type of building, the cooling demand is estimated to be between 10-20 kWh/m², with a peak cooling demand of 10-20 W/m² under the RCP4.5 scenario (median scenario) [Kapeller u. a., „The Effects of Climate Change-Induced Cooling Demand on Power Grids“.].

Those data indicate that the sizing of the adsorption heat pump (adHP) in heating mode is consistent with the cooling needs of existing buildings constructed before 2000. In heating mode, approximately 20-25% of the heat is transferred to the building by the adHP. For these buildings, the peak cooling demand is at most one-third of the peak heating demand. Consequently, the same substation with an [adHP could be used reversibly to lower the district heating network (DHN) return temperature during the heating season and to meet cooling needs in the summertime.

For more recent buildings (constructed after 2000), the heating and cooling needs are more balanced in terms of energy. These buildings have annual heating needs of 60-80 kWh/m². For the same category of buildings, cooling needs are estimated to be around 30-35 kWh/m² under the RCP4.5 scenario. In terms of thermal power, the peak cooling power can even exceed the peak heating power. The peak heating power for recent buildings is around 20-30 W/m², whereas the peak cooling power is around 40-60 W/m². For this category, cooling needs and peak power could be significantly reduced by combining night ventilation with window shading [Silva u. a., „Opportunities for Passive Cooling to Mitigate the Impact of Climate Change in Switzerland“].

3.1.7 Hydraulic integration

In this section, the hydraulic integration of a substation integrating an adHP is given for the two modes of operation described above. As mentioned above, in order to maximize the number of operating hours of the adHP, a hydraulic concept allowing to operate the adHP in a reversible way has also been defined. This hydraulic concept gives the possibility to operate the adHP for cooling application in summertime and to reduce the thermal grid return temperature during the heating season.

A possible hydraulic integration **for the heating mode** is given below in Figure 14. This hydraulic scheme is particularly adapted to replace a standard plate heat exchanger between a large high temperature DHN and a low temperature branch (for example for a new neighbourhood with high energy efficiency building).

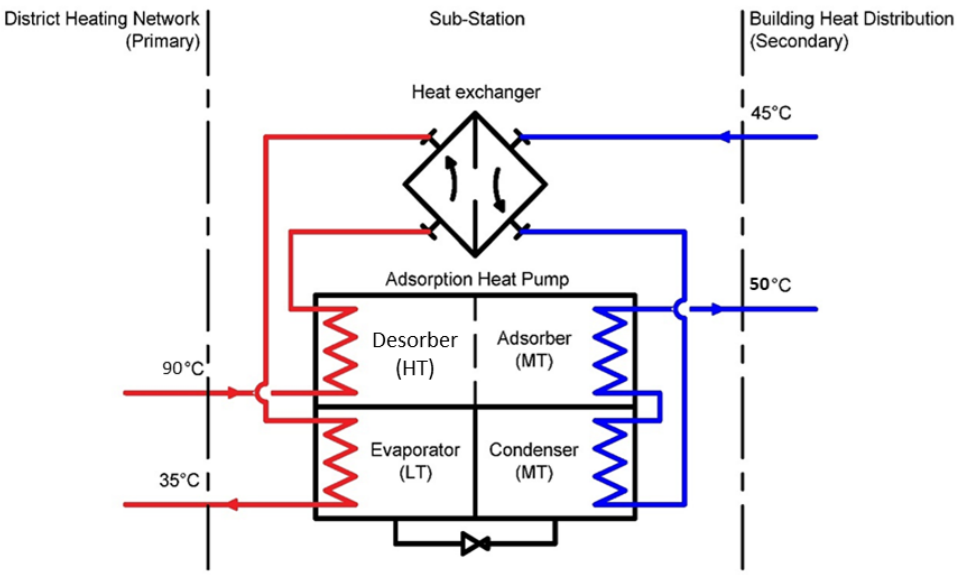

Figure 14: Hydraulic integration of a substation incorporating an adHP in “heating mode”

This type of integration is particularly interesting since the adHP in the substation could be operated outside the heating season (providing that the temperature difference between the high temperature DHN and the low temperature branch respect the constraints described above). As discussed above, a substation integrating an adHP requires important initial investment. To accelerate its financial amortization, it is important to increase its operation time per year as much as possible. This kind of configuration have been called sorption heat exchanger in the literature. It has already been successfully experienced on a large scale in China for waste heat transfer over long distance (Zhang, Yi, and Xie, 2022).

As mentioned above, in order to lower the cost of cooling, it is important to avoid using an aero cooler to dissipate heat from the building outside.

Consequently, a possible hydraulic integration for cooling shown in Figure 15 A have been proposed where the heat extracted from the building is used for DHW preheating. Figure 15 B presents an alternative hydraulic configuration where the heat evacuated from the building is used as heat source by a compression heat pump for DHW production. The main disadvantage of this kind of integration is that the cooling production potential is limited by the amount of DHW consumed by the building.

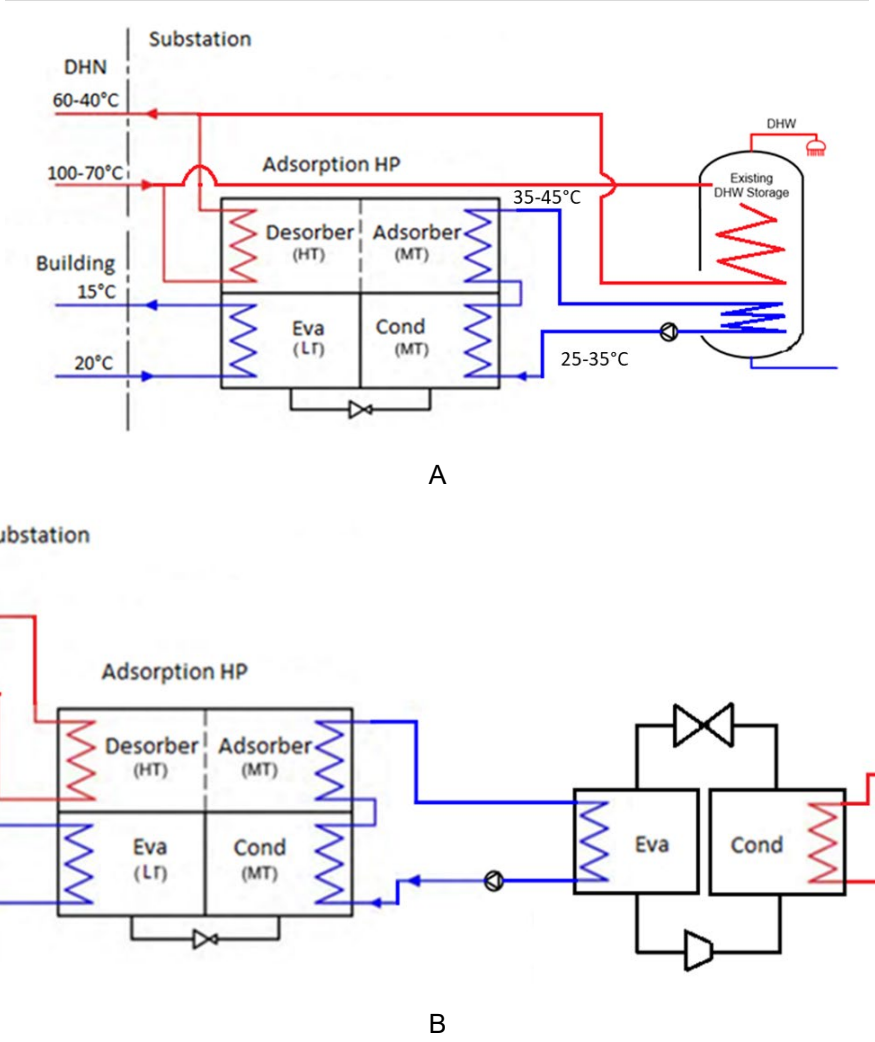

Figure 15: Hydraulic integration for the “cooling mode” with A. direct valorisation of the extracted heat for DHW preheating and B. valorisation of extracted heat through a compression heat pump for DHW production.

3.2 System performance simulation (WP2)

This section describes the results of the numerical modelling of an adsorption heat pump integrating the newly developed materials and the performance simulation. An existing adsorption heat pump model, TRNSYS type 820, was first modified to consider the new adsorption materials developed within the THRIVE and Characsorb projects, i.e., the activated carbon monolith (RMFAC). The modified model was then calibrated and validated against experimental measurements realized in the SPF test bench with the aged 1st generation RMFAC sorbent. The calibrated model has been used to map the performance of a substation integrating an AdHP in temperature return reduction mode. The results of the performance evaluation of the aged materiel was then compared to the 3rd generation materiel.

3.2.1 Modification of the TRNSYS Type 820

The original adsorption heat pump model type 820 was developed to work with adsorbent like silica gel or zeolite. To calculate the performance of an AdHP with the new material, new adsorption equilibriums

equation needed to be programmed from the correlation developed by EMPA in WP4. These take a hysteresis into account; thus, two set of equations/parameters are needed:

For adsorption:

$$w_{ad} = W_{0,1} \cdot \exp\left(-(F/C_1)^{n_1}\right) + W_{0,2} \cdot \exp\left(-(F/C_2)^{n_2}\right) \qquad \textit{Equation 6}$$

$$F = \frac{R \cdot T}{M} \ln\left(p/p_{\text{sat}}\right) \qquad \textit{Equation 7}$$

For desorption:

$$w_{de} = W_{0,1} \cdot \exp\left(-\left(\frac{F}{C_1+\Delta C_1}\right)^{n_1+\Delta n_1}\right) + W_{0,2} \cdot \exp\left(-\left(\frac{F}{C_2+\Delta C_2}\right)^{n_2+\Delta n_2}\right) \qquad \textit{Equation 8}$$

With parameters given in Table 2:

Table 2: water adsorption model fitted parameters for 1st generation RMFAC.

Code	$W_{0,1}$ $[g_w/g]$	C_1 $[J/g]$	$\Delta C1$ $[J/g]$	n_1 $[-]$	$\Delta n1$ $[-]$	$W_0 2$ $[g_w/g]$	$C2$ $[\,J/g]$	$\Delta C2$ $[J/g]$	$n2$ $[-]$	$\Delta n2$ $[-]$
RMFAC 1st gen	0.25	150	-	6.2	1.4	0.12	210	21	1.5	6.6-0.02T

No hysteresis effect was implemented in the model because of the extensive programming work required to carry out the task.

3.2.2 Model calibration and validation

Fit and validation of uncertain parameters were carried out on experimental data provided by SPF (WP3):

- The fit and validation is carried out only for the desorption phase. This is explained by the fact that type 820 is a two chambers heat pump model in contrast to the test object which is a one chamber system. Experimental conditions in the adsorption phase are not reproducible with type 820.
- 2 half-cycles were investigated under the same boundary conditions from a data set comprising of 8 half-cycles, 4 desorption cycle (cycle 2, 4, 6, 8) and 4 adsorptions (cycles 1, 3, 5,7). The first 2 half cycles are discarded from the analysis and serve the purpose of initialising the simulation.
- 3 uncertain parameters were fitted, overall heat transfer coefficient of the HMX (UA_{ads}), coefficient of diffusion (D_{s0}), adsorbent mass (m_{ads}).
- 3 physical variables were considered for the fitting of the parameter and validation:
    - Adsorber outlet temperature and desorber outlet temperature at 1 s time interval.
    - Cycled mass of water during a half cycle.
- This generation of HMX have 35% of monolith that show damages (cracks), and delamination of the monolith from the copper fins.

Fit of the parameter was carried out with a sensitivity analysis of the uncertain parameters. Validation is assumed with the best fitted parameters. Parametric runs are defined by the combination of the values given in Table 3: The total simulation runs account to 27.

Table 3: values chosen for the sensitivity analysis.

Parameters	D_s0 [m^2/s]	UA_{ads} [W/K]	m_{ads} [kg]
Values	2.90e-3	5	0.406
	2.90e-4	10	0.264
	2.90e-5	20	0.203

To evaluate the results several indicators listed in Table 4 are used and computed mostly with the sklearn.metrics python library.

Table 4: indicator description.

Indicator	Description	Computation method
r2	coefficient of determination	with sklearn.metrics.r2_score
RMSE	root mean square error	with sklearn.metrics.mean_square_error
MAPE	Mean absolute percentage error	With sklearn.metrics. mean_absolute_percentage_error
CvRMSE	coefficient of variation of the RMSE	according to : $cvRMSE = RMSE/\bar{y}$, with $\bar{y}$ mean value of the experimental quantities
APE	absolute percentage error	according to the Percentage Error: $PE = \|y - \hat{y}\|/y$, with y the experimental quantities and $\hat{y}$ the simulation quantities

Sensitivity analysis for desorption phase

Figure 16 shows the experimental outlet temperature of the desorber (solid line) and all the ones from the simulation's runs (dotted lines) during one half cycle (cycle 4). We see that for most the simulations results, the desorber outlet temperatures profile and values fit well to the experimental data for most of the parameter sets.

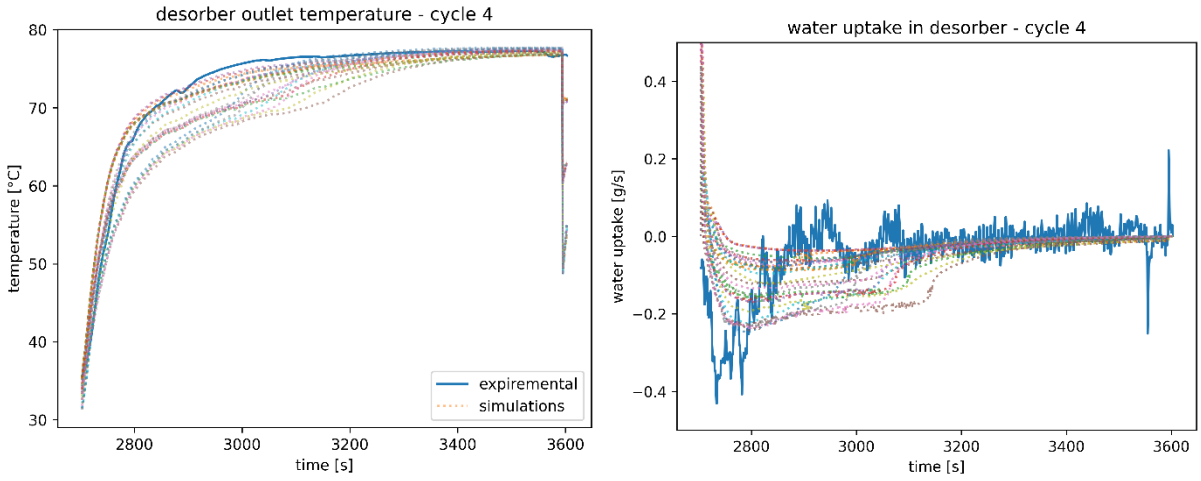

Figure 16: left: experimental (solid line) and simulated (dotted line) profiles of the desorber outlet temperature during cycle 4 ; right ; experimental (solid line) and simulated (dotted line) profiles of the water uptake during desorption

For the water uptake rate, the simulation initially underestimates the uptake rate during the early stages of desorption and subsequently overestimates it (see Figure 17). Achieving a balance between accurately representing the dynamic profile and the total mass of water desorbed during the cycle proved challenging, as suitable parameters for both aspects could not be identified simultaneously. A trade-off was therefore necessary, and priority was given to accurately representing the total cycle mass. This decision aligns with the project's focus on evaluating annual performance for various applications, where the precision of intra-cycle dynamics is of secondary importance.

In TRNSYS, a simplified 0D model was chosen to reduce computational complexity and input parameter requirements. While this approach sacrifices some accuracy in capturing the detailed adsorption and desorption dynamics, it ensures reliable predictions of the total refrigerant mass cycled. This trade-off is critical for the CharacSorb project, as the cycled refrigerant directly corresponds to the energy absorbed or delivered by the adsorption heat pump (adHP).

Given the project's objectives, prioritizing model simplicity over detailed dynamic accuracy enables efficient simulations while maintaining the capability to evaluate the thermal energy absorbed and released by the adHP for each application. This balance between model complexity and accuracy is essential to effectively address the needs of the project.

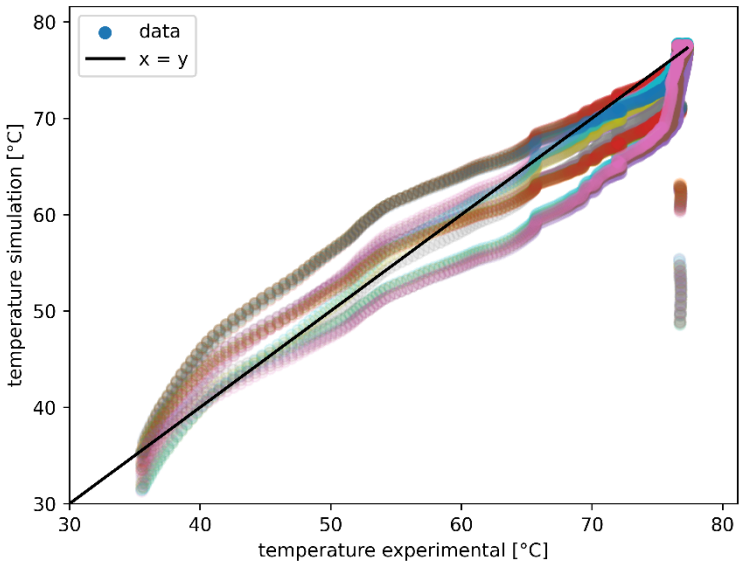

Figure 17: Experimental versus simulated outlet desorber temperature comparison

Based on the lowest percentage error on the cycle water mass, Table 5 shows the 3 best parameter sets of cycle 4 and of cycle 6. It shows that error of the mass of cycled water is lower than 15%. In addition, indicators for the desorber outlet temperature stay within the same range with satisfying values above 0.9 for coefficient of determination (r^2) and under 5% for the cvRMSE and MAPE. The merit order for cycle 4 and 6 is not the same between run 22 and 26. However, run 22 shows significant better results in cycle 4 compared to run 26. Thus, parameters from run 22 should be taken.

Table 5: indicator evaluation of the simulation results for the 3 best parameter sets according to the percentage error of the mass of water cycled.

					water cycled	Desorber outlet temperature			
		Ds0	UAads	mads	PE	r2	RMSE	MAPE	cvRMSE
		m²/s	w/K	kg	%	-	°C	%	%
cycle 4	Run 22	2.90E-05	10	0.406	1.9%	0.91	2.37	2.5%	3.2%
	Run 26	2.90E-05	20	0.264	11.3%	0.88	2.80	1.8%	3.8%
	Run 15	2.90E-04	10	0.203	13.4%	0.87	2.91	2.8%	4.0%
cycle 6	Run 26	2.90E-05	20	0.264	3.4%	0.88	3.11	2.1%	4.3%
	Run 22	2.90E-05	10	0.406	3.5%	0.91	2.65	2.8%	3.6%
	Run 23	2.90E-05	10	0.264	14.5%	0.93	2.29	2.2%	3.1%

Based on these results, the model is considered validated, with the parameter set of run 22. Figure 18, shows the corresponding profile of the parameter set of run 22 against the experimental results.

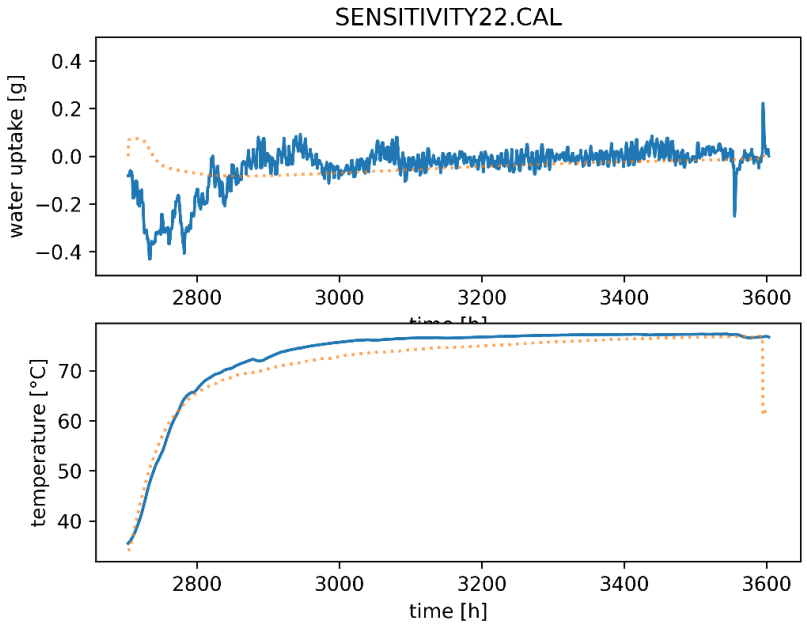

Figure 18: top: water uptake profile for cycle 4, experimental data (solid line) and simulation from run 22 (dotted line); bottom: desorber outlet temperature profile for cycle 4, experimental data (solid line) and simulation from run 22 (dotted line)

3.2.3 Performance mapping in heating mode (DH temperature reduction)

Figure 19 represents the TRNSYS model used for the performance mapping of an active substation integrating an AdHP for DHN return temperature reduction. This design and model were developed during the PACs-CAD project (“Sorption heat pump to improve DHN efficiency”, [“PACs-CAD – Interreg France-Suisse,” 2024]).

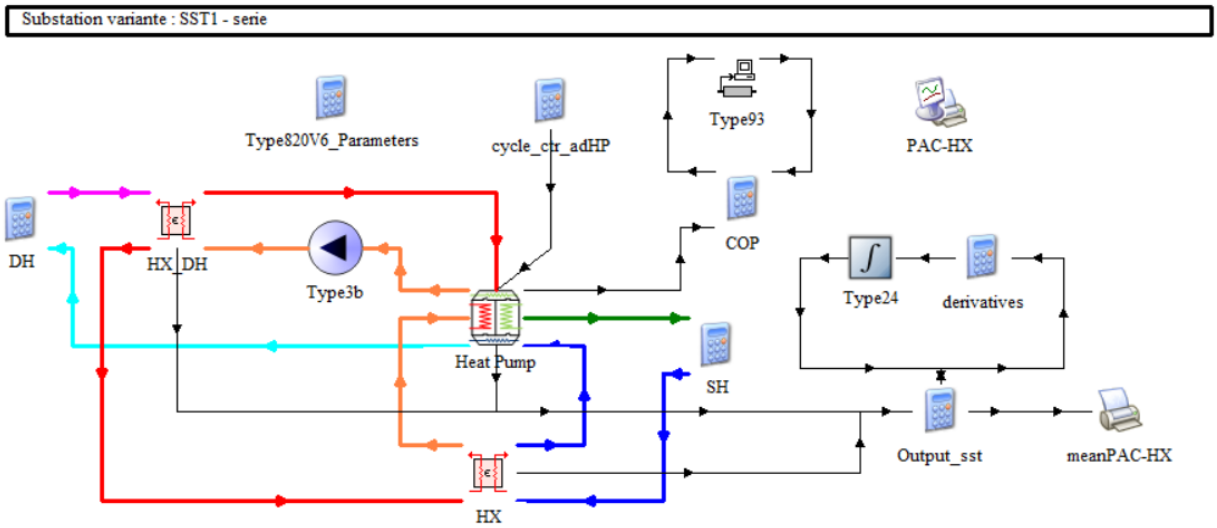

Figure 19: screenshot of the TRNSYS model for the performance mapping in heating mode.

Nonspecific parameters for type 820 were extrapolated from the values found during the fitting process for the adsorber and desorber, i.e., UA_{ads} and m_{sg}. The scaling factor was found to be 50 in order to

obtain heat flow rates close to the reference commercially available AdHP, the Fahrenheit eCoo 10. Parameters values for the evaporator and condenser are considered equal to the ones of the Fahrenheit eCoo 10 machine. Table 6 presents the parameters values of the test sample and of the scaled version.

Table 6: Comparison table between test sample and 10 kW scaled version of the fitted parameter of type 820

	Ds0 **m²/s**	**UAads** **w/K**	**mads** **kg**
Test sample	2.90E-05	10	0.406
Scaled to ~10 kW (x 50)	2.9E-05	500	20.3

The mapping of the performance was realized by varying the following 3 main inputs:

- The DH supply temperature: T_{DHi}
- The SH return temperature: T_{SHo}
- The flow rate ratio between the DH side and SH side: k (a ratio of 10 indicates that the secondary flowrate is 10 times higher than the primary flowrate)

From the results, performance indicators can be calculated. It was chosen to use the temperature reduction potential compared to a reference substation. This substation is defined as normal heat exchanger with an efficiency ε_{ref} of 0.9 that provide the exact same service on the secondary side. Therefore, the DHN return temperature can be calculated for the same transferred thermal power, and given space heating return temperature T_{SHo}, supplied DH temperature T_{DHi}:

$$T_{DHo,ref} = T_{DHi} - \varepsilon_{ref} \cdot (T_{DHi} - T_{SHo}) \qquad \textit{Equation 9}$$

The temperature reduction potential is then computed with the simulated return temperature of the active substation T_{DHo} as $T_{DHo,ref} - T_{DHo}$

Figure 20 compares the results obtained with the CharacSorb adsorbent with the results obtained with the Fahrenheit eCoo 10 AdHP (from PACs-CAD project). Results show the power range is very similar. However, the eCoo 10 (PACs-CAD) obtains better results in terms of temperature reduction potential. In number, Characsorb has a maximum temperature reduction potential of -12°C (for k=10 and T_{DH} = 90°C) whereas PACs-CAD is close to -16°C. The results are promising knowing that 35% of the HMX has visible damage.

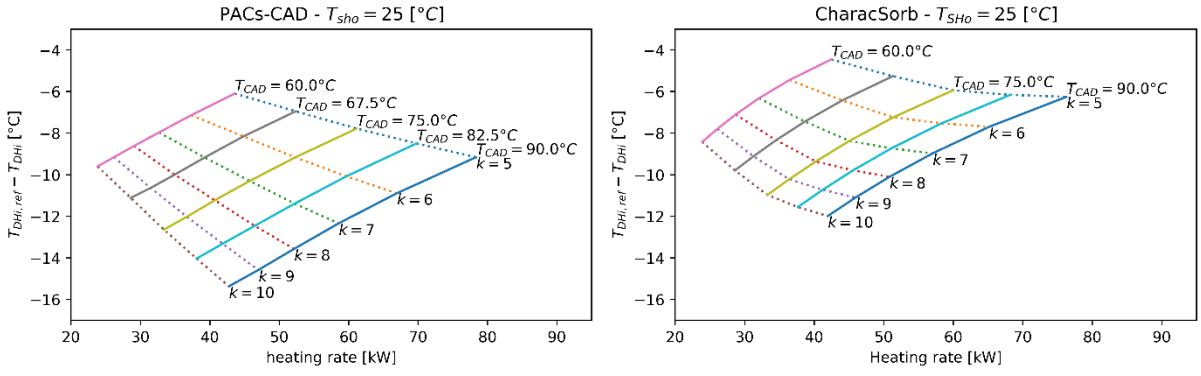

Figure 20: Comparison of results of the new CharacSorb results concerning the 1st generation HMX and aged 1st generation RMFAC (right) with results from PACs-CAD (left) for an SH return temperature of 25°C.

3.2.4 Performance mapping in cooling mode

This section details the performance mapping process of the adHP in cooling mode, focusing on the different generations of sorbent and heat and mass exchangers (HMX) developed and tested in this project. The analysis was conducted using dynamic simulations based on equilibrium data of the activated carbon (AC) sorbents and UA values of the HMX. Different generation of AC sorbent and HMX were evaluated:

1. First-Generation Sorbent and HMX:

The cooling performance of the first-generation HMX paired with the first-generation AC sorbent was evaluated using equilibrium data and experimental measurements of the HMX. Additionally, a sensitivity analysis was performed to assess the impact of variations in the UA value on the system's performance.

2. Second-Generation Sorbent and HMX:

The cooling performance of the second generation HMX, paired with the optimized second-generation AC sorbent, was subsequently evaluated. This step aimed to quantify the improvements achieved with the latest materials and design innovations.

Performance mapping was performed following the method outlined in Jobard et al. (2020) and is summarized as follows:

1. **Carnot COP for Cooling:** The Carnot coefficient of performance (COP) for cooling, $Carnot_c$, is calculated as a function of the operative temperature triplet of the adHP:

$$Carnot_c \equiv Q_{LT}/Q_{HT} = \left(\frac{1}{T_{MT}} - \frac{1}{T_{HT}}\right)/\left(\frac{1}{T_{LT}} - \frac{1}{T_{MT}}\right) \qquad \textit{Equation 10}$$

   This represents the ideal performance of adHP devices under given conditions.

2. **Cooling Technical Efficiency:** To account for irreversibilities and non-idealities in real-world devices, the cooling technical efficiency, η_{tech_c}, is introduced as the ratio of the actual COP to the Carnot COP:

$$\eta_{tech_c} = COP_c/Carnot_c \qquad \textit{Equation 11}$$

The mapping process involved varying the inlet temperatures of the adHP and the UA value of the HMX to evaluate potential improvements in the HMX design. A summary of the values used in the analysis is provided in Table 7. The inlet temperature to the evaporator is set constant to 18°C as well as the half cycle time to 640 s.

Table 7: Parameters' values chosen for the performance mapping in cooling operation

Parameters	UA of the HMX [W/K]	Temperature inlet of the absorber condenser [°C]	Temperature supply from the DH [°C]
Values	500	30	70
	1500	35	80.0
	3000	40	90.0

This section presents the performances of the 1st generation HMX constructed with the 1st generation AC sorbent. The sorbent has aged prematurely due to inadequate storage and the monolith of the HMX showed visible cracks on 35% of the HMX surface.

Figure 21 shows the variation of the COP in function of the Carnot COP. The better the UA is the better the COP is. Except for high Carnot COP values where the difference is less noticeable. Moreover, only small differences are seen between 1500 and 3000 W/K. Even though the highest COP is obtained for the highest UA value with a value 0.37, the maximum COP with 1500 W/K is 0.354 (4% less).

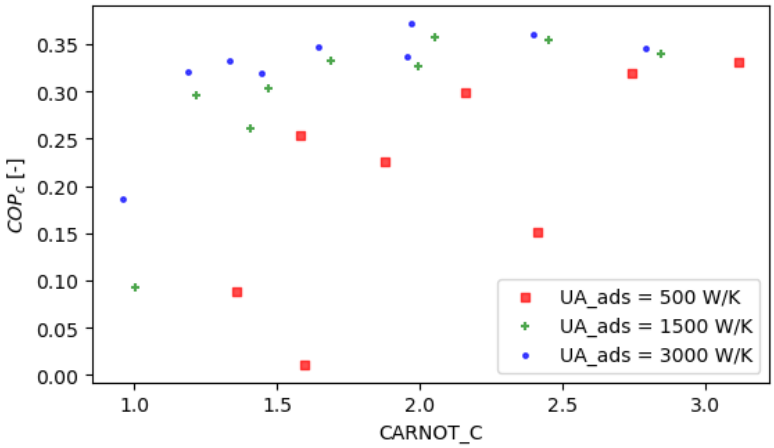

Figure 21: Evolution of the cooling COP COP_c as a function of the Carnot COP ($CARNOT_c$) for the performance mapping of the 1st generation HMX with the 1st generation of AC Sorbent.

To evaluate the performance of the newly developed sorbent material, Figure 22 compares the technical efficiency of the adHP across multiple datasets: (1) literature values from Demir et al. (2008), Meunier (2013), and Wang et al. (2007); (2) predictions from a thermodynamic model developed by Sharonov and Aristov; and (3) experimental results from the eCoo10 system reported by Jobard et al. (2020), alongside the performance mapping results for the considered HMX and sorbent material. The analysis reveals that the performance of the new development falls within the lower range of the literature values and aligns with the experimental data presented in Jobard et al. (2020).

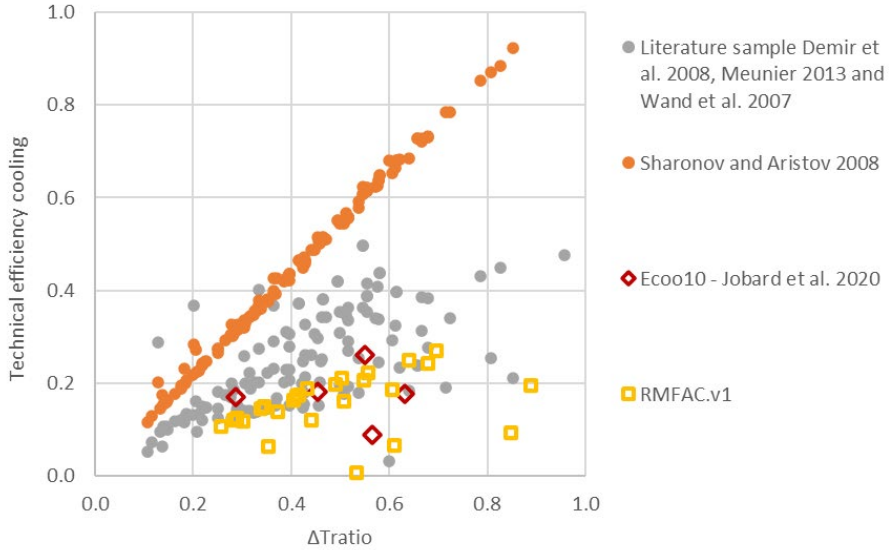

Figure 22: Comparison of the technical efficiencies of the new 1st generation AC sorbent and HMX with data from the literature.

To evaluate the performance of the latest generation of sorbent material developed by EMPA within the project (WP4) and HMX, the sorbent equilibrium parameters were implemented in TRNSYS, and the performance mapping was conducted using the same methodology described above. The results, presented in Figure 23, indicate no significant improvement in performance compared to the first-generation sorbent. The maximum COP remains unchanged, with a value of approximately 0.37.

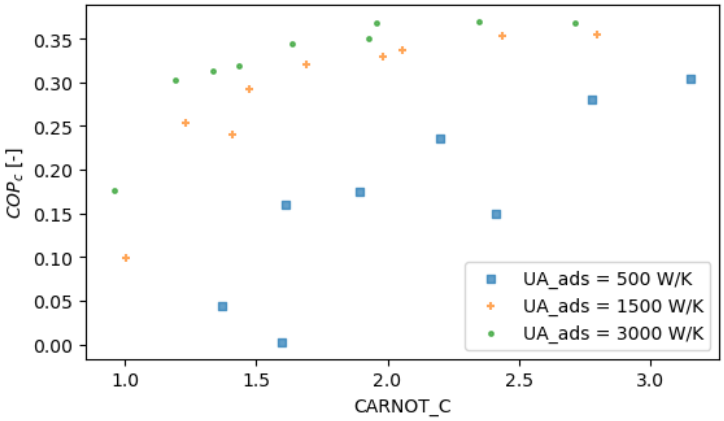

Figure 23: Evolution of the cooling COP COP_c as a function of the Carnot COP ($CARNOT_c$) for the performance mapping of the 2nd generation HMX with the 2nd generation of AC Sorbent.

3.2.5 Case studies for temperature reduction mode

To evaluate the performance of the substation for the temperature reduction mode, a case study was carried based on the eco-district “Les Vergers” in Meyrin (GE), see Figure 24. This is an ambitious district heating project, aligned with the Geneva cantonal objectives, includes 1,350 housing units and various public facilities spread across 33 high energy standard buildings, all certified Minergie A or P. Each building consumes heat for heating and hot water via a low-temperature district heating network and produces electricity with rooftop photovoltaic panels. Part of the electricity produced is self-consumed on-site, and the rest is fed into the power grid. The district heating network is mainly powered by a 5 MWth hydrothermal heat pump, the most powerful in the canton, supplemented by the high-temperature CADSIG network (71% from natural gas combustion and 29% renewable heat). Therefore, the district heating network in Les Vergers is almost entirely based on renewable resources. In 2019/2020, 82% of the heat distributed on this DHN was generated by the HP. The remaining 18% were supplied by the CADSIG DHN [Schneider et al., 2020].

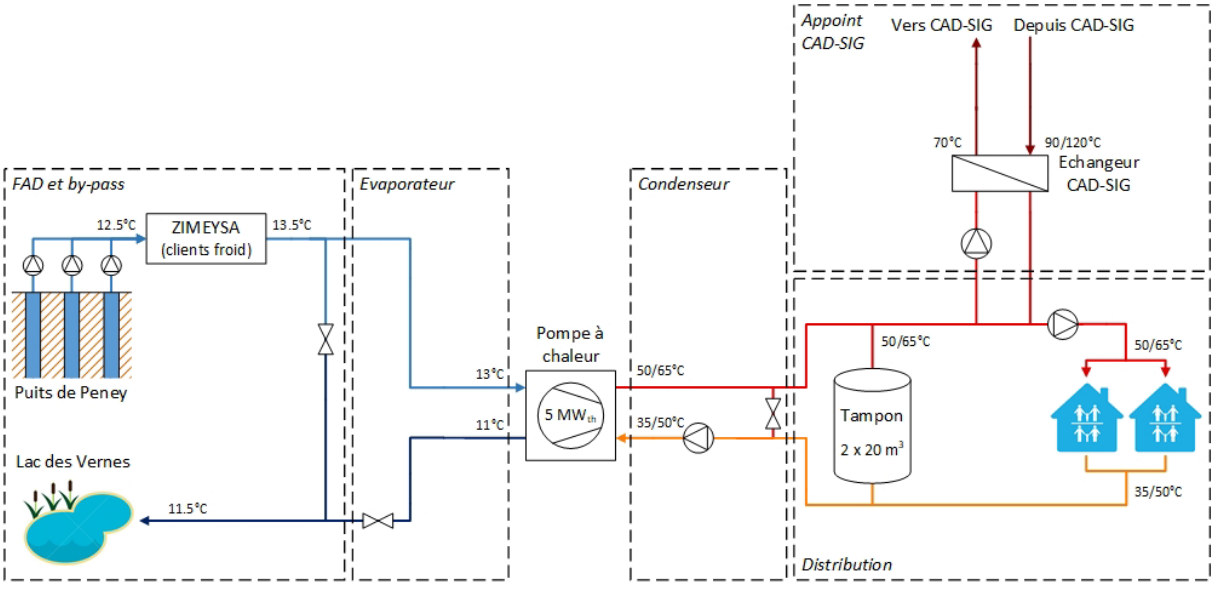

Figure 24 : Energy concept representation of the eco-district “ les Vergers” in Meyrin [Schneider et al., 2020].

The objectives of the case study:

- Evaluate the reduction potential of the return pipe temperature.
- Estimate the economic benefits of the novel concept

To carry out the work, the monitoring data provided by the group « systèmes énergétiques » of the University of Geneva are used to define the boundary condition in terms of the network forward and return temperatures as well as the volumetric flow rate. The data is available for 1 year from the July 1st, 2021, to June 30th 2022 at a timestep of 10 minutes.

Modelling method :

To evaluate the performances of the system, a performance map model of the substation developed within the PACs-CAD project was used[3]. This model is based on calibrated simulations of an experimental substation integrating a Fahrenheit eCoo 10 adsorption heat-pump. The model calculates the return temperature of the primary network for a given set of three parameters:

- the required heating power
- district heating supply temperature
- return temperature of the secondary network

The district heating supply temperature is taken constant at 90°C as it is the maximum operating temperature of the sorption substation model. The required power and return temperature of the secondary network is defined according to the hourly average of the monitoring data. The district operates at low temperatures (50°C) when only space heating is needed, and the domestic hot water is produced during specific hours of the day in batch mode, the forward temperature is then set to 65°C. In the latter case, the return temperature is most of the time outside the validity domain of the model given from 25 to 45°C. In these periods the substation is assumed to work as a regular heat exchanger with a pinch of 5K.

Reference case:

To compare the results, a reference substation is defined as a simple heat exchanger with a temperature pinch of 5K.

$$T_{PDHre} = T_{SDHre} + 5\ K \qquad \textit{Equation 12}$$

Performance indicators:

Power weighted return temperature : $\bar{T}_{PDHre} = \frac{\sum_t (T_{PDHre}(t) * P_{DH}(t))}{\sum_t P_{DH}(t)}$ *Equation 13*

Total specific volume flow : $\dot{V}_{spe} = \frac{\sum_t \dot{V}(t)}{\sum_t P_{DH}(t)}$ *Equation 14*

Average temperature difference : $\Delta\bar{T}_{PDH} = \frac{\sum_t (T_{PDHfo}(t) - T_{PDHre}(t))}{\sum_t dt}$ *Equation 15*

[3] This choice was made because the calibration of the model for the new sorbent did not show significant improvement in terms of performances.

Cost hypothesis and evaluation method

To evaluate the financial benefits of the installation of the substation, the payback period of the project is calculated considering only the over-cost linked to the installation of the sorption heat pump. Cost for general valves, controls and pumps are assumed of the same order as the CAPEX for a regular transfer station.

Table 8: Over-cost hypothesis for the adsorption heat pump with consideration of a scale effect factor.

Description	Value	Unit	Reference
kW cost for adHP	1000	CHF/kW	adHP up to 50kW [1]
Scale effect factor for adHP > 1MW	0.29	-	reduction based on absortion chiller cost [2]
kW cost for adHP for adhp > 1 MW	290	CHF/kW	

Table 8 present the considered specific cost for the adHP and taken from section 3.1.6. A scale effect factor of 0.29 is derived from observation on the absorption chiller market to determine the cost for adHP larger than 1 MW from cost of smaller units.

To assess the financial benefits of each degree of temperature reduction on the return pipe, we examine the cost reduction gradients (CRG). The CRG measures the savings on the levelized cost of heat for each degree of temperature reduction for a given heat supply technology. Table 9 presents the CRG values introduced and compiled in studies by Geyer et al. (2021) and Averfalk et al. (2021). To convert euros to swiss francs, an exchange of 1 is considered.

Table 9: Overview of assessed economic effects, indicated with the cost reduction gradient (CRG) in euro/(MWh.°C), of reduced system temperatures. Source : Averfalk et al. (2021).

Chapter section and the assessed heat supply technology, either by itself or dominating in a system	CRG in euro/(MWh·°C)	
	Investment cases when investment costs are reduced	Existing cases when operating costs are reduced
2.1 Low-temperature geothermal heat	0.45 – 0.74	0.67 – 0.68
2.2 Heat pump	0.41	0.63 – 0.67
2.3 Low-temperature waste heat	0.65	0.51
2.4 Solar thermal – flat plate collectors	0.35 – 0.75	Not available
2.4 Solar thermal – evacuated tube collectors	0.26	Not available
2.5 Biomass-boiler with flue gas condensation	Not available	0.10 – 0.13
2.6 Biomass-CHP with back-pressure turbine	Not available	0.10 – 0.16
2.6 Biomass-CHP with extraction turbine	Not available	0.09
2.6 Waste-CHP with flue gas condensation	Not available	0.07
2.7 Daily storage as tank thermal storage	0.01	0.07
2.7 Seasonal storage as pit thermal storage	0.07	0.07
2.8 Heat distribution losses	Not available	0 – 0.13

The savings induced by the adHP is then calculated with the following equation:

$$Yearly\ Savings = CRG \cdot (\Delta T_{red}) \cdot Q \qquad \textit{Equation 16}$$

With

- $Yearly\ Savings$: the yearly savings of the temperature reduction measure in CHF/y
- CRG: cost reduction gradient in or CHF/(MWh.°C)
- ΔT_{red}: Temperature reduction after application of the measure in °C
- Q : Yearly amount of heat supplied in MWh/y

The payback period is then obtained by the following equation by considering only the initial investment I_0 and the only cash flow are the yearly average savings :

$$Payback\ Period = \frac{I_0}{Savings} \qquad \textit{Equation 17}$$

This metric considers that the initial investment is supported totally by the investor regardless of capital costs.

Potential to reduce the return temperature

Figure 25 shows the temperature profile for 4 days in December. The return temperature of the main DH network with the novel substation (solid blue line) is reduced compared to the reference return temperature (dotted blue line) outside the DHW production batches. This is due to the validity domain of the numerical model. A maximum of -16.5 K is observed on the whole dataset.

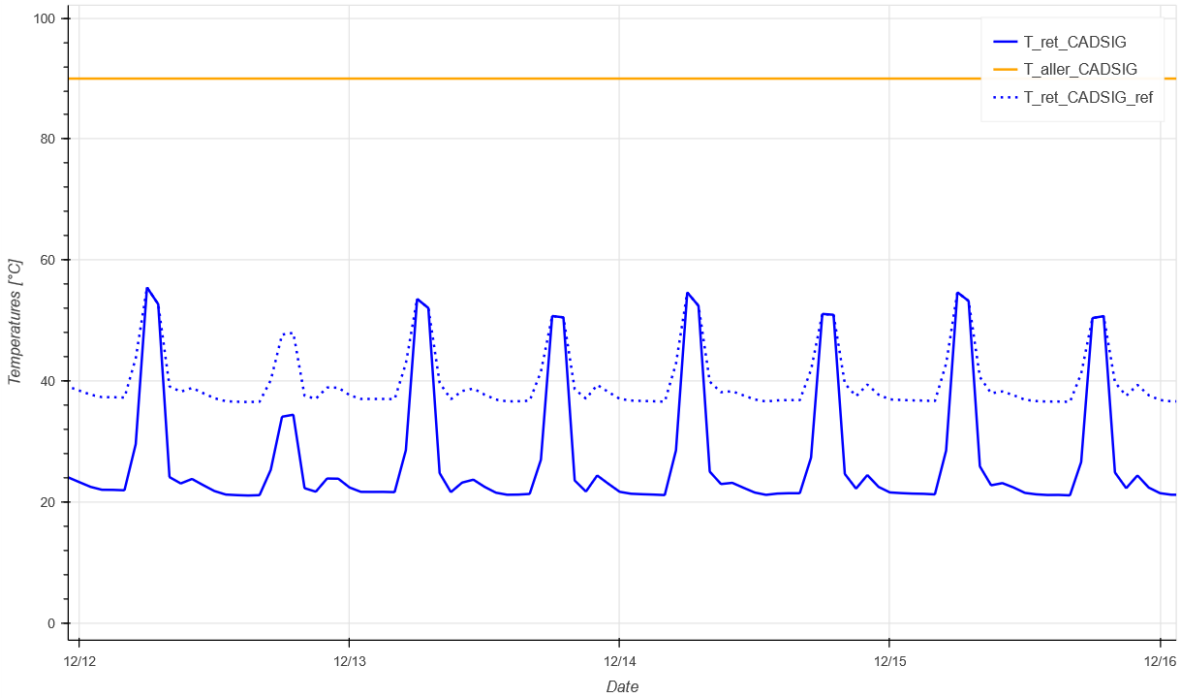

Figure 25: Comparison of the return temperature of the primary district heating network.

Figure 26 presents the annual performance indicators for the CharacSorb substation and the reference case. The power weighted mean return temperature is greatly decreased by 10.4K thanks to the adHP in comparison to the reference case. The same magnitude in benefit is observed on the the mean temperature difference between the supply and return pipe. However, the specific volume is only reduced from 19.2 to 16.4 m3/MWh (-14%).

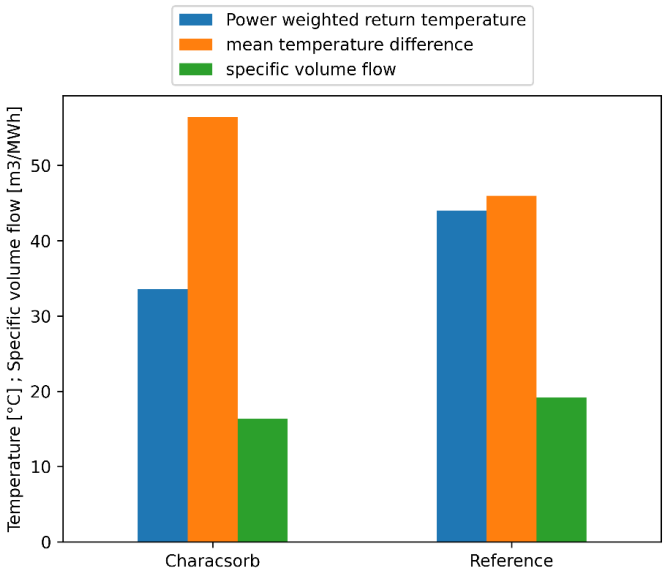

Figure 26: Comparison oft he annual performance indicators between the Characsorb substation and the reference.

The evaporator of adHP is assumed to cover 20% of the total heat flow rate of the substation. Therefore, the size of the adHP is assumed to be 1 MW for a substation covering 5MW. Table 10 present to needed inputs for the financial analysis.

Table 10: input and sizing data for the adsorption heat pump substation in the case study les Vergers

Total heating power of the Substation	5000	kW
Amount of heat supplied per year	8996	MWH/y
Cooling power of the adHP	1000	kW
Initial investment for the adHP	290	kCHF
Potential temperature reduction	10.4	K

From Table 9, the most promising heat supply technologies are geothermal heat, heat pumps and low temperature waste heat. Geothermal heat and heat pumps show respectively CRG ranges of 0.67 to 0.68 CHF/(MWh.°C) and 0.63 to 0.67 CHF/(MWh.°C). These values are similar and therefore results were regrouped and shown in Figure 27 under the CRG value of 0.67.

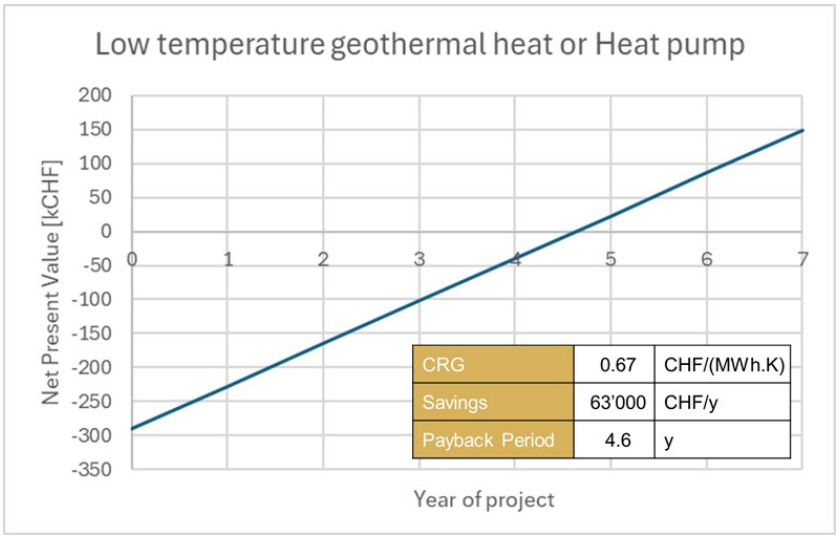

Figure 27 : Net present value according to the year of the project considering low temperature geothermal or heat pumps (CRG = 0.67 CHF/(MWh.K) leading to yearly savings of approximately 63'000 CHF/y)

The payback period is under 5 years which makes the project interesting for investors. For low temperature waste heat (Figure 28), the payback period is slightly higher occurring during the 6th year of the project.

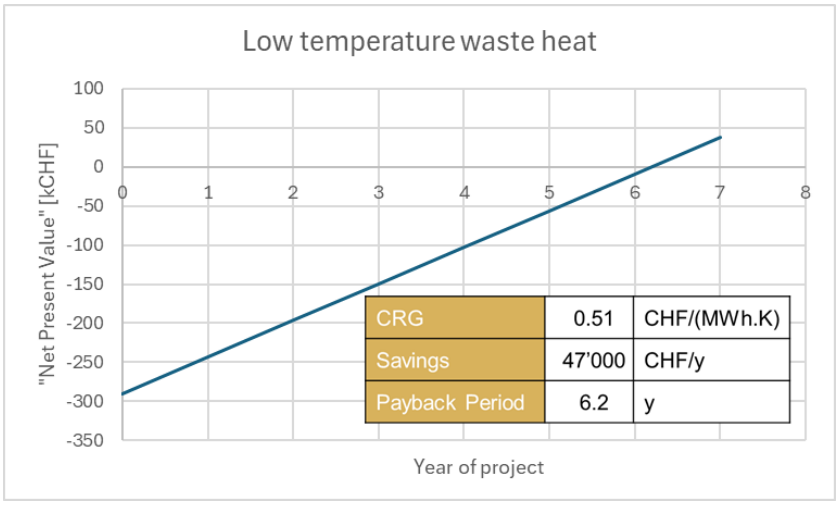

Figure 28: Net present value according to the year of the project considering low temperature waste heat (CRG = 0.51 CHF/(MWh.K) leading to yearly savings of approximately 47'000 CHF/y)

3.2.6 Case studies for cooling mode

This case study explores the potential of CharacSorb adsorption heat pump (AHP) technology for cold production in a commercial area located in Monthey. This area, currently not connected to the district heating network, is close to the central heating plant (CAD) of SATOM (Municipal Waste Incinerator and DHN operator in Monthey). In addition, it is located near a steam line connecting the SATOM incinerator to the Monthey chemical industrial park. Part of the steam needs of this industrial site are covered by this line, called "EcoTube", which has been transporting steam since 2022. This case study is an update of a case study conducted in collaboration with SATOM. The map below in Figure 29 illustrates the position of the commercial area in relation to the district heating network and the steam line.

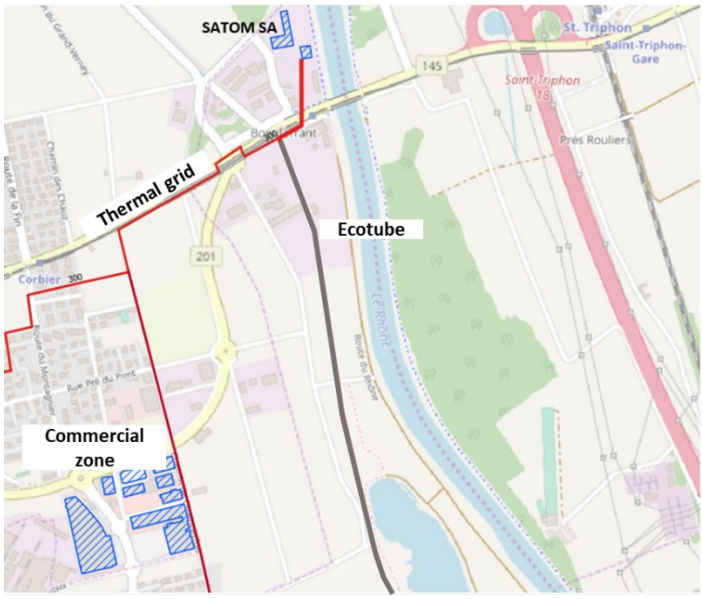

Figure 29: Site plan for the cold production case study showing the location of the commercial area, the SATOM heating network (in red), and the steam line (in grey)

The commercial zone encompasses approximately thirty diverse stores spanning a total area of 46,000 square meters (see Figure 30). Due to a lack of readily available data, the cooling requirements for these establishments were estimated using the SIA 2024 standard [SIA, 2024]. This standard outline energy consumption per square meter for various occupancies, encompassing both air conditioning and refrigeration needs. The overall cooling demand for this commercial area was determined to be 14 GWh per year (see Figure 30).

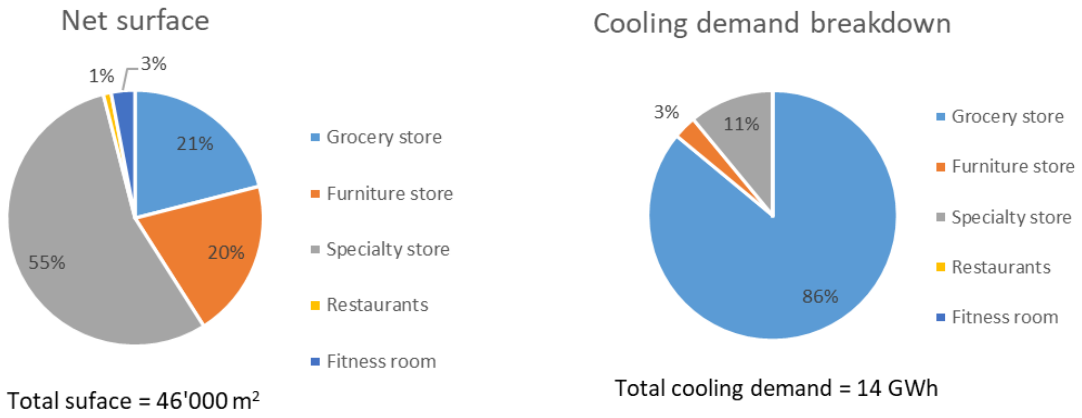

Figure 30 A. Surface and B. cooling needs for the commercial zone studied.

Interestingly, grocery stores account for a mere 21% of the total floor area yet contribute a staggering 86% of the cooling demand [Milona Z, 2017]. This is primarily attributed to the stringent requirement for maintaining an unbroken cold chain at subzero temperatures.

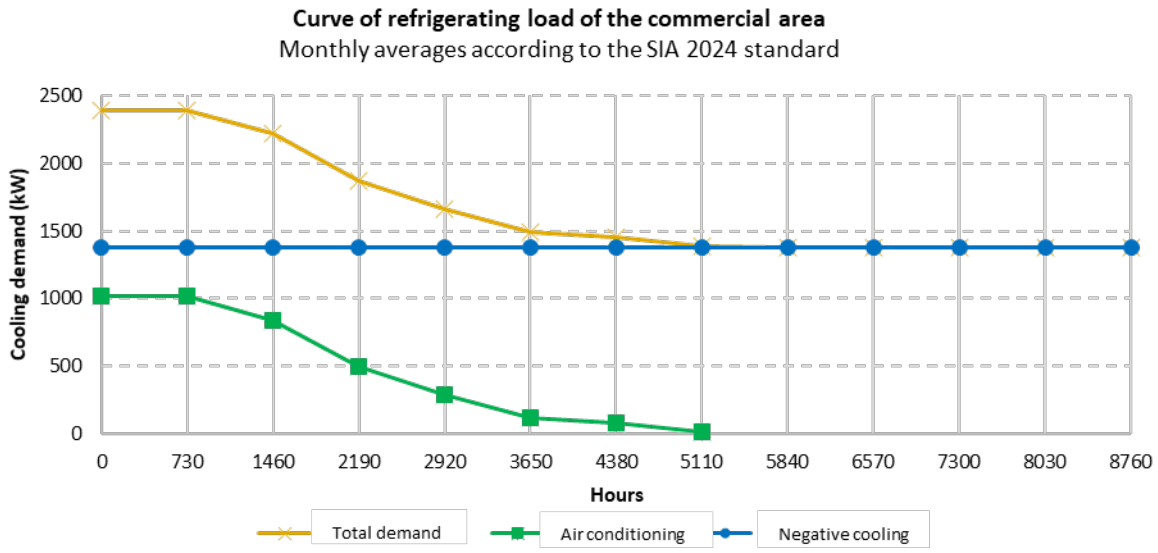

Figure 31 Monthly load cooling load curve for the commercial zone.

To better understand the cooling requirements and size the components of the cooling production system, a monthly load curve was generated for the two primary cooling applications: (1) space cooling for occupant comfort and (2) negative cooling for food preservation (base load over the year). This detailed load curve is presented in Figure 31. Interestingly, space cooling accounts for a relatively modest 15% of the total cooling demand, while negative cooling represents a substantial 85%.

To fulfil the cooling requirements of the commercial zone, two distinct scenarios have been devised:

Scenario 1: Business as Usual (BAU): This conventional approach employs a decentralized cooling system utilizing a cascade of two compression heat pumps. The first heat pump generates positive cooling for maintaining comfortable indoor temperatures, while the second produces negative cooling for preserving food items.

Scenario 2: District Cooling & Sorption Chiller: This innovative strategy involves centralized cooling production at 7°C using a sorption heat pump powered by SATOM's DHN (Ecotube return flow). The chilled water is then distributed to the commercial spaces via a dedicated chilled water network (District cooling). Negative cooling is generated decentrally by each store as per its specific needs, employing a compression heat pump that utilizes the district cooling water for heat dissipation. Scenario 2 necessitates the construction of a chilled water network and a connection to the ecotube return line. Notably, the centralized sorption heat pump in this scenario is sized to meet 100% of the negative cooling demand (base load, as a heat sink) and 50% of the space cooling demand. This approach prevents oversizing the absorption heat pump, ensuring efficient operation throughout the year.

To evaluate the energy efficiency of each scenario, an average annual COP was employed (see Table 11). The sorption chiller COP corresponds to the COP targeted by the CharacSorb project in cooling mode. Subsequently, operating costs were determined based on energy consumption figures. Investment costs were estimated using prevailing market prices for similar installations.

Table 11: COPs for the different Heat Pump (compression & sorption) required for the two scenarios presented above.

Scenario		COP [-]
100% Compression Heat Pump	Compression Heat Pump for air conditioning (10°C)	4
	Compression Heat Pump for negative cooling (cascade, -30°C)	3.5
District cooling with Sorption Heat Pump	Sorption Heat Pump (7°C)	0.8
	Compression Heat Pump for negative cooling (7°C → -30°C)	7

A financial study was conducted using the assumptions provided in Table 12. This study allows for comparing the two scenarios in terms of their cost-effectiveness.

Table 12: Hypothesis/assumptions summary for evaluating the financial performances of the two scenarios.

Financial model hypothesis	
Project duration	25 Years
Discount rate	3%
Electricity cost	0.20 CHF/kWh
Heat cost	0.02 CHF/kWh
Investment cost for compression, sorption heat pump and recooler	Based on “Absorption chillers: their feasibility in district heating networks and comparison to alternative technologies”, M.D. Schöpfer, 2015

Based on the assumptions, the Levelized Cost of Energy (LCOE) was calculated for both scenarios. The results, including a breakdown of the cost components, are presented in Figure 32.

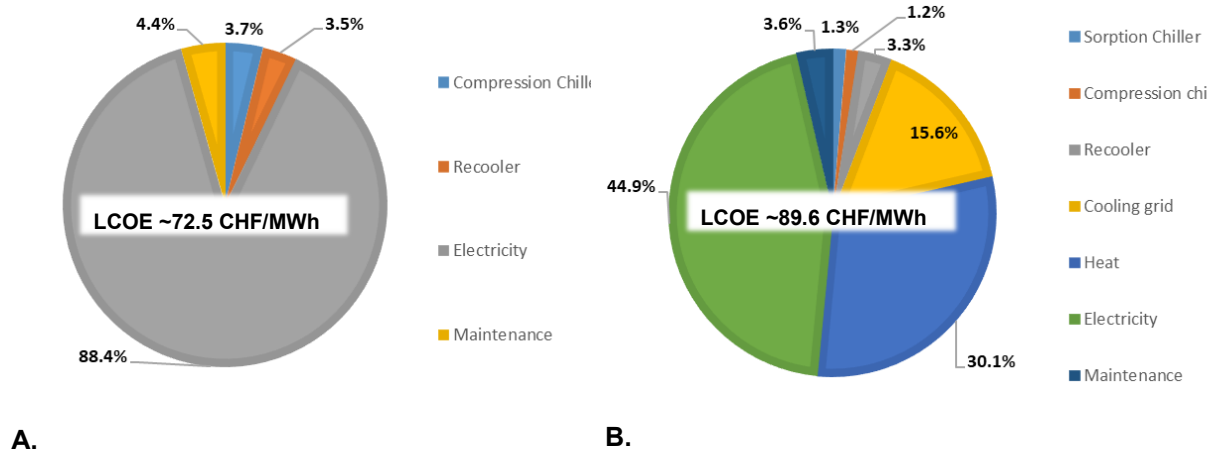

Figure 32 Levelized Cost of Cooling for the A. Scenario "Business as Usual2 and B. Scenario "District Cooling and absorption chiller".

Scenario 1 - Business as Usual (BAU): The total cooling production cost for the BAU scenario is 72.5 CHF/MWh. Initial investment amortization accounts for only 7.2% of this cost, while operating expenses represent approximately 92.8%. Electricity costs are the primary component of cooling production costs in this scenario.

Scenario 2 - District Cooling and Sorption Chiller: The total cooling production cost for the District Cooling and Sorption Chiller scenario is 89.6 CHF/MWh. Similar to the BAU scenario, investment amortization represents a minor portion of the total costs (~21%). The construction of the chilled water network accounts for approximately 15% of the production costs. Operating expenses constitute nearly 75% of the production costs and are divided between the heat bill (32.8%) and electricity costs (42.9%). Notably, the investment in an Sorption chiller accounts for only 1.2% of the production costs in this scenario.

Key Insights: This case study demonstrates that for baseload cooling requirements, the District Cooling scenario enables cooling production at a cost very close to the BAU scenario. The cost difference is mainly due to the amortization of the cooling grid (15.6% of the LCOH or 13.9 CHF/MWh). Cooling production using a sorption heat pump helps reduce electricity consumption and, consequently, the sensitivity of production costs to electricity price fluctuations. In the District Cooling scenario, heat is sold at a very low price (20 CHF/MWh). To make this scenario financially viable, it would be preferable for the DHN operator to invest in cooling production facilities and sell the cooling directly to users (contracting).

3.3 Upscaling of synthesis, pyrolysis and forming of chosen, optimized sorbent materials for second generation heat and mass exchanger

The Activated Carbons (AC) developed for THRIVE (Civioc et al., 2020; Huber et al., 2019) were based on petroleum-derived precursors for the phenolic networks. Therefore, to improve both the sustainability and the cost of the sorbent, we studied an alternative starting material: an activated carbon derived from Spent Coffee Grounds (SCG) with water adsorption characteristic is comparable with the one from more traditional resorcinol-based activated carbons; retaining an optimal performance is crucial for the efficiency of the project overall.

One of the advantages of using ACs as adsorbent material is the possibility of tailoring their properties to a given application. In particular, for SCG this can be controlled by changing the pyrolysis process to have more or less microporosity and macroporosity which will influence the adsorption characteristic, the density and the thermal diffusivity. In order to understand how the different pyrolysis conditions (CO_2 flowrate, max temperature and time above the critical temperature of the coffee) affect these properties, a Design of Experiment based on a central composite design was performed on the SCG. Based on the results, each material property P was described as a function of the maximum pyrolysis temperature $T \in [632, 968]$ ($°C$) and the duration of the pyrolysis above 300 °C $D \in [244, 429]$ (min):

$$P=a\cdot T+b\cdot D+c\cdot T\cdot D+d \qquad \textit{Equation 18}$$

Table 13 summarizes the results obtained for the SCG AC powder.

Table 13: Description of SCG AC properties as a function of the pyrolysis parameters

Material Property	Symbol [Units]	Temperature coeff. a	Time coeff. b	Temp./Time coeff. c	Constant coeff. d
Saturation Water Capacity	$W\ \left[\frac{g_w}{g_s}\right]$	0	-1.3e-3	2.4e-6	0
Char. Energy of Adsorption	$C\ \left[\frac{J}{g}\right]$	0.43	1.2	-2.0e-3	0
Ads. Curve Shape Factor	$N\ [-]$	0	0	0	2.0
Skeletal Density	$\rho_{skel}\ \left[\frac{g}{cm^3}\right]$	0	-2.1e-3	2.9e-6	1.7
Envelope Density	$\rho_{env}\ \left[\frac{g}{cm^3}\right]$	5.6e-4	1.4e-3	-2.4e-6	0

Given the requirements of DHN for heating and cooling purposes, the performance of the SCG ACs should be tailored accordingly. Therefore, we used the dynamic adsorption model to simulate the Key Performance Indicator (KPI) of the material in a range of process, material and application parameters. The KPI was selected to be a tradeoff between energy efficiency and specific cooling power reached by an adsorption/desorption cycle in steady state (i.e. after 50 cycles):

$$KPI_{heating} = \frac{(E_{con}+E_{ads})^2}{E_{hot}t_{cycle}} \qquad \textit{Equation 19}$$

$$KPI_{cooling} = \frac{E_{eva}^2}{E_{hot}t_{cycle}} \qquad \textit{Equation 20}$$

In order to ensure a feasible heat exchange with the heat transfer fluid, the desorption temperature is assumed to be 5 K below T_{hot} and the adsorption temperature is assumed to be 5 K above T_{cold}. To minimize the number of simulation required, the working temperatures T_{eva}, T_{cold} , T_{hot} were fixed to 293, 308, 368 K for the heating mode and to 288, 303, 363 K for the cooling mode respectively. Firstly, the

best pyrolysis conditions for the (improvable) not sieved SCG+RF AC were defined by calculating the KPI for long cycles (reaching full equilibrium). The best material was selected for 3 scenarios, for which the total KPI was calculated as $KPI_t = \left(\frac{\varphi_h}{KPI_{heating}} + \frac{\varphi_c}{KPI_{cooling}}\right)^{-1}$ where $\varphi_h + \varphi_c = 1$ are the scenario specific weights for heating and cooling:

· Current Demand (CD), serving only heating, with φ_h=1, φ_c=0

· Moderate Cooling (MC), where the cooling demand is less important than the heating demand, with φ_h=0.67, φ_c=0.33

· High Cooling (HC), where cooling demand is as important as the heating demand, with φ_h=0.5, φ_c=0.5

However, one of the main advantages of traditional resorcinol-based ACs is their monolithicity; they can be tailored thanks to the bottom-up synthesis approach by pouring the sol into a box of the desired shape. The results above on the other hand were collected on powders, while adapted strategies were determined to find ways to produce monolithic SCG AC. In the meantime, the reference thermal conductivity of 0.067 $W*m^{-1}*K^{-1}$ (obtained for a highly macroporous RMF AC monolith) was used instead for the lumped materials model. This means that the thermal resistance might be overestimated for the denser samples. Moreover, the specific heat capacity was assumed to be similar to the one measured for the RMF AC (Piccoli et al., 2021).
The ideal pyrolysis conditions for the three scenarios determined with our modelling approach are listed in Table 14. The material design is clearly limited by space in which they were investigated: higher temperature and lower duration of pyrolysis would be beneficial. Moreover, the cooling mode is by far the most constraining and it dominates the choice for MC and HC scenarios.

Table 14: Optimal pyrolysis parameter for the different application scenarios

Parameter	Current Demand	Moderate Cooling	High Cooling
T	968 °C	968 °C	968 °C
D	275 min	244 min	244 min

For the investigation of the optimal material thickness and cycle time, the material for MC and HC was used. When simulating different monolith thicknesses, thinner materials were able to produce much higher power, and therefore are preferred. For example, a thickness of 1 mm (one order of magnitude higher than conventional coatings), delivered maximum KPI with a full cycle time of about 25 s, that is at the limit of the capacity of conventional heat exchangers, which have important thermal inertia. This means that for thin coatings, work should be done towards fast heat exchangers design. For 2 mm monoliths, however, the transport resistances increase (figure 7) and the ideal cycle time increase to 100 s. The achieved thermal coefficient of performance reached 0.79 and the $KPI_{cooling}$ 1.4 $kW*kg^{-1}$.

The aim was then to produce monolithic materials according to the specification determined in the modeling. Comparing two compounding methods, with expanded graphene as well as with a minor amount of resorcinol and formaldehyde, the latter yielded better results, both concerning mechanical stability, shaping and thermal conductivity. Importantly, the compounding does not compromise the water adsorption performance of the materials. Our synthesis protocol involves the collection of spent coffee grounds, which are then mixed with a minimal amount of resorcinol and formaldehyde. Typically, 30 g of dry SCG and 25 mL of ethanol are mixed with 6 g of resorcinol and 12 mL of commercial formaldehyde aqueous solution. A catalytic amount of ammonia in the form of an aqueous solution,

around 1 mmol, is then added to the mixture. It is then poured into molds boxes of the desired shape. The materials are left to cure and dry in a convection oven before being pyrolyzed and physically activated in a one-step heat treatment. Additionally in an early step of optimization, it was found that a finer particle size of the AC was beneficial both for the mechanical properties and the water uptake. Therefore, before synthesis, SCGs is sieved and only the fraction with a diameter < 200 micrometers was used. This resulted in the 2nd generation optimized materials.

Throughout the project we experienced problems and had to contend with down time of our tube furnace, important equipment for the pyrolysis and activation of the AC. In the end, adaptations of the furnace set-up with additional isolation were necessary to hopefully avoid future down times of the furnace. The additional isolation however led to a significantly slower cooling ramp, influencing the heat treatment. Therefore, in addition to the upscaling of production, additional re-optimization / adaptation of the pyrolysis conditions were necessary. The final pyrolysis conditions used were 850 °C for 120 min. The less harsh conditions compared to the originally determined parameters (see table 5) can be explained by the slower cooling down ramp, leading to higher temperatures and longer duration of the heat treatment during this phase.

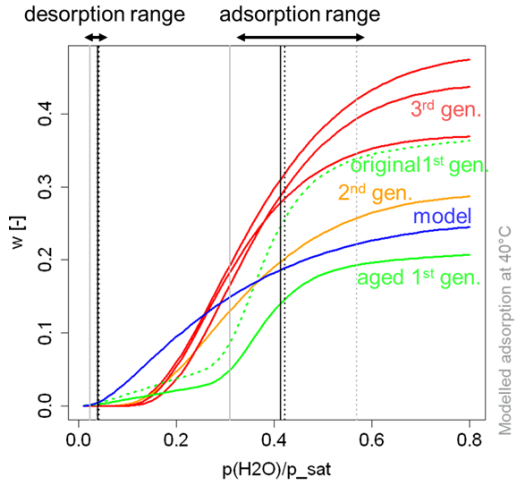

	1st gen	model est.	2nd gen	3rd gen
envelope density [g/cm3]	0.43	0.31	0.56	0.53
macroporosity [cm3/g]	1.4	~0.8	0.8	0.8
thermal conductivity [W/mK]	~0.06	~0.09	~0.09	~0.13

Figure 33: Water adsorption isotherms at 40 °C (left) and major performance influencing properties (right) of different generation of AC: Original as well as aged 1st generation RMF sorbents, 2nd generation SCG AC sorbents as well as the properties used for the A/D HEX 2.

A reproducibility study of the upscaled 3rd gen material synthesis and pyrolysis/activation showed better sorption properties than considered for the modelling as well as the 1st and 2nd generation of materials (see Figure 34). The envelope density is higher, the macroprosity as well as the thermal conductivity are in the same range, indicating that the performance of the model remains valid. Shrinkage was homogeneous and dimensions could be controlled within +/- 0.3 mm.

Based on these results, PTFE moulds were designed and ordered for the production of monoliths. Gluing tests have been performed and satisfactory gluing could be achieved by applying the glue on the monoliths before gluing on the fins. A different glue was used compared the 1st gen prototype, allowing for better distribution of the glue. For correct placement of the monoliths, a gluing rig was designed and produced (Figure 34).

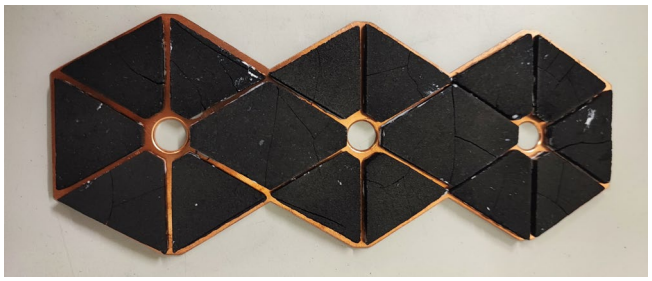

Figure 34: Copper fins glued with 3rd generation sorbent materials

During the production periodic water adsorption isotherms and weight measurement of the produced monoliths were done for quality control and better understanding of the final prototype. 18+/-1 g of dry activated carbons were glued with 5+/-3 g (reduced amount with later fins) on the copper fins with an initial weight of 20.9+/-0.05 g. The total mass of the dry fins is thus 44+/-3 g. Typically under ambient (winter) laboratory conditions an additional 2-3 g of water is adsorbed per fin.

The properties retained for modelling of the 3rd generation activated carbons used for the 2nd prototype are summarized in Table 15.

Table 15: Final parameters of the 3rd generation activated carbons integrated in the 2nd prototype.

			Adsorption $w = W_1 e^{-\left(\frac{F(p,T)}{C_1}\right)^{N_1}} + W_2 e^{-\left(\frac{F(p,T)}{C_2}\right)^{N_2}}$						Desorption $w = W_1 e^{-\left(\frac{F(p,T)}{C_1}\right)^{N_1}} + W_2 e^{-\left(\frac{F(p,T)}{C_2}\right)^{N_2}}$					
envel. density	macro-porosity	thermal cond.	W_1	C_1	N_1	W_2	C_2	N_2	W_1	C_1	N_1	W_2	C_2	N_2
g/cm3	cm3/g	W/(mK)	g/g	J/g	-	g/g	J/g	-	g/g	J/g	-	g/g	J/g	-
0.53	0.8	0.13	0.179	149	5.92	0.245	164	1.07	0.245	153	5.50	0.168	260	1.45

3.4 Design and manufacturing of the 2nd generation heat and mass exchanger

During the period under review, the mechanical design of the second-generation heat exchanger was developed. As it is depicted in Figure 35, the heat exchanger now has three parallel tubes with fluid flows in the same direction.

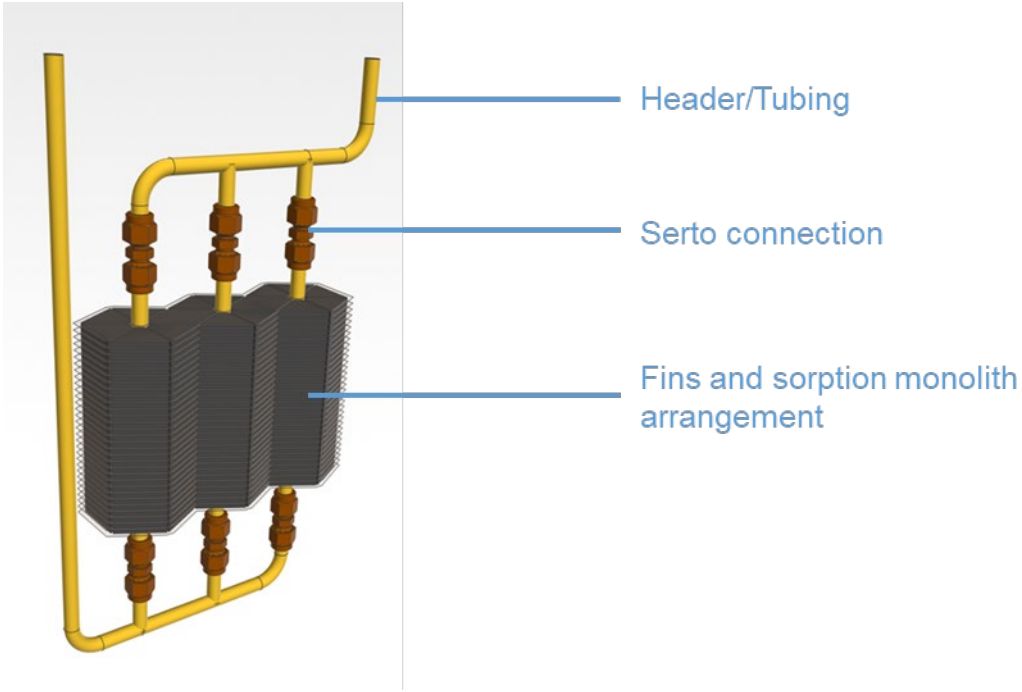

Figure 35: 3D model (CAD) of the heat and mass exchanger unit with a threefold tubing.

The design is now be broken down and discussed in several parts:

3.4.1 Tubing

The tubing is the same as in the first generation, with copper tubes (same exterior diameter of 10 mm) expended to match the fin holes in order to ensure optimum heat transfer. A Tichelmann distribution was retained to ensure the same mass flow of heat transfer fluid in each of the three tubes.

As a matter of assembly, the main line in contact is removable with SERTO parts. Compared to a soldered version, the retained version offers a very similar total weight (1.72kg instead of 1.77kg), no critical thermal distortion and some ease of assembly and disassembly. The tubing is therefore divided into three parts, which also has the advantage of keeping heat from soldering or welding away from the monoliths.

3.4.2 Fins and sorption monolith arrangement:

In the second-generation heat and mass exchanger, the monoliths have a new shape and arrangement. Unlike the circular shape of the first-generation HEX, the second-generation heat and mass exchanger is made up of multiple trapezoids arranged in a hexagonal structure around the tube (see Figure 36). The reference hexagonal monolith structure has a thickness of 4.4 mm and a weight of approximately 0.76 g of sorbent per trapezoid. For the peripheral area of the A/D HEX, the trapezoids are fabricated and cut from hexagonal monoliths.

This new arrangement offers the possibility of compactness and the ability to incorporate vapour channels. These 1.5 mm wide vapour channels (which meet both mass transport requirements and manufacturing tolerances) will allow for more uniform mass transport through the sorbent material. In addition, the resulting compactness of the parallel tubes allows for a tighter final assembly, drastically reducing the A/D HEX's height while increasing theoretical performance. Figure 36 shows the arrangement of the monoliths.

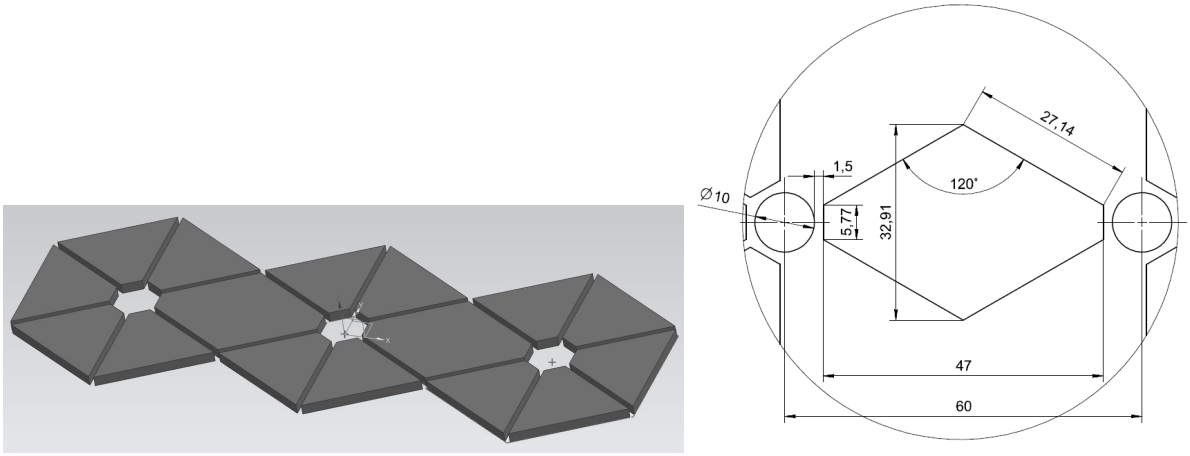

Figure 36: Sorbent monolith arrangement (right) as well as dimension of a trapezoid (reference monolith, left)

According to Table 16, the geometry with a row of 3 tubes includes the equivalent of 18 trapezoids, corresponding to approximately 14 g of dry sorbent. The geometry retained with 31 Cu fins corresponds to the equivalent of 540 half-monoliths, matching with a quantity of 0.41 kg of dry sorbent material (1% more active mass compared to the first generation A/D HEX).

Table 16: Details of the characteristics of the sorption material that makes up the second generation A/D HEX.

						full monolith		
half-trapezoid height	*mm*	23.5						
half-trapezoid short width	*mm*	5.77						
half-trapezoid long width	*mm*	32.91						
half-trapezoid thickness	*mm*	4.4						
averaged volume of one carbon monolith	*m3*	2.00E-06		*trapez assumption*				
specific density of a carbon monolith (dry)	*kg/m3*	380		*THRIVE RMF data*				
averaged dryed weight of one half carbon monolith	*g*	0.76				1.52		
total carbon monolith dryed weight required	***g***	**405.7**		**minimal configuration (THRIVE)**				
tubes mounted in paralell	-	3		*Thilleman configuration*				
number of half-monoliths pro tube	-	6						
number of half carbon monoliths pro fin	-	18				2		
carbon monolith dryed weight pro fin	*g*	13.68						
required number of fins for the HMX	-	30.7		*sandwitch configuration*				
retained number of fins for the HMX	-	31						
total number of half carbon monoliths required	-	540			full monoliths	60	monoliths to cut	210
total carbon monolith dryed weight required	*g*	410.3	1%					

3.4.3 Fin manufacturing

In order to reduce the inert thermal mass of the A/D HEX, the fins are cut to the monolithic pattern, including a slight overhang to the monolithic structure. They are produced using waterjet cutting to ensure accurate and good quality edges (see Figure 37). The material used is copper (CW004A) with a thickness of 0.22 mm.

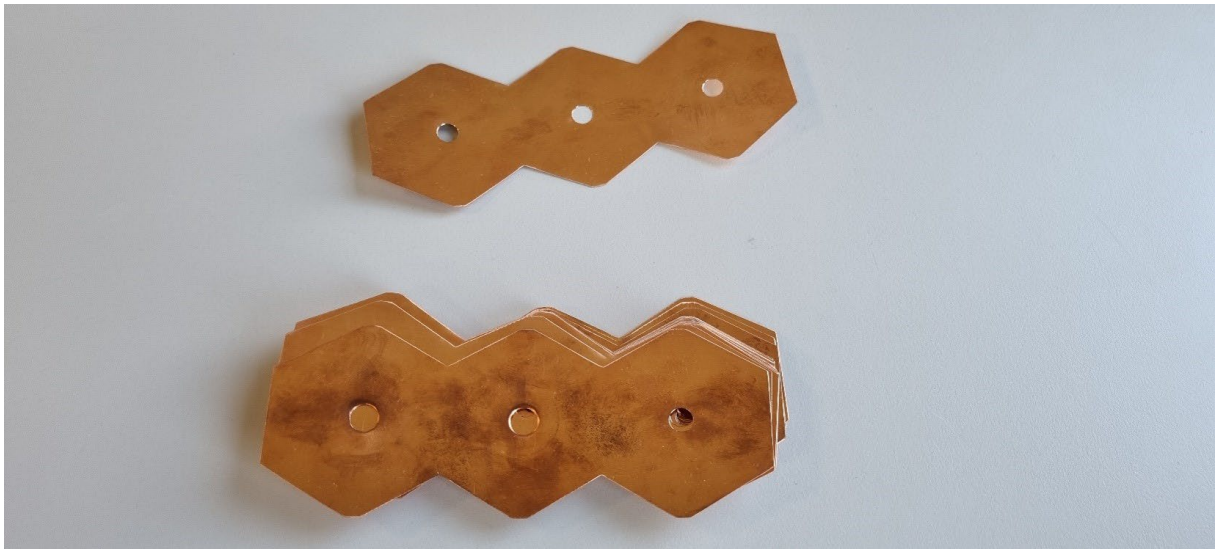

Figure 37: Manufactured (stamped) copper fins.

To ensure sufficient thermal contact with the tubes, a collar is stamped into the holes of the copper fins. For this purpose, a stamping die has been designed and manufactured in-house, as shown in Figure 38. The fin is precisely placed in the die, ensuring that the punch is collinear with the hole. The punches are then simultaneously pressed into the fin, enlarging and bending the holes to form a collar. A total of 31 fins are produced in this way and then shipped to EMPA for monolith application.

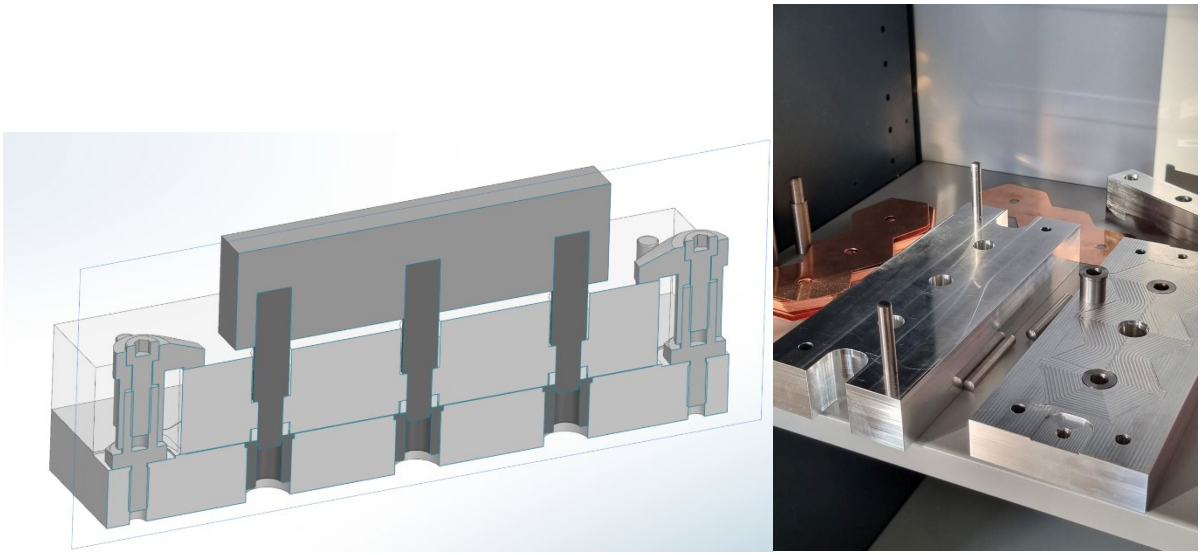

Figure 38: Clip section of collar stamping device (left) and in-house designed and manufactured stamping tool (right).

3.4.4 Heat and mass exchanger assembly preparation

Given that the monoliths are intended to be sandwiched (one side glued, the other with thermal paste to ensure thermal contact) between the copper fins, the vacuum compatibility of both the glue and the thermal paste had to be validated (outgassing). Associated virtual leak rates measured (see Figure 39) for the thermal paste and adhesive were 3.76E-6 and 1.86E-6 mbar*l/s respectively, which are quite low and will not cause any problems for the application considered.

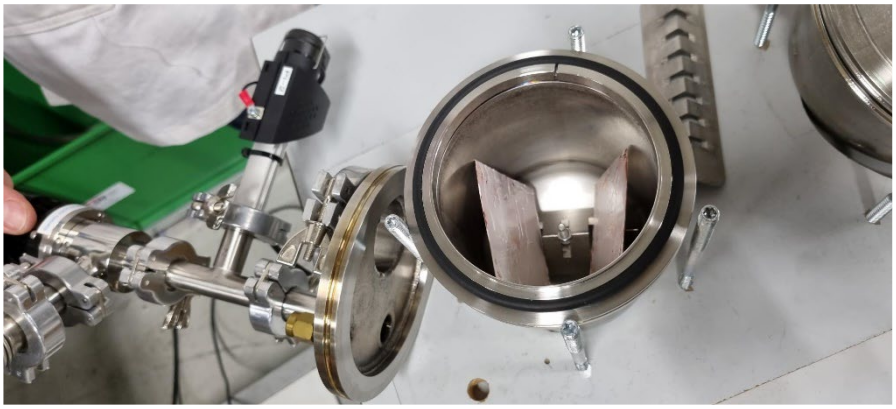

Figure 39: Vacuum chamber with thermal paste covered copper fin to test outgassing of the paste.

Preliminary calculations allow the risk of damaging the monoliths during the A/D HEX assembly process to be minimized. For example, the stress in the radial direction was calculated. Maximum values of the expected stress $\sigma_{\mathrm{m,therm}}$ around 145 MPa at the contact surface during heating should not lead to any expected material failure, as the high thermal conductivity compensates for the radial length variation of the fin and tube. Similarly, during tube expansion, an expected shrinkage of 0.24% (0.5 mm for 200 mm tube length) allows for sequential expansion of the tubes.

3.4.5 HEX Assembly

With all the monoliths glued onto the fins by EMPA, the heat exchanger was ready to be assembled by OST. Therefore, the same settling device was used as in Section 3.4.3, with addition of some parts manufactured to help with easier assembly.
Prior to assembly, the three tubes used have been held in a high temperature oven at 480 °C for the copper to soften. This step is crucial for the tube expansion tool to work properly.

The copper tubes are inserted into the settling device and the first fin layer is placed. Now, thermal paste is applied and distributed across the whole copper surface before a second layer is placed on top. Figure 40 shows the first layer. Approximately 5 grams of thermal paste is used per fin.
After the 31st fin is put, the tubes were expanded with the tool to an outer diameter of approximately 10.14 mm, which is an excess of 0.14 mm.

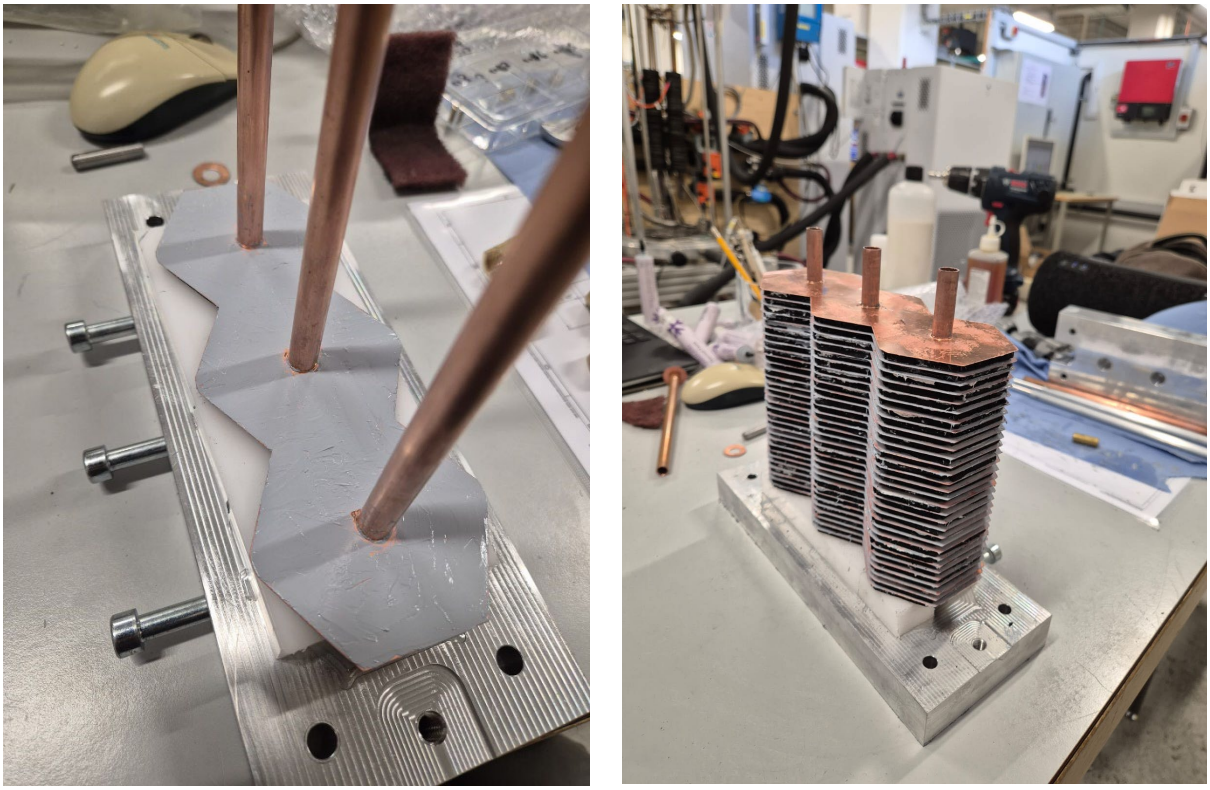

Figure 40: First layer of thermal paste (heat conduction) in the Copper fin (left). The stack of Copper fins sandwiched monoliths (right).

3.4.6 HEX integration into test rig

After the tubes have been expanded the Serto fittings are mounted and a leakage test is conducted as it is depicted in Figure 41. The main leakage problems arose with one of the Serto connectors which had a reduction element. But the problem could be solved to an extent where the leakage rate was in the range below 10^{-4} mbar*l/s which is an indication for a tight vacuum system.

Before integrating the heat exchanger, the whole assembly is weighted. Including Serto fittings and tubes the weight comes to a total of 2681 grams. The average dry sorbent mass per fin is 18.85 g, whilst the average wet sorbent mass per fin is 22.26 g. This means that the total dry sorbent mass comes to a total of 565.5 g.

A brief overview is given in the following table:

Table 17: Mass of different A/D HEX parts

Total dry sorbent mass (g)	Total mass of thermalpaste (g)	Total mass of glue (g)	Total mass of fin structure (g)	Total mass of A/D HEX 2 (g)
565.5	163g	160.2	1814.1	2681

The whole A/D HEX is then mounted into the test rig, as it is seen on the right in Figure 41 and the facility was commissioned for a calibration measurement.

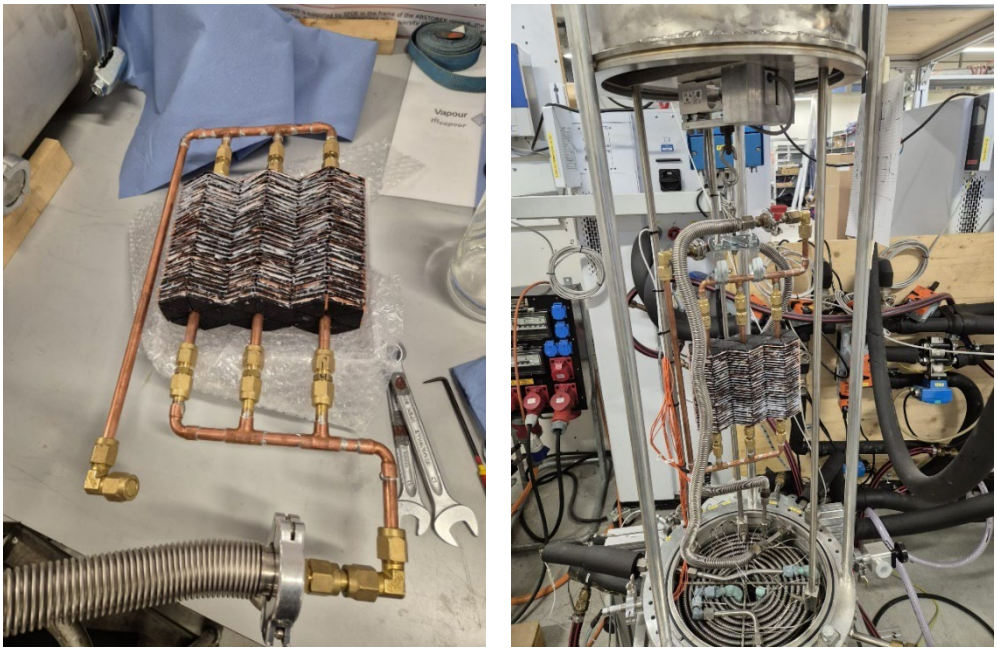

Figure 41: Assembled heat exchanger in (vacuum) leakage test (left) and after fulfillment, integrated into the test rig.

3.5 Heat and Mass exchangers characterization.

3.5.1 Characterisation of the first-generation A/D (HEX 1)

The heat and mass exchanger A/D HEX 1 (THRIVE) is characterized in the setup shown in figure 3 during a (sorbate water vapor) adsorption and desorption cycling procedure. Regarding the AdHP operation modes, the measurement parameters are shown in Table 18.

Table 18: Measurement parameters to characterize the A/D HEX 1 as well as A/D HEX 2

				Temperature Reduction Mode	Cooling Mode
Desorption	T_iAD_in	HTF temperature at the A/D inlet	*°C*	**85**	**80**
	F_iD	A/D HTF volume flow rate	*l/h*	**50**	
Adsorption	T_iAD_in	HTF temperature at the A/D inlet	*°C*	**35**	**35**
	F_iD	A/D HTF volume flow rate	*l/h*	**50**	
Evaporation / Condensation	T_iE_in	HTF temperature at the E/C inlet	*°C*	**25**	**15**
	F_iE	E/C HTF volume flow rate	*l/h*	**500**	
Top double jacket	T_iS_LD	HTF temperature at the double jacket inlet	*°C*	**60**	**57.5**
	F_iE	Double jacket HTF volume flow rate	*l/h*	**max**	

For a fist step, after the setup improvement, a cycle time of t_{cycle} 1800 s, i.e. a half cycle length $t_{cycle}/2$ of 900 s, is used. In Figure 42, an example of measurement data is shown for the temperature quadruple T_{ads} 35 °C, T_{des} 85 °C (T_iAD_in, T_iAD_out), T_{evap} & T_{cond} of 20 °C and a heat transfer fluid flow (F_iD) of 50 l/h. The arrow (showing to the left) in the graph indicates an improvement of the power, if the cycle time is reduced.

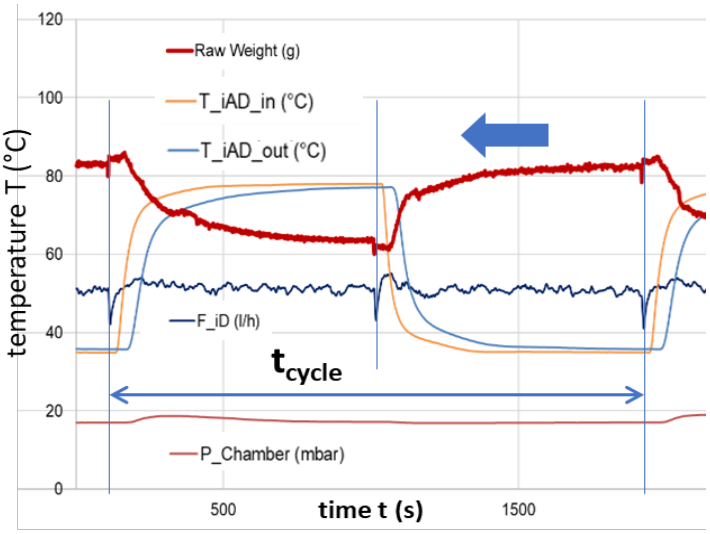

Figure 42: Measurement data section: adsorption and desorption (half) cycle measurement in the single chamber setup for A/D HEX characterisation. Raw Weight (g), heat transfer fluid inlet (T_iAD_in) and outlet (T_iAD_out) temperature, heat transfer fluid flow (F_ iD) and sorbent pressure P_Chamber in function of time t.

The following figures are showing weight measurement data for both adsorption (Figure 43) and desorption (Figure 44). At the onset of adsorption (resp. desorption) the behaviour with a high mass uptake (resp. decrease) per time can be seen. Due to the high kinetic behaviour in the first third of the cycle - weight increase (decrease) at the onset of the adsorption (desorption) mode - the cycle time t_{cycle} could be reduced to approx. 2*300 s ($t_{cycle}/6$ for each half-cycle).

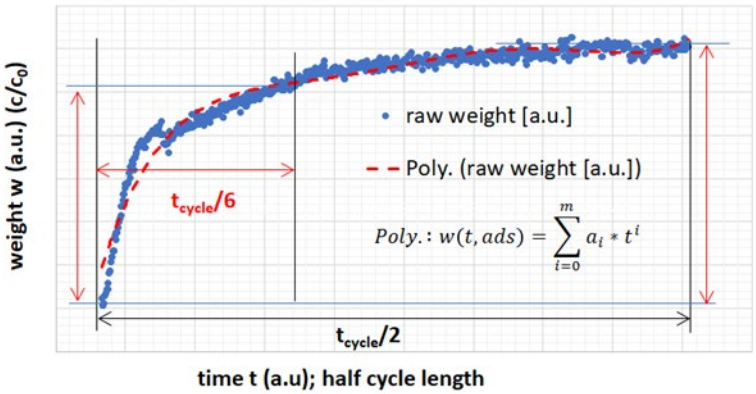

Figure 43: Measurement data section: A/D HEX 1 measurement data of the adsorption curve over the half cycle time $t_{cycle}/2$ (a. u. = arbitrary units) and concept of data curve analysis with peace wise fit-functions. At the onset of adsorption a high mass uptake (high kinetic) per time can be seen. With a reduction of the cycle time to, for example $t_{cycle}/6$, a strong increase of the power can be reached.

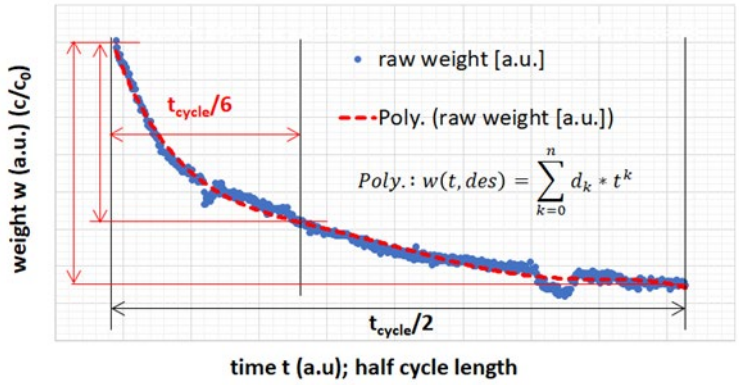

Figure 44: Measurement data section: A/D HEX 1 measurement data of the desorption curve over the half cycle time $t_{cycle}/2$ (a. u. = arbitrary units) and concept of data curve analysis with peace wise fit-functions. At the onset of desorption a high mass loss (high kinetic) per time can be seen. With a reduction of the cycle time to, for example $t_{cycle}/6$, a strong increase of the power can be reached.

After the measurements with the sorbent-sorbate combination, an appropriate data procedure follows to determine the efficiency parameters. This procedure comprises the measurement curve fitting to determine the coefficients a_l, d_k and the indices l, k for each temperature quadruple and cycle time. After this procedure the functions can be used the parameterise a sorption heat pump model.

The power of the A/D HEX I was determined by the sorbate mass uptake w(t) and mass loss through the adsorption desorption cycles. At a cycle time Tcycle/2 of 900 s the heat and mass exchanger A/D HEX I reaches an average power of (80+/-6) W at Tdes = 80 °C and (112+/-10) W at Tdes = 85 °C. Although the sorbent shows a high kinetic behaviour (steep increase of the mass uptake at the onset of adsorption) a low power in the range of 100 W was reached (SCP: 300 $W*kg^{-1}$) due to a long cycle time t_{cycle}.

As mentioned above, a closer look to the mass curve w(t) (figure 10 & 11) indicates to shorten the t_{cycle} down to approx. one third – and therefore nearly a double of the specific cooling power (SCP) would be reached. An even higher SCP is expected with unaged sorbent material and an unaged A/D HEX (no peeling/dissolution of sorbent from the heat conduction Copper fins, figure 8). In fact, the sorbent aging depends of the interaction with the sorbate and should not occur in normal operating conditions. Based on the defined temperatures of the scenarios the sorbate vapor pressure p_s is in the range of 17.1 mbar (15 °C) and 42.5 (30 °C) sub-atmospheric pressures. The understanding of the sorption kinetics in the 1 kW power range allows for the scaling of results to a several kW (heating and cooling) power adsorption heat pump.

Table 19: cycled water vapor in g theoretical (unaged) and measured (aged)

	cycling weight theoretical	**cycling weight measured**		**relative difference**
	g_H2O	*g_H2O*	*Δg_H2O*	-
Cooling mode @80/50_aged	49.7	32	±3	-45%
District Heating @85/50_aged	50.6	42	±4	-20%

3.5.2 Characterisation of the second-generation A/D (HEX 2)

Almost 24 months elapsed between the first and second measurement campaigns. Despite some maintenance of the test rig, several hardware problems occurred during the second measurement campaign. These problems were independent from HEX2 implementation and on one hand linked with aging hardware that does not fully support the latest software security updates and on the second hand with the thermostatic bath responsible for the desorption liquid line.

This Thermostatic bath had problems with its level sensors, as shown in orange in Figure 45. As it turned-out, one of the two level-sensors (one for safety, the other for control) was not moving properly due to deterioration of the inner tube (probably corrosion). The difference in level between the two sensors caused a system failure, while the entire thermostatic bath shut down and the measurement was ruined. This happened several times, even after the intervention of technicians. Although the problem was partially solved for a short period of time, it returned with a force that prevented any measurements, and the long delivery time (3-4 weeks) of the replacement part prevented complementary measurement campaigns.

Figure 45: Lauda thermostatic bath featuring its level sensors.

Finally, partial evaporation problems were encountered with the heat transfer fluid (Minoltherm), a mixture of water and ethanol. According to refraction measurements, the alcohol content of the heat transfer fluid mixture decreased from 20 wt.% to nearly 14 wt.%, necessitating several fluid changes to avoid having measurements affected by varying heat capacity of the heat transfer fluid.

At the end, several measurements campaigns were conducted on the second-generation A/D HEX with the parameters already used for the characterization of the first A/D HEX generation (Table 18). To confirm the results, two measurement campaigns were performed with the cooling mode boundary conditions, three measurement campaigns were performed with the district heating mode boundary conditions, as well as two calibrations (see section 2.3) for each mode. Each measurement campaign represents at least half a day of measurement and several temperature cycles. From these multiple cycles, the four most representative cycles for both cooling and district heating modes were selected. From these four cycles, an average and absolute uncertainty of both the average power and the water uptake were calculated and are presented in Table 20.

Table 20: Averaged measurement values obtained with the second-generation heat and mass exchanger.

	A/D HEX weight variation		**Ad-/De-sorption averaged power (based on water uptake)**	
	average value [g]	abs uncertainty [g]	average value [W]	abs uncertainty [W]
cooling mode	23	2	57	9
district heating	44	4	115	12

According to Table 20, in cooling mode an average power of about 57+/-9 W, corresponding to a water adsorption/desorption of about 23+/-2 g, is achieved for a half-cycle length of 900 s. The A/D HEX2 performs better in district heating mode, with an average heat exchange of about 115+/-12 W, corresponding to about 23+/-2 g of water adsorption/desorption.

Figure 46 gives some more details about the parameter evolution inside the A/D HEX for two selected cycles. According to this graph, the dynamics of both the desorption and adsorption processes are fast during the first 100 s and then slow down. The pressure increase inside the measurement chamber during the first phase of the desorption process may be related to a limiting design of the condenser in terms of heat exchange. However, this pressure decreases gradually until the end of the cycle and should not limit too much the A/D HEX performance on the considered 900 s desorption process.

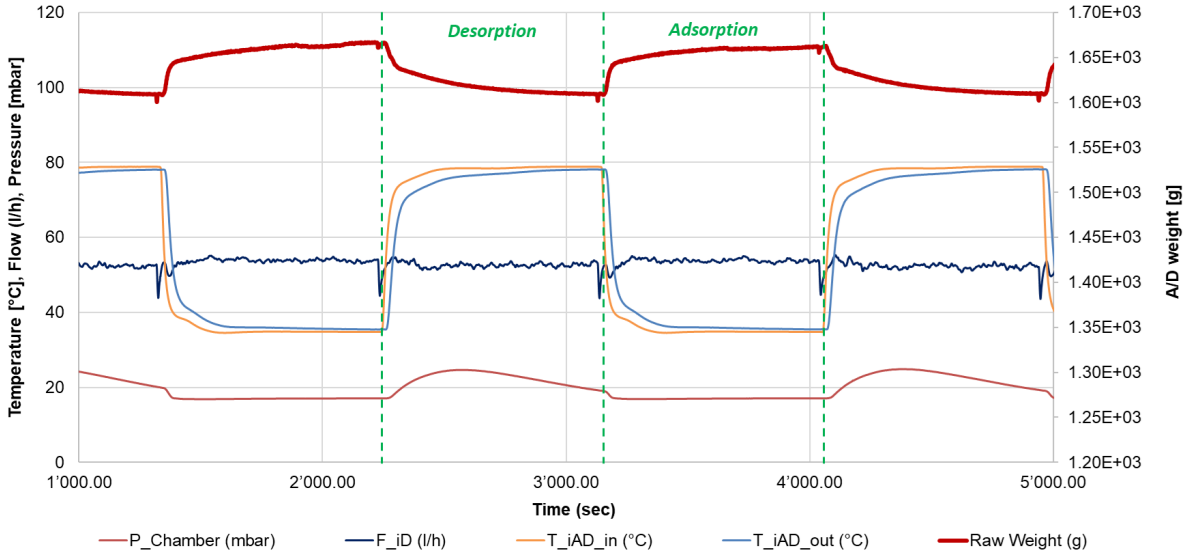

Figure 46: Measurement data: Evolution of temperatures, pressure, flow and weight of the A/D HEX 2 (cooling district mode).

No pressure variation occurs during the adsorption process, which means that the limitation is not related to the evaporator, but more likely to the A/D HEX design (limiting mass transfer or more likely limiting heat transfer, since the process is not linear with time).

The following figures show the weight measurement data of the A/D HEX2 for both adsorption (Figure 47) and desorption (Figure 48 and confirm that at the onset of desorption, the mass variation per time behavior is higher than at the onset of desorption (higher kinetic).

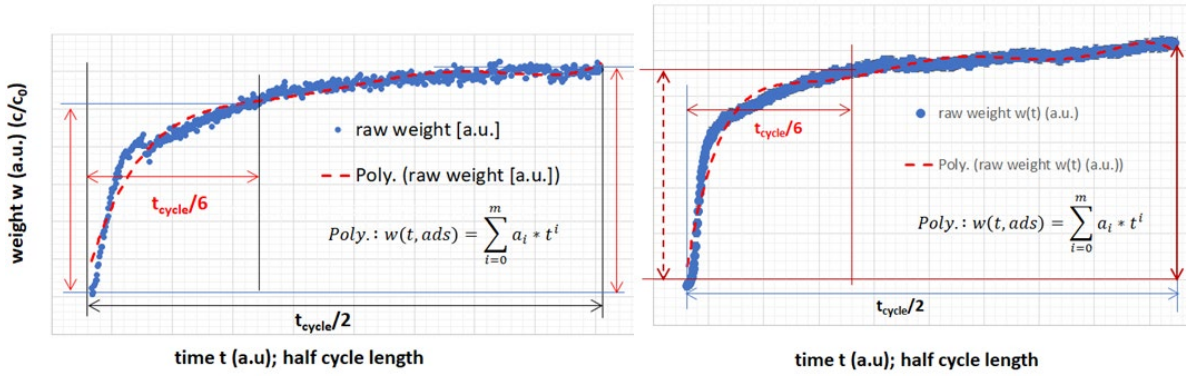

Figure 47: Measurement data: AD HEX 2 measurement data of the adsorption curve over the half cycle time $t_{cycle}/2$ (a. u. = arbitrary units) and concept of data curve analysis with peace wise fit-functions (first generation left, second right)..

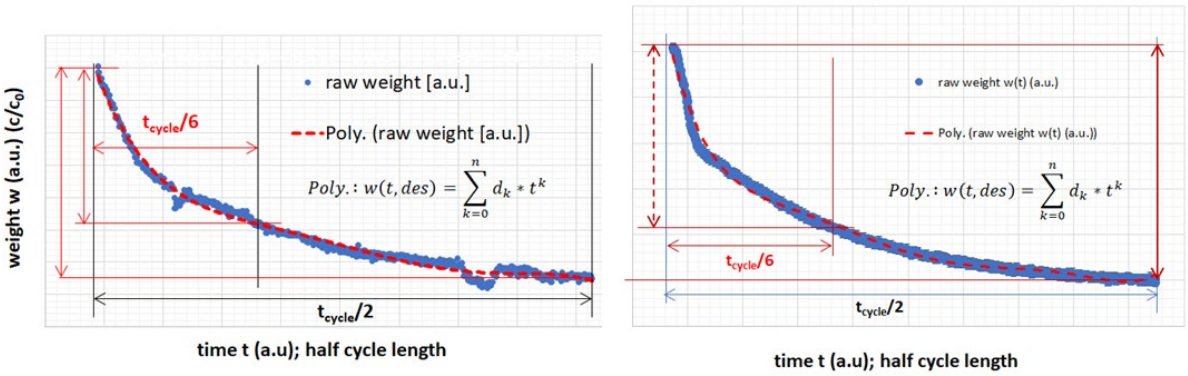

Figure 48: Measurement Data: AD HEX 2 measurement data of the desorption curve over the half cycle time $t_{cycle}/2$ (a. u. = arbitrary units) and concept of data curve analysis with peace wise fit-functions (first generation left, second right).

For this second generation of heat and mass exchangers, as for the first, the cycle time t_{cycle} could be reduced to about 2*300 s due to the high kinetic behaviour in the first third of the cycle.

3.5.3 Comparison of the first and second-generation A/D results

Comparing the average performance of the second generation A/D HEX 2 with that of the first generation A/D HEX 1 for a half cycle duration of 900 s, the performance of the second generation A/D HEX 2 is lower by about 30 % in cooling mode whereas the HEX works slightly better (+5 %) in district heating mode.

These results are difficult to explain. From the materials properties much higher performance was expected, especially for the cooling mode. Even if we would consider a similar ageing as the 1 generation of material, this would not explain the measured values fully. One possible explanation can lie in the pressure within the A/D HEX 2. In the pressure curve of the A/D HEX 2 measurements it can be clearly seen that the pressure rises and does not reach the target value within the measurement, in other words the desorption process seems to be kinetically driven by the condensor and the capacity of the material will be negatively influenced by this. Also even in the case of adsorption there seems to be a slow adsorption dynamics in addition to the initial fast uptake, which is unexpected. In conclusion there are likely several factors, partially coming from the measurement setup, partially from the A/D HEX design and partially from the material all contributing to the observed low performance. However a full investigation was not possible due to the project end.

As already mentioned, the designed A/D HEX 2 has a high (mass uptake) kinetic during the first part of the cycle. By shortening the cycle length to one third (300 s half-cycle), 70% of the water mass is still cycled, as shown in Figure 49 and For such a cycle time, the power is increased by more than 200%.

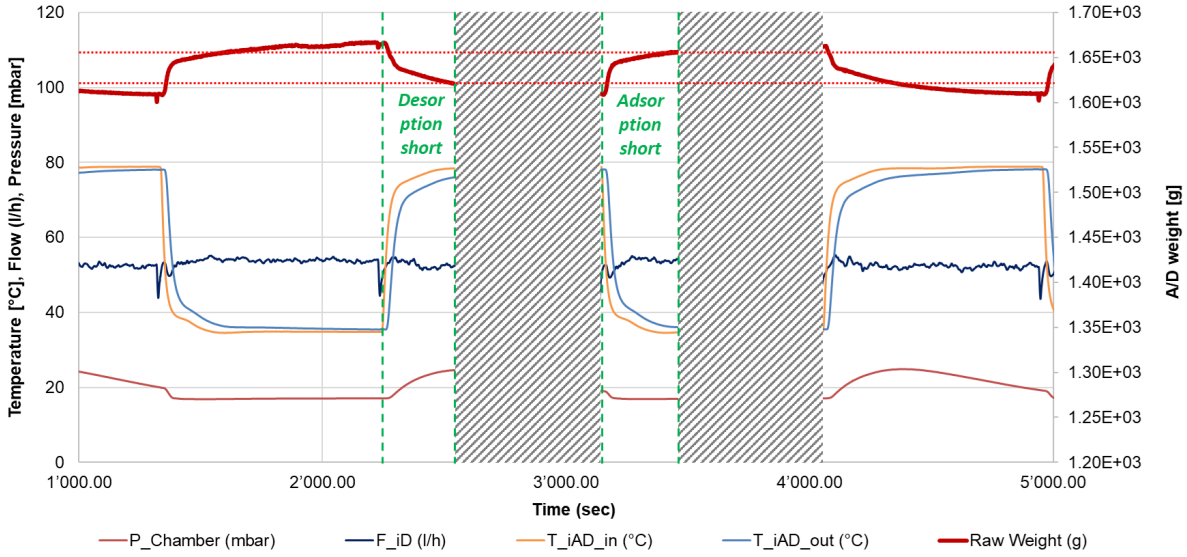

Figure 49: Measurement data: Evolution of temperatures, pressure, flow and weight of the A/D HEX 2 (cooling district mode, reduced cycle length)

Additional investigations (modeling of the heat and mass transfer, further measurement campaign with shortened cycle time lengths and different condenser boundary conditions) may allow a better understanding of the limitation of the second-generation (AD HEX 2) heat and mass exchanger.

3.6 Results summary

Section 3 evaluates the results and challenges of integrating adsorption heat pumps (adHPs) into district heating networks, focusing on their operation, performance, and the development of supporting materials and components.

The project examined two modes of operation for adHPs, based on an updated model that has been calibrated and validated against experimental measurements realized in the SPF test bench. A case study in temperature reduction mode was carried out, integrating an active substation between a low-temperature subnetwork (outgoing: 50°C/65°C, return: 40°C/50°C) supplying a district of 33 buildings (5MW of power and 9 GWh/year of consumption) and a 90°C structural network. The results show that the active substation enables return temperatures to be reduced by 10K, with paybacks of less than 5 and 7 years respectively, considering cost reduction gradients of 0.67 and 0.51 CHF/(MWh.°C). A case study for a commercial zone's cooling application was conducted, comparing two scenarios: 1) Business as Usual (BAU) with decentralized compression chillers, and 2) District Cooling (DC) integrating a sorption chiller powered by the DHN. The DC scenario (89.6 CHF/MWh) is more expensive than the BAU scenario (72.5 CHF/MWh), with higher initial investment amortization (~21% vs. 7.2%) and additional costs from the chilled water network. The BAU scenario's costs are primarily driven by electricity (92.8%), whereas the DC scenario has a more balanced cost distribution between heat (32.8%) and electricity (42.9%), mitigating energy tariff volatility.

Performance simulations validated the potential of adHPs to enhance DHN operations. In temperature reduction mode, the systems achieved temperature efficiencies up to 1.2, surpassing the 0.9 efficiency of conventional setups, while also reducing flow rates by 30% on the DHN side. Cooling mode

simulations yielded coefficients of performance (COPs) between 0.6 and 0.8, depending on temperature conditions, indicating reasonable efficiency for renewable cooling applications.

Significant progress was made in sorbent material development, with the successful upscaling of activated carbon-based sorbents. These materials showed promising adsorption properties, although structural issues, such as cracks and delamination in prototypes, highlighted the need for further refinement. Two generations of heat and mass exchangers (A/D HEX) were also developed and tested. The second-generation exchanger incorporated improved hydraulic distribution and sorbent layout but exhibited only modest performance improvements in heating mode (+5%) and a drop in cooling performance (-30%).

Overall, the study underscores the potential of adHPs to enhance DHN efficiency and provide sustainable cooling solutions. However, further work is needed to optimize heat transfer in exchanger designs and address structural challenges in sorbent materials. Future research, including advanced 3D modelling, is recommended to refine system performance and reduce experimental efforts.

Regarding the objectives defined in chapter 1.3, the objective of defining the technical and operational constraints for integrating reversible adHPs into substations (a) was achieved. The project successfully outlined temperature and flow requirements for both temperature reduction and cooling production modes, guiding material and system development. Integration guidelines addressed hydraulic configurations, temperature levels, and cost considerations. Despite challenges in material performance and exchanger design, the defined constraints proved feasible and economically viable, fulfilling the objective.

The objective of extending a physical reversible adHP simulation model, including hydraulic implementation for DHN cooling applications (b), was partially achieved. The numerical model was successfully modified to incorporate the new adsorption materials and calibrated using experimental measurements from the first-generation heat exchanger (HEX). While the model accurately mapped system performance for temperature reduction and cooling modes, some discrepancies in dynamic water uptake and material integration were noted. These challenges highlight the need for further refinement to fully align experimental results with simulated performance.

The objective of developing targeted sorbent materials with a thermal $COP_{th} > 0.6$ in cooling mode and optimal recooling temperatures (c) was partially achieved. Promising activated carbon-based sorbents were developed and successfully upscaled, demonstrating good adsorption properties. However, performance limitations in the system were primarily linked to heat transfer inefficiencies in the exchanger design rather than the sorbent materials themselves. While the materials showed potential, further optimization is needed to fully meet the energy density and thermal efficiency targets.

The objective of upscaling material synthesis and integrating ~100 g of sorbent into a custom-designed adsorber-desorber HEX with ~1 kW cooling power (d) was partially achieved. While sorbent production was upscaled, the system did not reach the targeted cooling power of 1 kW due to performance limitations in heat transfer within the HEX. There are likely several factors, some from the measurement setup (the desorption process appears to be kinetically driven by the condenser), some from the A/D HEX design (likely limiting heat transfer within the heat and mass exchanger), and some from the material (limited producable amount), all contributing to the observed low performance. Characterization highlighted these challenges, and further optimization is needed to achieve the desired performance and scaling targets.

The objective of conducting a technical and financial evaluation of the new reversible sorption substation for return temperature reduction and cooling modes (e) was achieved. Validated simulation models demonstrated that the return temperature reduction mode significantly improved DHN efficiency, achieving up to a 10K reduction with favorable payback periods of 5–7 years. In cooling mode, the system was technically feasible but incurred higher costs than conventional solutions. The findings

provided valuable insights into the performance and economic viability of the substation in both operational modes.

The objective of formulating practical implementation guidelines for reversible adHPs in district heating networks (f) was achieved. The project provided detailed guidelines for hydraulic integration to maximize efficiency in both heating (return temperature reduction) and cooling applications. These included optimal temperature and flowrate requirements, design configurations, and strategies to enhance operational hours, such as reversible substations and integration between high- and low-temperature networks. The guidelines offer a clear pathway for implementing adHPs to improve DHN efficiency and support room air conditioning applications.

4 Conclusions

The CharacSorb project advanced the development and evaluation of reversible adsorption heat pumps (adHPs) for district heating networks (DHNs), yielding significant insights and achievements across technical and economic dimensions, while highlighting areas for further improvement.

In temperature reduction mode, adHPs demonstrated the ability to lower DHN return temperatures by up to 10K, significantly enhancing network efficiency. This improvement allows for increased heat distribution capacity, reduced thermal losses, and optimized energy utilization. Economic analysis indicated favourable payback periods of 5–7 years, making this mode a viable enhancement for DHNs.

In cooling mode, adHPs provided renewable cooling using DHN heat, offering a balanced cost distribution between heat and electricity, which mitigates exposure to energy price fluctuations. However, cooling costs were higher than those of decentralized chillers, reflecting the need for continued cost and performance optimizations to improve competitiveness.

The project made substantial progress in material and system development. By using a combination of modelling and experiments, it was still possible to find mitigation strategies for ageing observed on the A/D HEX I to develop an upscaled synthesis and pyrolysis protocol for monolithic carbons based on spent coffee grounds with target properties and to finish production of ACs for the second prototype. The design and manufacturing of second-generation heat and mass exchangers (A/D HEX 2) was successfully achieved, incorporating improved hydraulic distribution and sorbent layouts. While the second-generation HEX exhibited slightly improved heating performance (+5%) compared to its predecessor, cooling performance was lower (-30%), largely due to heat transfer limitations. Both heat and mass exchangers having a high (mass uptake) kinetic during the first part of the cycle, reducing the cycle length to one third (300 s half cycle) would increase the SCP by more than 200%. These findings underscore the need for enhanced HEX designs to unlock the full potential of the sorbents.

Validated simulation models provided critical insights into the performance of adHPs in both operational modes, bridging experimental data with practical applications. These models guided the formulation of comprehensive implementation guidelines, which address hydraulic configurations, temperature and flowrate requirements, and strategies to maximize system operation hours.

In summary, the CharacSorb project highlights the significant potential of reversible adHPs to improve the efficiency and sustainability of DHNs while offering renewable cooling as a valuable energy service. The findings emphasize the importance of optimizing heat and mass exchanger designs and reducing system costs to fully realize this technology's potential. The progress achieved in material development, system integration, and performance evaluation lays a robust foundation for future advancements and commercialization of adHP technologies.

5 Outlook and next steps

Case studies investigated in **WP2** gave promising results for the temperature reduction mode and for district cooling applications, especially for large projects where scale effects can be found (>1 MW). Commercial project is already being implemented in Europe but with Asian technology providers. For smaller units like building substations, further studies are required to determine if reversible substations are feasible at cost and compacities adapted to dense urban areas. An increase in performance of the sorbent and of the HMX will only increase the financial attractiveness of the technology.

For **WP4**, it will be tried to characterize a piece of the sorbent after the disassembly of the A/D HEX II to investigate possible origins of the lower-than-expected performance. Depending on results, supplemental modelling might give further insights and will be envisaged depending on results and available resources after the project termination. This can give further insights into materials performance, stability and lifetime.

Further investigations (modeling of heat and mass transfer, further measurement campaign with shortened cycle times and different condenser boundary conditions) would be interesting within **WP3** to better understand the limitations of the second-generation heat and mass exchanger and to enable its improvement.

6 National and international cooperation

In the SFOE financed project CharacSorb 3 institutions – Empa, SPF of OST & HEIG-VD - are cooperating as a system development team.

A short summary of each of the previous or current R&D projects on which the CharacSorb project is based is given below.

1. ***SNF THRIVE – "Thermally driven adsorption heat pumps for substitution of electricity and fossil fuels":*** *The objectives of this project that was funded by the NRP70 was to develop an adsorption heat pump technology able to valorise waste and renewable heat for building heating and cooling. Different AdHP application scenario were generated and investigated by LESBAT. A new sorption material was developed and characterized for the most interesting specific application scenario by EMPA. This material was integrated in a HEX which was characterized by SPF. One very promising integration scenario was the use of AdHP in DHN substation in order to reduce DHN return temperature while providing heat to the customer at higher temperatures. The THRIVE project results will be directly used as a starting point for the CharacSorb project. This project has been completed in 2018.*

2. ***Interreg PACs-CAD projects – "Adsorption heat pump for more efficient DHN":*** *the objective of the PACs-CAD project was to map and characterize all the possible integration of AdHP technology in DHN. The most promising integration scenario were evaluated with experimental measurements and numerical models. The impacts of AdHP on DHN energy efficiency, financial and environmental performances were evaluated. The PACs-CAD project will be completed in summer 2021. One of the main conclusion of this project so far is that the most interesting integration scenario of AdHP in DHC is to reduce return temperature in heating season and to produce cooling in summer time. The experimental measurements carried out with a commercial adsorption chiller (eCoo10 from Fahrenheit GmbH) have confirmed the interest of the two integration scenarios. In addition, those experimental results have shown that*

a dedicated adsorption technology need to be developed for performances improvements (further decrease of return temperature in return temperature reduction mode and increase of temperature differences and heat rejection temperature in cooling mode).

3. ***EU HYCOOL:*** *Industrial Cooling through Hybrid system based on solar heat with a cascaded (adsorption and compression) heat pump with a focus on increasing the current use of Solar Heat in Industry Processes. The results will contribute to the CharacSorb project.*

4. ***EU ProDIA – "Production, control and demonstration of structured hybrid nano-porous materials for industrial adsorption application"(www.prodia-mof.eu):*** *HEX integration of MOF and measurement of the adsorption kinetics regarding cooling machine application. SPF completed a sub-atmospheric HEX characterisation containing a metal organic framework (MOF) sorbent produced by a French-UK-Norwegian consortium.*

5. ***Project DecarbCH – "Decarbonisation of heating and cooling in Switzerland":*** *this project was submitted in the first SWEET SFOE call. SPF and LESBAT are both involved in this project. LESBAT will be mainly working on the decarbonisation of existing District Heating Network (DHN). The technology developed in the CharacSorb project will be used in the portfolios of technologies to reduce greenhouse gas emission from DHN. So the results of CharacSorb will be directly valorized in this ambitious project.*

7 Communications

Alexis Duret. Cas d'application d'optimisation de sous-stations pour un réseau thermique villageois. Programme 5à7 Institut des Energies, Réseaux thermiques, 20th of June 2024, Yverdon-les-bains, Switzerland.

Xavier Jobard. Abaissement niveaux température - PAC à sorption. Programme 5à7 Institut des Energies, Réseaux thermiques, 20th of June 2024, Yverdon-les-bains, Switzerland.

Sandra Galmarini, Xavier Jobard, Alexis Duret, Kevin Meili, Xavier Daguenet. Optimized Adsorption Heat Pump for Efficiency Increase of District Heating Networks. Swiss Heat Pump Conference, 26th of June 2024, Bern, Switzerland.

8 Publication

Emanuele Piccoli, Romain Civioc, Sandra Galmarini, Xavier Jobard, Alexis Duret, Xavier Daguenet and Paul Gantenbein. Optimized Adsorption Heat Pump for Efficiency Increase of District Heating Networks. EuroSun 2022, ISES and IEA SHC International Conference Solar Energy for Buildings and Industry, 25 – 29 September 2022, Kassel, Germany.

9 References

Ammann, Jens, Bruno Michel, and Patrick W. Ruch. “Characterization of Transport Limitations in SAPO-34 Adsorbent Coatings for Adsorption Heat Pumps.” *International Journal of Heat and Mass Transfer* 129 (February 2019): 18–27. https://doi.org/10.1016/j.ijheatmasstransfer.2018.09.053.

Ammann, Jens, Bruno Michel, André R. Studart, and Patrick W. Ruch. “Sorption Rate Enhancement in SAPO-34 Zeolite by Directed Mass Transfer Channels.” *International Journal of Heat and Mass Transfer* 130 (March 2019): 25–32. https://doi.org/10.1016/j.ijheatmasstransfer.2018.10.065.

Aristov, Yuri “Challenging offers of material science for adsorption heat transformation: A review,” Applied Thermal Engineering - APPL THERM ENG, vol. 50, Feb. 2013, doi: 10.1016/j.applthermaleng.2011.09.003.AL-Hasni, Shihab, and Giulio Santori. “The Cost of Manufacturing Adsorption Chillers.” *Thermal Science and Engineering Progress* 39 (March 2023): 101685. https://doi.org/10.1016/j.tsep.2023.101685.

Averfalk, H., T. Benakopoulos, I. Best, F. Dammel, C. Engel, R. Geyer, O. Gudmundsson, et al. “Low-Temperature District Heating Implementation Guidebook. Final Report.” Accessed September 24, 2024. https://doi.org/10.24406/PUBLICA-FHG-301176.

Carslaw, H. S., J. C. Jaeger, and Herman Feshbach. “*Conduction of Heat in Solids*.” *Physics Today* 15, no. 11 (November 1, 1962): 74–76. https://doi.org/10.1063/1.3057871.

Civioc, Romain, Marco Lattuada, Matthias M. Koebel, and Sandra Galmarini. “Monolithic Resorcinol–Formaldehyde Alcogels and Their Corresponding Nitrogen-Doped Activated Carbons.” *Journal of Sol-Gel Science and Technology* 95, no. 3 (September 2020): 719–32. https://doi.org/10.1007/s10971-020-05288-x.

Dalibard, Antoine, “Advanced control strategies of solar driven adsorption chillers,” Forschungsberichte des Deutschen Kälte- und Klimatechnischen Vereins e.V. DKV e.V., Deutscher Kälte- und Klimatechnischer Verein, Hannover, 2017.

DeMeester, T. R., and L. F. Johnson. “Evaluation of the Nissen Antireflux Procedure by Esophageal Manometry and Twenty-Four Hour pH Monitoring.” *American Journal of Surgery* 129, no. 1 (January 1975): 94–100. https://doi.org/10.1016/0002-9610(75)90174-9.

Demir, Hasan, Moghtada Mobedi, and Semra Ülkü. “A Review on Adsorption Heat Pump: Problems and Solutions.” *Renewable and Sustainable Energy Reviews* 12, no. 9 (December 2008): 2381–2403. https://doi.org/10.1016/j.rser.2007.06.005.

Dubinin, M. M., and V. A. Astakhov. “Development of the Concepts of Volume Filling of Micropores in the Adsorption of Gases and Vapors by Microporous Adsorbents: Communication 1. Carbon Adsorbents.” *Bulletin of the Academy of Sciences of the USSR Division of Chemical Science* 20, no. 1 (January 1971): 3–7. https://doi.org/10.1007/BF00849307.

EnDK, 2022. MuKEn. Accessed September 24, 2024. https://www.endk.ch/de/energiepolitik-der-kantone/muken.

FAHRENHEIT, eCoo 40X. Accessed December 20, 2024. https://fahrenheit.cool/en/product/ecoo-40x/.

Farrusseng, David, Cécile Daniel, Conor Hamill, Jose Casaban, Terje Didriksen, Richard Blom, Andreas Velte, et al. “Adsorber Heat Exchanger Using Al-Fumarate Beads for Heat-Pump Applications – a Transport Study.” *Faraday Discussions* 225 (2021): 384–402. https://doi.org/10.1039/D0FD00009D.

Fernandez, L. A., J. M. MacSween, and G. R. Langley. “Effect of Treatment on T-Cell Function in Chronic Lymphocytic Leukaemia.” *British Journal of Haematology* 38, no. 2 (February 1978): 171–78. https://doi.org/10.1111/j.1365-2141.1978.tb01033.x.

Gantenbein P. et al., Adsorption Heat Pump – Development and Application, 26. Tagung des BFE-Forschungsprogramms "Wärmepumpen und Kälte", 24. Juni 2020 BFH Burgdorf.

Geyer, Roman, Jürgen Krail, Benedikt Leitner, Ralf-Roman Schmidt, and Paolo Leoni. “Energy-Economic Assessment of Reduced District Heating System Temperatures.” *Smart Energy* 2 (May 2021): 100011. https://doi.org/10.1016/j.segy.2021.100011.

Gonseth, Camille, Philippe Thalmann, and Marc Vielle. “Impacts of Global Warming on Energy Use for Heating and Cooling with Full Rebound Effects in Switzerland.” *Swiss Journal of Economics and Statistics* 153, no. 4 (October 2017): 341–69. https://doi.org/10.1007/BF03399511.

Huber, Lukas, Stefanie Beatrice Hauser, Eric Brendlé, Patrick Ruch, Jens Ammann, Roland Hauert, Remo N. Widmer, et al. “The Effect of Activation Time on Water Sorption Behavior of Nitrogen-Doped, Physically Activated, Monolithic Carbon for Adsorption Cooling.” *Microporous and Mesoporous Materials* 276 (March 2019): 239–50. https://doi.org/10.1016/j.micromeso.2018.09.025.

Jobard, Xavier, Pierryves Padey, Martin Guillaume, Alexis Duret, and Daniel Pahud. “Development and Testing of Novel Applications for Adsorption Heat Pumps and Chillers.” *Energies* 13, no. 3 (February 1, 2020): 615. https://doi.org/10.3390/en13030615.

Kapeller, Rudolf, Marianne Bügelmayer-Blaschek, Barbara Herndler, Lukas Kranzl, Andreas Müller, Simon Moser, Thomas Natiesta, Johannes Reichl, and Roman Schwalbe. “The Effects of Climate Change-Induced Cooling Demand on Power Grids.” *Energy Reports* 11 (June 2024): 674–91. https://doi.org/10.1016/j.egyr.2023.07.028.

Meunier, Francis. “Adsorption Heat Powered Heat Pumps.” *Applied Thermal Engineering* 61, no. 2 (November 2013): 830–36. https://doi.org/10.1016/j.applthermaleng.2013.04.050.

“MuKEn.” Accessed September 24, 2024. https://www.endk.ch/de/energiepolitik-der-kantone/muken.

Mylona, Zoi, Maria Kolokotroni, and Savvas A. Tassou. “Frozen Food Retail: Measuring and Modelling Energy Use and Space Environmental Systems in an Operational Supermarket.” *Energy and Buildings* 144 (June 2017): 129–43. https://doi.org/10.1016/j.enbuild.2017.03.049.

“PACs-CAD – Interreg France-Suisse.” Accessed September 24, 2024. https://www.interreg-francesuisse.eu/beneficiaire/pacs-cad/.

Piccoli, E., Frazzica, A., Galmarini, S., 2021. D4.3: Model capable of estimating the performance of a given ad-sorption chiller set-up and a given adsorber material for a given application scenario, Hycool project public deliverables. https://hycool-project.eu/download/d4-3-model-capable-of-estimating-the-performance-of-a-given-adsorption-chiller-set-up-and-a-given-adsorber-material-for-a-given-application-scenario/.

Quiquerez, Loïc. “Quel rôle pour le chauffage à distance dans la transition énergétique?,” In: Cycle de formation Energie-Environnement 2016-2017. Genève. 2017.

QUIQUEREZ, Loic et al. Températures de distribution de chauffage du parc immobilier genevois. 2013

Ruch, P., Duret, A., Rommel, M., Gantenbein, P., Michel, B., Frank, E., Koebel, M., Burgherr, P., 2015. THRIVE «Thermally driven adsorption heat pumps for substitution of electricity and fossil fuels».

Rüetschi, M. “The Return Temperature in DH Networks : A Key Factor for the Economical Operation of DH.” *Euroheat and Power*, 1997. https://www.semanticscholar.org/paper/The-return-temperature-in-DH-networks-%3A-a-key-for-R%C3%BCetschi/270e63d81fcd126734493c03780dc2625da5ba07.

Schneider, S., Brischoux, P. , Santandrea, D. and Hollmuller, P. “Retour d’expérience énergétique sur le quartier des Vergers à Meyrin (Genève) - Rapport intermédiaire,” Université de Genève, 2020. Accessed: Dec. 06, 2024. [Online]. Available: https://archive-ouverte.unige.ch/unige:147702

Schöpfer, M. “Absorption Chillers : Their Feasibility in District Heating Networks and Comparison to Alternative Technologies,” 2015. https://www.semanticscholar.org/paper/Absorption-chillers-%3A-their-feasibility-in-district-Sch%C3%B6pfer/2c17fb077b4575bafd1af092e3c81ba5771ec09e.

SIA, 2024 - Donnees d’utilisation des locaux pour l’energie et les installations du batiment 2015:154.

Silva, Ricardo, Sven Eggimann, Léonie Fierz, Massimo Fiorentini, Kristina Orehounig, and Luca Baldini. “Opportunities for Passive Cooling to Mitigate the Impact of Climate Change in Switzerland.” *Building and Environment* 208 (January 2022): 108574. https://doi.org/10.1016/j.buildenv.2021.108574.

Stahl, Th., S. Brunner, M. Zimmermann, and K. Ghazi Wakili. “Thermo-Hygric Properties of a Newly Developed Aerogel Based Insulation Rendering for Both Exterior and Interior Applications.” *Energy and Buildings* 44 (January 2012): 114–17. https://doi.org/10.1016/j.enbuild.2011.09.041.

Streicher, Kai Nino, Pierryves Padey, David Parra, Meinrad C. Bürer, Stefan Schneider, and Martin K. Patel. “Analysis of Space Heating Demand in the Swiss Residential Building Stock: Element-Based Bottom-up Model of Archetype Buildings.” *Energy and Buildings* 184 (February 2019): 300–322. https://doi.org/10.1016/j.enbuild.2018.12.011.

Tarazona, P. “Free-Energy Density Functional for Hard Spheres.” *Physical Review A* 31, no. 4 (April 1, 1985): 2672–79. https://doi.org/10.1103/PhysRevA.31.2672.

“Températures de distribution de chauffage du parc immobilier genevois,” July 5, 2013. https://www.unige.ch/sysener/fr/services/wwwelectricite-vertech/energie/tempdist/.

Wang, D.C., Z.X. Shi, Q.R. Yang, X.L. Tian, J.C. Zhang, and J.Y. Wu. “Experimental Research on Novel Adsorption Chiller Driven by Low Grade Heat Source.” *Energy Conversion and Management* 48, no. 8 (August 2007): 2375–81. https://doi.org/10.1016/j.enconman.2007.03.001.

Zhang, Hao, Yuhao Yi, and Xiaoyun Xie. “Performance and Optimization of Absorption Heat Exchanger under Different Flow Rate Ratio Conditions.” *Applied Thermal Engineering* 212 (July 2022): 118603. https://doi.org/10.1016/j.applthermaleng.2022.118603.